PRODUCTION AND CHARACTERIZATION OF SUGARCANE BAGASSE BASED ACTIVATED CARBON FOR THE TREATMENT OF CHROMIUM AND ZINC IONS FROM ELECTROPLATING EFFLUENT

BY

OGUNDEJI, Olorunseun Joshua
(MEng/SEET/2017/6722)

DEPARTMENT OF CHEMICAL ENGINEERING
FEDERAL UNIVERSITY OF TECHNOLOGY
MINNA

OCTOBER, 2021

ABSTRACT

Sugarcane is cultivated in large quantity and it creates serious disposal problems. In light of the increased recognition of the health and environmental impacts of insufficient wastewater treatment, several measures need to be put in place to mitigate these impacts. This study reports the potential of sugarcane based activated carbon for the treatment of chromium and zinc ions from electroplating effluent. A preliminary study was done on the raw sugarcane bagasse through proximate and ultimate analysis and the thermo graphic analysis (TGA). The characterization of raw sugarcane (RSCB), modified sugarcane bagasse (MSCB) and Sugarcane Bagasse Activated Carbon (SCBAC) was carried out using Fourier Transform Infra-Red Spectroscopy (FT-IR), Brunauer-Emmett-Teller (BET) and Scanning Electron Microscopy (SEM). The proximate and ultimate analysis showed the composition of SCB a carbonaceous material. The TGA result showed stages of moisture loss, decomposition of hemicellulose and lignin. The BET surface area of RSB, MSCB and SCBAC were found to be 178 m^2/g, 423 m^2/g and 954.4 m^2/g respectively. The FT-IR analysis showed the presence of hydroxyl, amine, carbonyl and phenolic groups, which are responsible for the adsorption of the Cr and Zn ions from the effluent. In the adsorption study, the individual and interaction between process parameters including contact time, pH of the solution, temperature and adsorbent dosage on removal efficiency of Cr and Zn ions were optimized by applying the response surface methodology combined with the central composite design. The Langmuir model fitted more adequately with regression coefficient (R^2) closer to one and equilibrium parameter R_L between zero & one and it better describes the adsorption process, indicating that the adsorption process is favorable, and a monolayer adsorption. The regression coefficient (R2) showed that the pseudo-second-order kinetics was closer to one and thus, have better fit to the kinetic behavior of the adsorption process. The thermodynamic parameters studied include; ΔG^0which values were negtives, ΔS^0were positives and ΔH^0values were negatives for the adsorption process and thus, suggests that the process was spontaneous and exothermic.

CHAPTER ONE

1.0 INTRODUCTION

1.1 Background of the Study

Nigeria and South Africa are two countries considered as the largest economies in Africa. In 2015, the gross domestic product (GDP) of these countries was estimated at 525 (Nigeria) and 350.63 (South Africa) billion USD. Sugarcane bagasse (SCB) is an abundant agro-industrial by product worldwide and it is used in many different applications (Sulaiman *et al.,* 2015, Bachrun *et al.,* 2016).

Sugarcane is the raw material used for manufacturing sugar in Nigeria, which accounts for about 61% of the total world sugar production. Two types of sugarcane are grown in Nigeria - industrial and soft (chewing) cane. The industrial cane is the hard or tough type generally processed into sugar by the sugar estates. The soft cane is mainly chewed raw for its sweet juice. Some of it is also processed into different crude sugar products. Local farmers grow soft cane all over Nigeria. Soft cane production accounts for about 60% of total sugarcane production in many years in Nigeria .The exact total land area currently under cane cultivation and the total production in Nigeria is not known, but it is estimated at between 25,000-35,000 hectares, out of which soft cane covers 18,000 hectares (Bachrun *et al.,* 2016).

SCB a carbonaceous byproduct of cane sugar processing, is generated in large quantities in Nigeria and it is considered as one of the largest natural fibre resources because of its high cellulose content has great potential in metal bisorption capacity high yield and annual regeneration capacity. Sugarcane bagasse consists of cellulose 43.8%, hemicellulose 28.6%, lignin 23.5%, ash 1.3%, and other components 2.8% (Kumar *et al.,* 2013).

Sugarcane bagasse (SCB) is suitable for preparing activated carbons due to their excellent natural structure and low ash content. SCB is a byproduct of sugarcane industries obtained after the extraction of juice for production of sugar. Conversion of sugarcane bagasse into activated carbons which can be used as adsorbents, ion exchange, carbon molecular sieve, catalyst would add value to these agricultural commodities, help reduce the cost of waste disposal, and provide a potentially cheap alternative to existing commercial carbons (Bachrun *et al.,* 2016).

Continuous discharge of untreated heavy-metals contaminated industrial effluents into water bodies is a major cause of environmental pollution problem because of their high solubility in the aquatic environments and ease of being absorbed by living organisms. Once they enter the food chain, large concentrations of heavy-metals may accumulate in the human body and if the metals are ingested beyond permitted concentration, they can cause serious health disorders (Babel and Kurniawan, 2004). This may include reduced mental and central nervous function, lower energy levels, and cause damage to blood composition, lungs, kidneys, liver, bones, other vital organs and death in the extreme case(s). For these reasons, environmental scientists are challenged to developing effective means of combating the problem (Bediako *et al.,* 2015).

Due to the need to remove toxic heavy-metals from wastewater and industrial effluents before being discharged into the water bodies, collective efforts of scientists brought about the development, use of methods and technologies such as chemical precipitation, coagulation/flocculation, stabilization, ion exchange, liquid ion exchange/liquid-liquid extraction, floatation, complexation/sequestration, electrochemical operations, extraction with chelating agents, cementation, membrane operations/reverse osmosis, evaporation/distillation, electrolysis and vitrification for removing contaminants such as

heavy-metals. However, these techniques have disadvantages that include high capital and operational costs, complex treatment and disposal methods for the residual metal sludge generated (Mohanty *et al.,* 2006).

Based on the disadvantages enumerated above and the need for effective, and affordable methods/technologies for heavy-metals pollution treatment, especially in developing countries like Nigeria, continuous efforts have suggested the use of adsorption/bisorption processes as an alternative (Cronje *et al.,* 2012). Abundant waste materials from industrial and agricultural activities have been reported as potential inexpensive alternatives for heavy-metals removal (Garg *et al.,* 2009). Many agricultural waste by-products such as coconut shell, grain sorghum, coffee bean husks, pine wood, peat, rubber wood saw dust, chestnut wood, wood, cotton, hemp, flax, sisal, sugarcane bagasse, corncob, cassava bagasse, banana rachis, soy hulls, mengkuang leaves (Pandanustectorius), Phormiumtenax leaf fibres, rice husk and jute and fruit stones have been discovered to be a better sources of cellulose and suiTable for activated carbon due to their high carbon and low ash contents by implication as an adsorbent for water and wastewater treatment (Akl *et al.,* 2014).

Literature shows that some works have been done in the area of application of SCB as an adsorbent and for activated carbon (AC) production for heavy treatments. For instance, Putra *et al.,* (2014) studied SCB in its natural form as an adsorbent for the removal of Cu (II), Pb (II) and Zn(II) with a maximum adsorption capacity of 3.65, 21.28 and 40.00 mg/g respectively. Bahadur and Paramatma (2014) worked on H_2SO_4 modified Sugarcane biomass to remove Cr (VI) from solution, the maximum adsorption capacity was found to be 131.68 mg/g at optimum pH of 1.Tran *et al.,* (2017) prepared activated carbon from SCB using $ZnCl_2$ as activating agent for the removal of Cu(II) ion by

applying Response Surface Methodology (RSM), the optimized conditions attained for the preparation of AC and removal of Cu (II) ions were temperature of 673 K, impregnation ratio of 1.5 and activation time of 35.2 minutes, which resulted to 48.8% of AC yield and 92.3 % Cu(II) ion removal. Alhassan *et al.*, (2017) did a comparative studied of CO_2 capture using acid and base modified activated carbon from sugarcane bagasse, the base modified activated carbon had the most effective adsorption for CO_2 compared with acid modified and unmodified activated with 148.5 mg/g at 25^oC and 25 minute.

The use of SCB as a potential adsorbent in its raw form and in the synthesis of AC for the treatment of heavy-metals contaminated industrial effluent has not been fully exhausted. Therefore, the current study shall focus on the area of optimization, isothermal, kinetics and thermodynamics of synthesized sugarcane bagasse based activated carbon for the removal of heavy metals from industrial effluent.

1.2 Statement of the Research Problem

The deleterious effects of accumulation of heavy metals on human health cannot be overemphasized. In light of the increased recognition of the health and environmental impacts of insufficient wastewater treatment, several measures need to be put in place to mitigate these impacts.

Sugarcane is cultivated in large quantity in Niger State; it creates serious disposal problems in Minna metropolis. Sugarcane bagasse waste may cause different menace in our environment, ranging from the waste lithering the floor, blocking the drainage system during the raining period as well as causing widespread outbreak of infectious disease.

Production of activated carbon/adsorbent from material like sugarcane bagasse still need better understanding of how its yield and quality are affected by process parameters (such

as temperature, pH, contact time, adsorbent dosage), and the study of kinetics, isotherms and thermodynamics in adsorption of heavy metals. Thus, the challenges of this study.

1.3 Aim and Objectives of the Study

The aim of this research work is to produce and evaluate the performance of raw sugarcane bagasse (RSCB), modified sugarcane bagasse (MSCB) and activated carbon from sugarcane bagasse (SCBAC) for the removal of chromium and zinc ions in electroplating effluent.

This aim will be achieved through the following objectives:

i. Proximate and Ultimate analysis of the raw SCB sample
ii. Modification and characterization of SCB
iii. Preparation and characterization of activated carbon from SCB
iv. Investigation the influence of contact time, mass of adsorbent, pH and temperature on the efficient removal of heavy metals using response surface methodology.
v. Study of adsorption isothermal, kinetic and thermodynamic parameters of chromium and zinc ions adsorption using RSCB, MSCB and SCBAC

1.4 Justification of the Study

Adsorbent are solid particles that present porous structure and volume which justify their use in adsorption process. Sugarcane bagasse is raw material that are naturally abundantly available at little or no cost, rich in cellulose and therefore a good biosorbent.

However, the need to minimize disposal problem of sugarcane bagasse an agricultural waste, compelled scientist towards the development of low-cost adsorbent that is readily available and eco-friendly for the removal of heavy harmful metals.

1.5 Scope of the Study

This research work is limited to

Selection of adsorbent (SCB), modification of SCB and preparation of AC the selected adsorbent, characterization of the adsorbents, optimization of process parameters (contact time, mass of adsorbent, pH and temperature) using response surface methodology (RSM) and adsorption studies of RSCB, MSCB and SCBAC in the removal of chromium and zinc from electroplating effluent.

The characterization of RSCB, MSCB and SCBAC will be evaluated by means of Brauner-Emmert-Teller (BET), screening electronic microscopy (SEM), and Fourier's transformed infrared (FTIR).

The isotherm, kinetics and thermodynamics studies of adsorption in the removal of chromium and zinc ions using RSCB, MSCB and SCBAC will be evaluated.

CHAPTER TWO

2.0 LITERATURE REVIEW

2.1 Historical Background

Recently, a great deal of interest in the research for the removal of heavy-metals from industrial effluent has been focused on the use of agricultural by-products as adsorbents, the use of agricultural waste in bioremediation of heavy-metals ions, is known as bio-sorption. This utilizes inactive (non-living) microbial biomass to bind and concentrate heavy-metals from streams by purely physio-chemical pathways (mainly chelation and adsorption) of uptake (Barakat, 2011). The development of low-cost and high capacity sorbents for removing or recovering heavy-metals ions has recently become crucial (Chao *et al.*, 2014).

2.2 Heavy Metals in Industrial Effluent

The environmental pollution due to the development in technology is one of the most important problems of this century (Bahadur and Paramatma, 2014). Because the high toxicities associated with heavy metals, their continual ejection and presence in our surrounding water bodies by industries, place great environmental threats that demand to be addressed urgently (Li *et al.*, 2015). Heavy metals are a group of a loosely defined subset of elements that exhibit properties and mainly include the transition metals, some metalloids, lanthanides and actinides (Bediako *et al.*, 2015). Heavy metals are generally considered to be those whose density exceeds 5 g per cubic centimeter. They are defined as metallic elements that have a relatively high density compared to water (Fergusson, 1990).

In recent years, there has been an increasing ecological and global public health concern associated with environmental contaminant by these metals. In addition, human exposure has risen dramatically because of an exponential increase of their use in several industrial, agricultural, domestic and technological applications (Bradl, 2002). He, (2005) reported sources of heavy metals in the environment include geogenic, industrial, agricultural, pharmaceutical, domestic effluent and atmospheric sources. Environmental pollution is very prominent in point source areas such as mining, foundries and smelters, and other metal-based industrial operations (Tchounwou *et al*., 2012)

Heavy metals are also considered as trace elements because of their presence intrace concentrations (ppb range to less than 10 ppm) in various environmental matrices (Kabata-Pendia, 2001). Their bioavailability is influenced by physical factors such as temperature, phase association, adsorption, and sequestration. It is also affected by chemical factors that influence speciation at thermodynamic equilibrium, complexation kinetics, lipid solubility, and octanol/water partition coefficients (Hamelink *et al*., 1994). Biological factors, such as species characteristics, trophic interactions, and bio chemical/physiological adaptation, also play an important role (Hamelink *et al*.,1994).

2.3 Industrial Effluent Sources and Effects

2.3.1 Cadmium

The use of cadmium by man is relatively recent and it is only with its increasing technological use in the last few decades that serious consideration has been given tocadmium as a possible contaminant. Cadmium is naturally present in the environment in air, soils, sediments and even in unpolluted seawater. Cadmium is emitted to air by mines, metal smelters and industries using cadmium compounds for alloys, batteries,

pigments and in plastics, although many countries have stringent controls in place on such emissions. Tobacco smoke is one of the largest single sources of cadmium exposure in humans. Tobacco in all of its forms contains appreciable amounts of the metal. Because the absorption of cadmium from the lungs is much greater than from the gastrointestinal tract, smoking contributes significantly to the total body burden. In general, for non-smokers and non-occupationally exposed workers, food products account for most of the human exposure burden to cadmium. People are exposed to cadmium when consuming plant- and animal-based foods. Seafood, such as molluscs and crustaceans, can be also a source of cadmium accumulates in the human body affecting negatively several organs: liver, kidney, lung, bones, placenta, brain and the central nervous system, other damages that have been observed include reproductive, and development toxicity, hepatic, haematological and immunological effects (Morais *et al.*, 2014).

2.3.2 Chromium

Chromium (Cr) is a naturally occurring element present in the earth's crust,with oxidation states (or valence states) ranging from chromium (II) to chromium (VI). Chromium compounds are sTable in the trivalent [Cr(III)] form and occur in nature in this state in ores, such as ferrochromite. The hexavalent [Cr(VI)] form is the second most sTable state. Elemental chromium [Cr (0)] does not occur naturally. Chromium enters into various environmental matrices (air, water, and soil) from a wide variety of natural and anthropogenic sources with the largest release occurring from industrial establishments (Bediako *et al.*, 2015).

Industries with the largest contribution to chromium release include metal processing, tannery facilities, chromate production, stainless steel welding, and ferrochrome and

chrome pigment production. The increase in the environmental concentrations of chromium has been linked to air and wastewater release of chromium, mainly from metallurgical, refractory, and chemical industries. Hexavalent chromium [Cr(VI)] is a toxic industrial pollutant that is classified as human carcinogen by several regulatory and nonregulatory agencies. The health hazard associated with exposure to chromium depends on its oxidation state, ranging from the low toxicity of the metal form to the high toxicity of the hexavalent form. All Cr(VI)-containing compounds were once thought to be man-made, with only Cr(III) naturally ubiquitous in air, water, soil, and biological materials. Recently, however, naturally occurring Cr(VI) has been found in ground and surface waters at values exceeding the World Health Organization limit for drinking water of 50 mg of Cr(VI) per liter. Cr(VI) compounds, which are powerful oxidizing agents and thus tend to be irritating and corrosive, appear to be much more toxic systemically than Cr(III) compounds, given similar amount and solubility. Although the mechanisms of biological interaction are uncertain, the variation in toxicity may be related to the ease with which Cr(VI) can pass through cell membranes and its subsequent intracellular reduction to reactive intermediates (Tchounwou *et al*. 2012).

2.3.3 Lead

Lead as a toxicologically relevant element has been brought into the environment by man in extreme amounts, despite its low geochemical mobility and has been distributed worldwide. Lead amounts in deep ocean waters is about 0.01-0.02 μg/L, but in surface ocean waters is ca. 0.3 μg/L (Castro-González and Méndez-Armenta, 2008). Lead still has a number of important uses in the present day; from sheets for roofing to screens for X-rays and radioactive emissions. Like many other contaminants, lead is ubiquitous and can be found occurring as metallic lead, inorganic ions and salts. Plant food may be

contaminated with lead through its uptake from ambient air and soil; animals may then ingest the lead contaminated vegetation. In humans, lead ingestion may arise from eating lead contaminated vegetation or animal foods. Another source of ingestion is through the use of lead-containing vessels or lead-based pottery glazes (Ming-Ho, 2005). In humans, about 20 to 50% of inhaled, and 5 to 15% of ingested inorganic lead is absorbed. In contrast, about 80% of inhaled organic lead is absorbed, and ingested organic Pb is absorbed readily. Once in the bloodstream, lead is primarily distributed among blood, soft tissue, and mineralizing tissue (Ming-Ho, 2005). The bones and teeth of adults contain more than 95% of the total body burden of lead. Children are particularly sensitive to this metal because of their more rapid growth rate and metabolism, with critical effects in the developing nervous system. The Joint FAO/ World Health Organization Expert Committee on Food Additives (JECFA) established a provisional tolerable weekly intake (PTWI) for lead as 0.025 mg/kg body weight (bw). The WHO provisional guideline of 0.01 mg/L has been adopted as the standard for drinking water (Castro-González and Méndez-Armenta, 2008).

Heavy-metals pollution is one of the major environmental problems that will lead to ecological imbalance and indirectly a threat to human health. The Table 2.1 below shows World Health Organization (WHO) and United States Environmental Protection Agency (USEPA).

Table 2.1: Permissible Limits and Health Hazards of Various Heavy Metals (Khoo *et al*., 2018)

S/N	HEAVY-METALS	PERMISSIVE LIMITS OF DRINKING WATER QUALITY (µg/L)		HEALTH HAZARD
		WHO	USEPA	
1	Arsenic	10	50	Carcinogenic (skin, lung, bladder, kidney and liver cancer), neurological, respiratory effects
2	Cadmium	3	5	Lung damage, carcinogenic, kidney, lung and bone disease
3	Chromium	50	100	Carcinogenic, severe cardiovascular, respiratory, hematological and neurological effects
4	Copper		- 1300	Cellular damage leading to Wilson disease, nose, mouth and eyes irritation, headache, dizziness
5	Lead	10	5	Damage to central nervous system, kidneys, liver, endocrine and reproductive system,
6	Mercury	1	2	Carcinogenic, corrosive to skin, eyes, and muscle, neurological change
7	Zinc		- -	Acute intoxication, lethargy, anemia and dizziness

2.4 Methods of Treating Heavy Metals

Generally, the technique employed for heavy metals removal include; precipitation, membrane filtration, ion exchange, adsorption, electrodepositing, reverse osmosis. Chemical precipitation requires a large amount of chemicals to reduce metals to an acceptable level for discharge. Other drawbacks are its excessive sludge production that requires further treatment, slow metal precipitation, poor settling, the aggregation of metal precipitates and the long-term environmental impacts of sludge disposal (Barakat, 2011).

Ion exchange is another method used successfully in the industry for the removal of heavy metals from effluent. An ion exchanger is a solid capable of exchanging either cations or anions from the surrounding materials. Commonly used matrices for ion exchange are synthetic organic ion exchange resins. The disadvantage of this method is that it cannot handle concentrated metal solution as organics and other solids in the wastewater easily foul the matrix. Moreover, ion exchange is nonselective and is highly sensitive to the pH of the solution (Aziz *et al.*, 2008).

Electrolytic recovery or electro-winning is one of the many technologies used to remove metals from process water streams. This process uses electricity to pass a current through an aqueous metal-bearing solution containing a cathode plate and an insoluble anode. Positively charged metallic ions cling to the negatively charged cathodes leaving behind a metal deposit that is strippable and recoverable. A noticeable disadvantage was that corrosion could become a significant limiting factor, where electrodes would frequently have to be replaced (Kurniawan *et al.*, 2006).

2.5 Adsorption Process

Adsorption is used to remove individual components from a gas or liquid mixture. The component to be removed is physically or chemically bonded to a solid surface. The solid is referred to as adsorbent and the adsorbed component as the adsorbate. Adsorption method is relatively low-cost process and certain advantages over conventional methods, which include minimized chemical and biological sludge, low-cost, high efficiency, and regeneration of adsorbents and possibility of metal recovery (Renu and Singh, 2017).

Adsorption is a spontaneous process where forces of attraction exist between adsorbent and adsorbate. Based on surface interaction, adsorption is divided in four types: ion

exchange, physisorption, chemisorption, and specific adsorption. Ion exchange adsorption involves an attachment of ionic species to the opposite charge at the surface of an adsorbent (Weber Jr., 1985). Physisorption occurs when van der Waals forces are involved, this type of adsorption has the characteristics of low enthalpy (less than 80 kJ/mol), it can be monolayer (unimolecular) or multilayer adsorption, there is no dissociation of adsorbed species, and decreasing adsorption capacity with increasing temperature in physical adsorption (Ruthven, 1984). On the contrary, chemisorption involves chemical forces or bonding between adsorbent and adsorbate that resulting in a change in the chemical form of adsorbate. Due to its strong interaction, chemisorption has high enthalpy (80 to 800 kJ/mol), adsorption occurs at monolayer only, and involves dissociation of adsorbed species (Ruthven *et al.*, 1984). Specific adsorption is resulted from specific interaction between adsorbate molecules and adsorbent, which do not result in chemical change of adsorbate. This type of adsorption has binding energy value in between those of physisorption and chemisorption (Putro, 2017).

To understand the mechanism of an adsorption process, usually it can be conducted with either isotherm or kinetic point of view. There are three types of adsorption isotherms for a solid-liquid system: type I (favorable), type II (linear), and type III (unfavorable). For favorable adsorption isotherm, adsorption normally occurs on microporous adsorbents where pore size is not greater than the molecular diameter of the adsorbate (Ruthven, 1984). Type II shows linear isotherm at low concentration, this type is well known as the classical Langmuir form (Basmadjian, 1997), and type III is commonly observed for a wide range of adsorbents pore size (Ruthven, 1984).

Adsorption is influenced by adsorbate-solvent properties, system properties, and adsorbent properties. For adsorbate-solvent properties, it can be shown in the form of

solubility. If the adsorbate molecule has high solubility in water, then adsorption removal will decrease. System properties such as pH can give major influences on adsorption mechanism. In many published works, the authors always studied the effect of pH since in some pH the adsorbent can either be protonated or deprotonated. Adsorbent properties are usually referred to surface area and the distribution of area with respect to pore size as a primary determinant in adsorption capacity (Weber Jr., 1985). Adsorption occurs in three consecutives step: bulk diffusion, external diffusion, and intraparticle diffusion. Bulk diffusion is usually rapid due to the effect of mixing. External diffusion concerns about the diffusion of adsorbate molecule through a hydrodynamic boundary layer. Then adsorbate molecules diffuse to the active sites of adsorbent, where this step is called intraparticle diffusion. Usually, the rate limiting step lays on the second step where it controls the diffusion of solute through boundary layer to the external surface of adsorbent (Weber Jr., 1985).

2.5.1 Types of adsorption

Depending upon the nature of force existing between adsorbate molecule and adsorbent, types of adsorption can be distinguished

Physical adsorption (Physiosorption): Dawood and Sen (2014) define this type of adsorption as the effect of intermolecular attraction between the adsorbent and the adsorbate. Whereby the adsorbate bond itself to the adsorbent surface through intermolecular interactions such as; hydrogen bonding, hydrophobicity polarity, static interactions, dipole-dipole interactions and Van der Waals forces which are all considered weak bonds. Physical adsorption is an easily reversible process and that this reversibility is for the recovery of substances, or some fractions of the substance for recycle.

Chemical adsorption (Chemisorption): Amari (2018) defines this type of adsorption as a contact between the adsorbate and the adsorbent in which the adsorbate molecules bond to the adsorbent surface through the formation of a chemical type of bond, which involves the exchange of electrons. The amount of heat released and adhesive forces here are greater than in the physical. Unlike the other type, chemisorption is not mostly reversible, and substances under high temperature undergo chemisorptions more than low temperature substances, but in some cases low temperature substances too under this kind of adsorption. In catalysis, chemisorption is of specific significance in catalysis.

2.5.2 Adsorption isotherm

According to Putro, (2017) in order to obtain proper design of an adsorption process, reliable adsorption equilibriums data are required. Adsorption equilibria can be represented in mathematical form called adsorption isotherm. Various adsorption models are available to represent the liquid phase adsorption equilibria, and the most widely used models are Langmuir and Freundlich.

Langmuir model was originally developed to describe monolayer surface adsorption on flat surface based on a kinetic viewpoint. The model assumes that the rate of adsorption equals to the rate of desorption from flat surface. Langmuir is the simplest theoretical adsorption model. Three assumptions were used to develop this model:

i. Energy of adsorption is constant over all adsorption sites due to surface homogeneity.
ii. Adsorption occurs on definite sites on adsorbent surface (adsorption on homogeneous surface is localized).

iii. Adsorption energy is the same at all sites, and each active adsorption site only accommodates one molecule of adsorbate.

According to Olorundare (2017), by applying these assumptions and kinetic principle, the Langmuir Equation is expressed as

$$q_e = q_{max}\left(\frac{K_L C_e}{1+K_L C_e}\right) \quad (2.1)$$

Equation 3.1 can also be written in linearized form as outlined in Equation 2.2-2.3

$$\frac{1}{q_e} = \left(\frac{1}{K_L Q_m}\right)\frac{1}{C_e} + \left(\frac{1}{Q_m}\right) \quad (2.2)$$

Where C_e is the equilibrium concentration$\left(\frac{mg}{L}\right)$, q_m the amount adsorbed at equilibrum$\left(\frac{mg}{g}\right)$. $Q_o$and b is the Langmuir constants related to the model.

Temkin and Pyzhev suggested that, because of the existence of adsorbent–adsorbate interactions, the heat of adsorption should decrease linearly with the surface coverage (Awala and El Jamal, 2011).

The corresponding adsorption isotherm can thus be adjusted by Equation 2.3:

$$Qe = B * lnA + B\ln(Ce) \quad (2.3)$$

where B is related to the heat of adsorption (L/g), and A is the dimensionless Temkin isotherm constant.

2.6 Materials used for adsorption process

2.6.1. Sugarcane (Saccharum officinarum)

Sugarcane is a tall perennial plant that belong s to the grace family, which has fibrous stalks that are rich in sugar, and measure two to six meters (6-9 ft.) (Mugure, 2014). Sugarcane is one of the most important crops in the word because of its strategic position and immense uses in the daily life of any nation as well as for industrial uses aimed at nutritional and economic sustenance. Sugarcane contributes about 60% of the total world sugar requirement while the remaining 40% came from sugar beet. It is a tropical crop that usually takes between 8 and 12 months to reach its maturity, it can be green, purplish, yellow or reddish when ripe and sugar content is at its peak (Sulaiman *et al.*, 2015). Current taxonomy divides sugarcane into six species, two of which are wild and always recognized (*Saccharum spontaneum* L. and *Saccharumrobustum* Brandes and Jewist ex Grassl). The other species are cultivated and classified variously. Of the four domesticated species of sugarcane, S.*officinarum* L. was first named and is the primary species for production of sugar (Moore, *et al., 2014*).

World population of sugarcane stood at 1.5 billion tonnes, Brazil, China, Cuba, Mexico, Pakistan, Thailand, USA, Colombia, Australia and Indonesia are the leading countries in sugarcane production, Africa countries like Mauritius, Kenya, Sudan, Zimbabwe, Madagascar, Cote dlvoire, Ethiopia, Malawi, Zambia, Tanzania, Nigeria, Cameroon and Zaire (Sulaiman *et al., 2015*).

Sugarcane was first introduced in Nigeria by the European sailors in the 15th century through the eastern and western coasts. Sugarcane was primarily cultivated for making juice and preparing of feeds for animals. Sugarcane is the raw material used for

manufacturing sugar in Nigeria, which accounts for about 61% of the total sugar production (Nmadu *et al.,* 2013). Nigeria's first sugarcane bio-refinery was established in Zaira in 2015. Despite the plans to increase sugarcane production in Nigeria, strategies to manage the residues such as straw and bagasse are not in place (1 ton of sugarcane generates about 270 kilos of bagasse) (Mohala *et al.*, 2016). Two types of sugarcane are grown in Nigeria – industrial and soft (chewing) cane. The industrial is the hard or tough type generally processed into sugar by the sugar estates. The soft cane is mainly chewed raw for its sweet juice. The exact total land area currently under cane cultivation and total production in Nigeria is not known, but it is estimated at 25,000-35,000 hectare, out of which soft cane covers 18,000 hectares (Nmadu *et al.,* 2013).

2.6.2 Sugarcane bagasse (SCB)

Sugarcane bagasse (*Saccharum officinarum L.*) is a fibrous residue originated from sugarcane after the crushing of the cane stalk and its juice extraction. Structurally, sugarcane is composed of an outer rind and inner pith. The majority of sucrose together with bundles of small fibres are found in the inner pith. The outer rind contains longer and finner fibers, in a random arrangement throughout the stem and bound together by lignin and hemicelluloses (Ullah *et al.*, 2013).

Sugarcane is as the potential to become an important raw material for applications ranging from animal feed, enzymes, paper and biofuel conversion (Pereira *et al.*, 2011; Chemienez *et al.,* 2013). SCB consist of cellulose 43.8%, hemicellulose 28.6%, lignin 23.5%, ash 1.3 % and other components 2.8% (Kumar *et al.,* 2013). The cellulose, hemicellulose, lignin, rind, comrind, pith and ash are the components of SCB wastes that

are being used in production of composites, additives in concrete manufacturing and ceramic refractory products (Loh *et al.,* 2013).

2.6.3 Cellulose

In 1838, AnselmePayen a French chemist while studying different types of wood, obtained a substance which could be broken down into basic units of glucose just as starch and he called it cellulose because it was obtained from cell walls of plants. It consists of long chains of anhydro-D-glucopyranose units (AGU) with each cellulose molecules have three hydroxyl groups per AGU, with the exception of the terminal ends (Lavanya *et al.*, 2011).

According to Zaini *et al* (2013) Cellulose is the most abundant bio-renewable material on earth. It is an infinite source of raw material for environmentally friendly and bi-composite products. The yearly biomass production of cellulose has been estimated at about 1.5 million tons (Klemm *et al.*, 2005).

Figure 2.1 shows the sorption of various pollutants using SCB and its derivatives. The modification of sugarcane bagasse is done through mechanical, chemical, magnetic and immobilization.

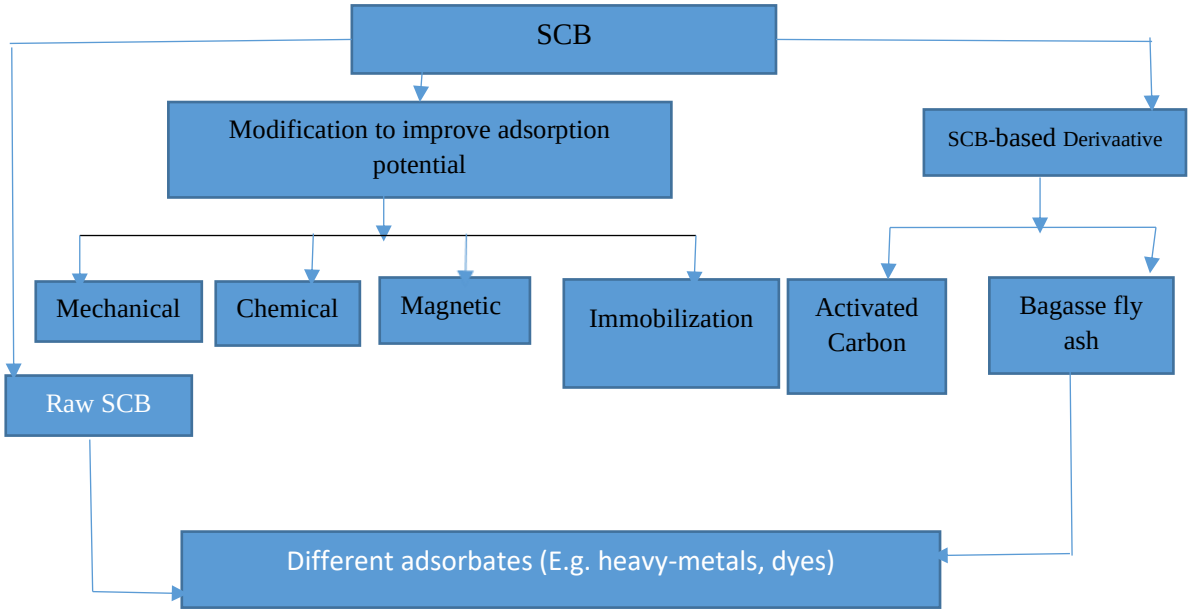

Figure 2.1: Sorption of various pollutants using SCB and its derivatives (Sarker, *et al.*, 2017).

2.6.4 Sugarcane bagasse as adsorbent

Various treatment methods are currently used to eliminate organic pollutants from wastewater, including flocculation, coagulation, biological oxidation, sedimentation, photo -Fenton treatment, advanced oxidation processes, chemical degradation, chemical oxidation, incineration, wet oxidation, reverse osmosis, solvent extraction and adsorption (Duran *et al.*, 2011, Salman *et al.*, 2011, Joseph *et al.*, 2011). Adsorption by agro-industrial residues has again been proven to be one of the best processes available for the elimination of organic pollutants, because of its universal nature, ease of operation, flexibility, and insensitivity of organic pollutants, as well as its high efficiency and efficacy. Moreover, this process can eliminate both solute and insoluble pollutants without generating hazardous by-products (Ali *et al.*, 2012).

SCB possesses several unique binding site, including carboxylic, carbonyl, amine, and hydroxyl groups, which make raw and modified sugarcane bagasse and its derivatives proficient in the adsorption of a variety of hazardous materials. Recently the function of SCB as a heavy-metals adsorbent had been investigated due to the increase attention of using agricultural waste as adsorption materials, because of the advantages of it being inexpensive, large supply quantities and high regeneration (Khoo *et al.,* 2018). The adsorption potential of adsorbents depends on their chemical nature, as well as different physicochemical experimental conditions including the solution pH, initial concentration of the pollutant, adsorbent dosage, and the contact time of the system (Sark *et al.*, 2017).

In recent decades, sugarcane bagasse and its derivatives have been successfully tested for use in the removal of a variety of hazardous materials. It has been utilized as a potential biosorbent in three main forms: (1) raw bagasse, (2) bagasse fly ash, and (3) bagasse-based activated carbon. Raw sug-arcane bagasse is a well-studied biosorbent used to remove pollutants (Alomá *et al*. 2012) without the need for other chemicals or physical treatments (Moubarik and Grimi 2015) and is therefore particularly environmentally friendly. Modified sugarcane bagasse can also be effective; for example, Raghuvanshi *et al*. (2004) found that dye removal was faster and more efective using chemically activated sugarcane bagasse compared with the raw bagasse.

Sugarcane bagasse-based activated carbon and bagasse fly ash are also effective adsorbents, able to eliminate various types of pollutants including metals (Tao *et al*. 2015), dyes (Amin 2008), phenolic compounds (Akl *et al*. 2014), and herbicides and pesticides (Deokar *et al*. 2016) from aqueous solution. It was reported that bagasse fy ash can remove up to 96% of diferent heavy metals ions from an aqueous solu-tion in optimum conditions (Gupta and Ali 2004). Abdelhafez and Li (2016) employed

sugarcane bagasse biochar and orange peel biochar for Pb (II) removal, reporting that the sugarcane-derived biochar was more efcient (86.96 mg g−1) than the orange peel biochar (27.86 mg g−1) in the elimina-tion of these ions. Contrasting results were found by Adamu and Ahmadu (2015), however, who reported that activated carbon prepared from sugarcane bagasse is less efcient at adsorbing heavy metal ions from wastewater than activated carbon prepared from Parkia biglobosa(locust bean) pods. However, biochar is a well-studied biosorbent; its utilization is sometimes restricted because of its higher cost (Sark *et al.*, 2017).

2.7 Biosorption

Biosorption is the passive sorption of organic and inorganic substances in soluble or insoluble forms from an aqueous solution using dead biological materials. Biosorption is distinct from bio-accumulation, which is the active, metabolically driven accumulation of metals and other substances by living organisms. Biosorption is highly effective compared to bio-treatmentprocesses, (Fomina and Gadd, 2014), reducing concentration of pollutant ions to very low levels, and in a few cases removing them altogether, through the employment of low-cost bisorbent materials (Moubarik and Grimi, 2015). Factors such as bisorbent dosage, initial pollution concentration, solution pH and temperature, contact time, and sorbent particle size significantly influence sorption processes and their potential. Biosorption involves two phases, a solid phase (sorbent) and a liquid phase (solvent) containing a dissolved species to be sorbed. Pollutant ion species often have very high sorbent afnities and are bound together by particularly complex processes that must be overcome by the biosorption process. The principal mechanisms in the adsorp-tion of metals and dyes by cellulosic biosorbents are ion exchange, chelation and complexation with the functional groups on the surface of the sorbent, and the release of

H_3O into the synthetic aqueous solution. Ion exchange takes place because of the electrostatic interaction between positive cati-ons and the negatively charged groups in the biosorbent. Biosorption mechanisms can be varied, but are predictable with an understanding of the sorbent surface structure and its associated functional groups, which can be determined using thermodynamic and kinetic studies, as well as combinations of Fourier transform infrared spectros-copy, scanning electron microscopy, transmission electron microscopy, X-ray photoelectron spectroscopy, and several traditional methods such as titration and the chemical blocking of functional groups (Witek-Krowiak 2012).

2.8 Activated Carbon

The term of activated carbon is come from the word “carbon” and “active” which meant a raw material undergoes a carbonization process (burning in high temperature) while active meant a material in carbon condition undergoes an activation process to open a pore surface area as a maximum as can to increase adsorption rate of activated carbon (Khadijah *et al.,* 2012).

Activated carbon is defined as a carbonaceous material with a large internal surface area and highly developed porous structure resulting from the processing of raw materials under high temperature reactions. It is composed of 87% to 97% carbon but also contains other elements depending on the processing method used and raw material it is derived from. Activated carbon’s porous structure allows it to adsorb materials from the liquid and gas phase. Its pore volume typically ranges from 0.20 to 0.60 cm^3/g, and has been found to be as large as 1 cm^3/g. Its surface area ranges typically from 800 to 1500 m^2/g but has been found to be in excess of 3,000 m^2/g. The surface area contains mostly micropores with pore diameter smaller than 2 nm. These favourable properties make

activated carbon a popular adsorbent for many applications (Leimkuehler and Suppes, 2010).

In some of the earliest recorded examples of adsorption, activated carbon was used as the adsorbent. Naturally, occurring carbonaceous materials such as coal, wood, coconut shells or bones are decomposed in an inert atmosphere at a temperature of about 800 K. Because the product will not be porous, it needs additional treatment or activation to generate a system of fine pores. The carbon maybe produced in the activated state by treating the raw material with chemicals, such as zinc chloride or phosphoric acid, before carbonizing. Alternatively, the carbon from the carbonizing stage may be selectively oxidized at temperatures in excess of 1000 K in atmosphere of materials of materials such as steam or carbon dioxide (Richardon, *et al.,* 2002).

2.9 Methods of Activated Carbon Production

According to Tadda *et al.,* (2016) generation of activated carbon can be classified into pyrolysis process, physical activation, and chemical activation process and carbonization and steam/thermal activation.

2.9.1 Pyrolysis process:

Thermochemical conversion of organic biomass into gaseous or/and liquid fuels at extremely high temperature in the presence of halogen (mainly oxygen) is termed *pyrolysis*. Pyrolysis is a simultaneous process that changes both the chemical composition and physical phase of materials and is irreversible. Pyrolysis process is mostly observed when materials are exposed to higher temperature. Some features of pyrolysis such as temperature has the most significant effect and then followed by retention time, eating rate and nitrogen flow rate. Normally, when the reaction temperature increases, it causes

reduction in both activated carbon and char production, while at the sme time the pyrolysis temperature leads to a drop off of solid yield and an increase in both gases and liquid percentages yield. On the other hand, raising the temperature leads to raised ash and activated carbon percentage, whereas the volatile matter gets reduced. Therefore, activated carbon with greater quality is obtained at a higher temperature (Renu *et al.*, 2017).

2.9.2 Physical activation process:

This is a two-step process. Carbonization of carbonaceous materials comes first, then activation of the resulting char at high temperature in the presence of CO_2, steam, air or three mixture serving as oxidizing gases. The $CO_2$is usualy used as activating gas being easy to handle, clean and possesses a slow reaction rate at a temperature around 800^{o}C, which facilitates control of the activation process. A temperature of 400^{o}C - 850^{o}C was found to be the carbonization temperature, though it may sometimes reach up to 1000^{o}C while activation temperature between 600^{o}C and 900 ^{o}C (Tadda *et al.*, 2016)

2.9.3 Chemical activation process:

In the chemical activation process, involves multiple two steps occurring simultaneously, with the chemical activating agents mixing with the precursor, as oxidants and dehydrates. Performing activation and carbonization simultaneously during the chemical activation process at lower temperature results in having better porous structures of AC, even though, concern about environmental protection may limit the use of chemical agents for activation. Moreover, some chemicals that are widely used as activating agents are zinc chloride ($ZnCl_2$), potassium hydroxide (KOH), trihydroxidooxidophosphorus, phosphoric acid (H_3PO_4) and potassium carbonate (K_2CO_3). Whereas the agricultural

wastes that are being reduced with the earlier mentioned chemicals consist of; olive seed, apricot stones, macadamia, pecan-shells, peanut-hulls, nut-shells, almondshells, corn-cob, hazelnut shells, rice husks, rice straw and cassava peel (Tadda *et al.,* 2016).

2.10 The Nature of Adsorbents

The following are the features of adsorbent to be attractive commercially as stated by Coulson and Richardson, (2002).

i. It should have a large internal surface area
ii. The area should be accessible through pores big enough to admit the molecules to
iii. be adsorbed. It is a bonus if the pores are also enough to exclude molecules which it is desired not to adsorb.
iv. The adsorbent should be capable of being easily regenerated.
v. The adsorbent should not age rapidly, that is lose its adsorptive capacity through continual recycling
vi. The adsorbent should be mechanically strong enough to withstand the bulk handling and vibration that are a feature of any industrial unit.

The summary of summary literature reviewed is listed in the table 2.2. Sugarcane bagasse was used as adsorbent to remove different heavy metals and the adsorption capacity was stated with their references.

Table 2.2: Summary of Related Work on SCB

S/N	HEAVY-METALS	SCB ADSORBENT	CAPACITY ADSORPTION (mg/g)	REFERENCES
1	Pb(II)	Natural SCB	21.28	Putra *et al.,* (2014)
2	Pb(II)	Natural SCB	8.288 (0.04 mmol/g)	Yu *et al.,* (2013)
3	Pb(II)	Magnetic modified SCB	2468.4 (1.2 mmol/g)	Yu *et al.,* (2013)
4	Zn (II)	Natural SCB	40.0	Putra *et al.,* (2014)
5	As (V)	Hydrous ferric oxide treated	22.1	Pehlivan *et al.,* (2013)
6	Co (II)	Caroxlyated functionalized	67.18 (1.140 mmol/g)	Ramos *et al.,* (2015)
7	Co (II)	Phthalate-functionalized SCB	33.06 (0.561mmol/g)	Ramos *et al.,* (2016)
8	Hg (II)	Natural and chemically modified	35.71	Khoramzadeh*et al.,* (2013)
9	Ni (II)	Caroxlyated functionalized	91.74 (1.563 mmol/g)	Ramos *et al.,* (2015)
10	Ni (II)	Phthalate-functionalized SCB	54.70 (0.932mmol/g)	Ramos *et al.,* (2016)
11	Ni (II)	Bagasse powder (<1 mm)	2.0	Aloma *et al.,* (2012)
12	Ni (II)	NaOH	12.76	Tchoumou *et al.,* 2015
13	Cu (II)	Nitric acid Modified	31.53	Dos Santos *et al.,* (2012)
14	Cu (II)	HCL	16.98	Tchoumou*et al.,* 2015
15	Cu (II)	NaOH	24.57	Tchoumou*et al.,* 2015
16	Cr (VI)	Con H_2SO_4	131.68	Bahadur and Paramatma, 2014
17	Ni (II)	Activated Carbon	140.85	Krishman, *et al.,* 2011

2.11 Optimization

Optimization is the use of specific method to determine the most cost-effective and efficient solution to a problem or design for a process. A wide variety of problems in the design, construction, operation, and analysis of chemical plants and other industrial processes can be solved by optimization. Optimization is concerned with selecting the best among the entire set by efficient quantitative methods. Computers and associated

software make the necessary computations feasible and cost effective. To obtain useful information using computers, however, requires critical analysis of the process or design, insight about what the appropriate performance objectives are (i.e., what is to be accomplished), and use of past experience, sometimes called engineering judgement (Edgar *et al.,* 2001).

2.12 Response Surface Methodology

Response Surface Methodology (RSM) is a collection of mathematical and statistical techniques useful for analysing problems where several independent variables influence a dependent variable or response, and the goal is to optimize this response. The independent variables are denoted by x_1, x_2, x_3 ….x_k. It is assumed that these variables are continuous and controllable by the experimenter with negligible error. The response, 'y' is assumed to a random variable. RSM is used for design and analysis of experiments, it seeks to relate an average response to the value of quantitative variables that effect response Trans *et al.,* (2017). RSM answers different kind of questions, such as the following.

a) How is a particular response affected by a given set of input variables over some specified region of interest?
b) To what level the inputs are to be controlled, to give a product, simultaneously satisfying desired specification?
c) What values of inputs will yield a maximum for a specific response, and what is the nature of response surface close to the maximum? (Pehlivan *et al.,* 2013)

The relationship between the dependent variable and independent variables can be represented as

$y = f(x_1, x_2, x_3 \ldots xk) + \varepsilon$ (2.4)

Where ε represents the noise or error observed in the response 'y'

If the response is well modelled by a linear function of the independent variable, then the approximating function is the first-order model.

$$\eta = \beta 0x0 + \beta 1x1 + \beta 2x2 + \ldots . \beta kxk \qquad (\mathbf{2.5})$$

If there is curvature in the system, then a polynomial of higher degree must be used, such as second-order model.

Almost all RSM problems use one or both of these models. Of course, it is unlikely that a polynomial model will be a reasonable approximation of the true functional relationship over the entire space of the independent variable, but for relative small region they usually work.

CHAPTER THREE

3.0 MATERIALS AND METHODS

This chapter contains a list of materials, chemicals, equipment, as well as methods used during the experiment.

3.1 Materials

The major feedstock used in this research work was sugarcane bagasse obtained from Kasuwan Gwari Market, Minna, Niger State, Nigeria. Table 3.1 summarized the properties of chemical used, while the list of equipment and materials used are represented in Table 3.2 and 3.3 respectively.

3.2 List of Chemicals

The list of chemicals used in this research work with their purity, manufacturer and where they were sourced are shown in Table 3.1

Table 3.1: List of Chemicals Used In This Research Work

S/N	Chemicals	Purity	Manufacturer	Source
1	Ortho-phosphoric acid	85%	BHD	Chemical Eng'g Depart, FUT, Minna
2	Sodium Hydroxide Pellet	99%	Avondale	Chemical Eng'g Depart, FUT, Minna
3	Distilled Water			WAFT
4	Hydrochloric acid	99%	JHD	WAFT
5	Buffer solution			WAFT

*****WAFT: Water and Fisheries Technology Department, FUT, Minna

3.3 List of Equipment

The list of equipment used in this research work with their model, manufacturer and their location are shown in Table 3.2.

Table 3.2: List of Equipment, Manufacturer and Sources

S/N	Equipment	Manufacturer	Model	Location
1	Electric Water Bath and Shaker	LabTech	-	Chemical Eng'g FUT, Minna
2	Electric Oven	GAllenkamp	GB36SR	WAFT
3	Kitchen Electric Blender	Kenwood	BL330	-
5	Muffle Furnace	Gallenkamp	OH85TR	WAFT
6	pH meter	REX	pH 25	WAFT
7	X-ray diffraction (XRD) Machine	Empyrean	DY 674	Nigeria Geographical & Survey Agency, Kaduna
8	Digital Weighing Balance Machine	OHAUS	E11140	Chemical Eng'g, FUT, Minna
9	Brunauer-Emmett-Teller (BET) Machine	NOVA	2400	STEP-B

*****WAFT: Water and Fisheries Technology Department, FUT, Minna

3.4 List of Materials

The list of materials used in this research work with their model, manufacturer and their location are shown in Table 3.3.

Table 3.3: List of Materials, Description, Manufacturer and Sources

S/N	Materials	Description	Manufacturer	Sources
1	Desiccator	Glass		WAFT
2	Crucibles	Ceramic		WAFT
3	Tong	Metal		WAFT
4	Sieves	Metal		WAFT
5	250 mL beaker	Glass	Pyrex England	Chemical Eng'g Lab, Futminna
6	1000 mL beaker	Glass	Pyrex England	Chemical Eng'g Lab, Futminna
7	100 mL measuring cylinder	Glass	Pyrex England	Chemical Eng'g Lab, Futminna
8	100 mL Conical flask	Glass	G.G- 17	
9	Funnel	Glass		Chemical Eng'g Lab, Futminna
10	Filter Paper		Whatman (15 cm)	Panlac, Minna
11	Air-tight containers	Plastic	Seward	Panlac, Minna

*****WAFT: Water and Fisheries Technology Department, FUT, Minna

3.5 Research Methodology

Figure 3.1 summarizes the experimental procedure that was used in the production of activated carbon from sugarcane bagasse for the removal of industrial effluent

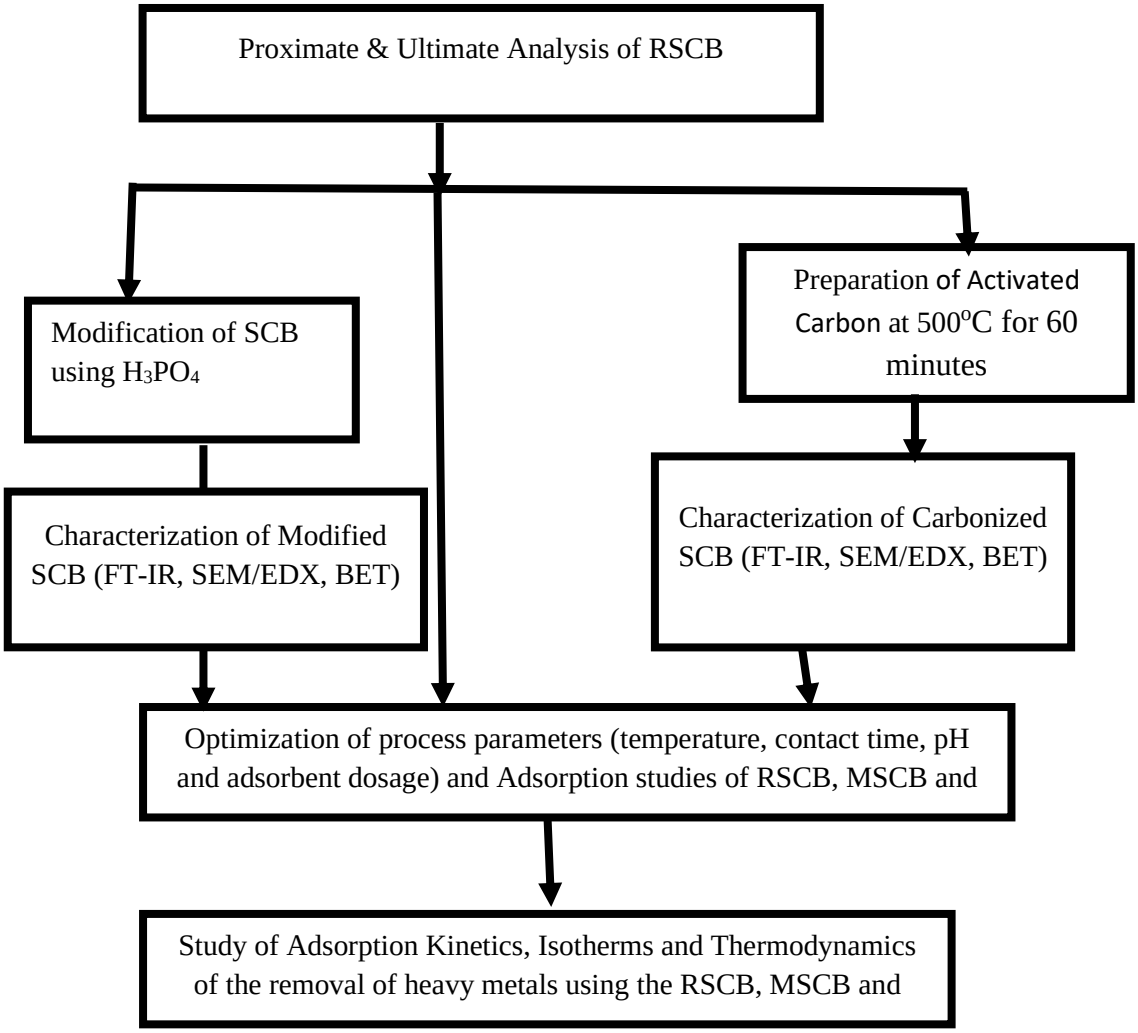

Figure 3.1: Block flow diagram of the procedure involved in the methodology of this research

3.6 Sourcing and Preparation of the Raw Sample

The sugarcane bagasse (SCB) was sourced in Minna and all chemicals that were used in this study were of analytical grade. The effluent was obtained from an electroplating section of the Scientific Equipment Development Institute (SEDI). SCB was washed to remove trapped contaminants. The effluent was gotten from an electroplating unit of an industry. The bagasse was dried in the oven for 24 hrs at 90^{o}C. The dried sample was ground using electric blender and was sieved to pass through 200 mesh (U.S standard) to obtain a more homogenous size of 74 µm and then stored at room temperature in airtight container for further study (Giusto *et al.,* 2017).

3.7 Proximate Analysis

The proximate and ultimate analysis of the raw SCB to determine the moisture content, volatiles, ash content, hydrogen content, carbon content, oxygen content of the RSCB

3.7.1 Moisture content determination

This was done to determine the amount of water present in the snail shell powder. The analysis was carried out in accordance with ASTM D2709. One gram (1 g) of SCB was added to the petri-dish and spread uniformly upon the surface of the petri-dish and the weight were taken and recorded. The prepared specimen was kept in the oven at 105ºC for a time period of 1 hr 30 min after which, it was placed in a desiccator for 15 min and then the new weight was taken.. The moisture content was computed using Equation 3.1

$$\%M_c = \frac{\text{weight of RSCB before drying (g)} - \text{dry weight of RSCB(g)}}{w\text{weight of RSCB before drying}(g)} * 100 \qquad (3.1)$$

3.7.2 Ash content determination

In accordance to American Standard Test Method (ASTM) E1755 for ash in biomass, about 1.0 g of dried SCB sample was measured into an empty crucible of known weight. SCB sample and the crucible was ignited in the furnace at 600ºC for 1 hr 30 min. The crucible was removed and placed in the desiccator. The SCB sample was weighed after cooled to room temperature. The ash content (A_c) value was calculated using Equation 3.2

$$\%A_c = \frac{ash\ weight(g)}{sample\ weight(g)} * 100 \qquad (3.2)$$

3.7.3 Volatile matter content determination

The volatile content was determined in accordance with American Standard Test Method (ASTM) E872 as reported by Aragaw (2016). About 2g of the sample was weighed and put into a crucible and transferred into the furnace and left for 8 min at 600°C. After which the crucible was placed in the desiccator and allowed to cool to room temperature and weighed. Equation 3.3 was used to compute the volatile content.

$$\%V_c = \frac{sample \text{ mass before heating(g)} - sample \text{ mass after heating(g)}}{\text{mass of sample before heating (g)}} * 100 \qquad (3.3)$$

3.7.4 Fixed carbon content determination

The fixed carbon value, was determined by subtracting the sum of percentage compositions of moisture content, volatile matter content, and ash content from 100 (Aragaw, 2016).

3.8 Ultimate Analysis

The ultimate analysis includes determination of elements in the sugarcane bagasse such as carbon, hydrogen, and nitrogen (ASTM D5373-13: 2013) and oxygen (ASTM D3176: 1990) as reported by Winarno *et al.,* (2018).

3.8.1 Determination of carbon, hydrogen and nitrogen

The analysis was done by preparing a raw sugarcane bagasse with a weight of 1 g. Carbon, hydrogen and nitrogen in the RSCB sample were sought simultaneously in an instrumental procedure using furnaces operating at temperatures in the range of 900°C - 1050°C. Conversion of carbon, hydrogen and nitrogen values into the corresponding gases (CO_2, H_2O, and NO_x) occured during sample combustion at high temperatures in the presence of oxygen gas. Combustion results that interfered with gas analyses were subsequently discarded. The nitrogen oxide (NO_x) was converted to N_2 before it was analyzed. Carbon dioxide, moisture and nitrogen elements in the gas stream were determined by appropriate analytical procedures. The total carbon, hydrogen and nitrogen deposited were recorded as a percentage of mass according to ASTM D5373-13: 2013.

3.8.2 Determination of oxygen

Determination of oxygen content was not done directly, but determined based on the difference of carbon, hydrogen, nitrogen, sulphur, and ash content. The percentage of oxygen content was obtained from the calculation of 100% – (% C + % H + % N + % ash) (ASTM D3176).

3.9 Thermo-Gravimetric Analysis (TGA) analysis

The TGA curve of the raw sample was obtained by using PerkinElmer TGA 4000 instrument. The preliminary thermal behaviour of the sugarcane bagasse was obtained by recording the TGA curves in the range of 30 to 900^{o}C under conditions of nitrogen atmosphere using weighed samples of about 13 mg at 10^{o}C /min. Data generated were .captured and reported accordingly (Pereira *et al.*, 2011).

3.10 Preparation of H_3PO_4 Modified SCB Sample (MSCB)

About 10 g of SCB was impregnated with H_3PO_4 (10, 20, 30, 40, 50 %). The impregnation ratio of acid to precursor was 2:1 (Castro *et al.,* 2000 and ALOthman *et al.,* 2013) then stirred for 30 minutes and left for 24 hrs. The purpose of treating the carbon with acid was to create a suiTable environment for its ring opening which increase the number of adsorption site. The sample was then washed with hot water up to a pH of about 6.7 to remove excess undiluted ortho-phosphoric acid and dried in the oven at 90 ^{o}C for 24 hrs, this was labelled modified SCB. The samples were then characterized.

3.11 Preparation of Sugarcane Based Activated Carbon using H_3PO_4

As reported by Adib *et al.,* (2015) the Sugarcane bagasse was impregnated with H_3PO_4 for 24 hrs. The impregnation ratio of acid to precursor was 2:1 (Castro *et al.,* 2000). After impregnation for 24 hrs, the sample was carbonized at different temperatures of 400, 450, 500, 550 and 600^{o}C according to the TGA for various time (40, 60, 80 and 100 minutes) in order to establish optimum conditions (Gin *et al.,* 2014). The sample was then washed with hot water to remove excess undiluted ortho-phosphoric acid and dried in the oven at 90^{o}C for 24 hrs.

3.12 Characterizations of the RSCB, MSCB and SCBAC

The RSCB, MSCB and SCBAC samples were characterized.

3.12.1 Fourier Transform Infra-Red Spectroscopy (FT-IR) analysis

This was carried out according to the method by Chao *et al*., (2014), the FT-IR spectra was recorded using the Nicolet 6700 spectrophotometer instrument and the result was obtained by feeding the dry samples (RSCB, MSCB, and SCBAC) into an impact 360 FT-IR spectrometer under dry air at room temperature using KBr pellets.

3.12.2 Scanning Electron Microscopy (SEM) analysis

The morphological characteristics of the RSCB, MSCB and SCBAC was examined by scanning electronic microscopy (SEM) according to the method of Kolawole *et al.,* (2017) where the ASPEX 3020 scanning electron microscope machine was operated at an accelerated voltage of 5 to 15 kV and this electron gets narrowed after passing through the apertures and electromagnetic lenses. SEM micrographs of the surfaces of samples were taken using SEM ASPEX 3020 to observe the surface morphologies. A thin layer of gold was coated on the specimens prior to measurement to prevent electrical charge accumulation on the surface during the examination.

3.12.3 Brunauer-Emmett-Teller (BET) analysis

This was carried out according to the method by Akl *et al.,* (2014) where the BET surface area measurement of the samples (RSCB, MSCB and SCBAC) using area & size analyzer NOVA 2400e to generate the surface area, pore volume and pore diameter. The BET apparatus analyzed the nitrogen adsorption-desorption isotherm at liquid nitrogen temperature. Out gassing at 77k with equilibrium interval of 10 secs before each

measurement ensured accurate results on all the samples (BET was used to analyze the specific surface, microporous area, microporous volume and pore-size distribution, specific surface respectively).

3.13 Electroplating Wastewater and Characterization

The wastewater sample was collected from the effluent discharge point of electroplating section of the Scientific Equipment Development Institute (SEDI), Niger State. It was carefully bottled in a plastic container and taken to the laboratory for further analyses. For preservation, 5 ml of 2.0 M nitric acid was added per liter of the sample. The sample was refrigerated at approximately 4^{o}C to avoid any heavy metal precipitation and to allow the samples to be kept for further use (Gin, *et al.,* 2014).

3.14 Heavy Metal Analysis

The effluent collected was analyzed for presence of heavy metals (zinc, lead, copper, colbat, cadmium, nickel and chromium) by digesting 100 ml of the effluent using 10ml triple acid mixture (5:1:1 HNO_3: HCl:H_2SO_4) in a 250 ml conical flask placed in a fume cupboard. the samples were covered properly with aluminium foil to avoid spillage and heated on a hot plate until the solution was reduced to 10 ml. the solution was then allowed to cool and it was made up to mark with distilled water before filtering into 50 ml standard flask, labeled for further analysis (Gin *et al.,* 2014). The concentration of the heavy metals in the wastewater was determined using Atomic Absorption Spectrometer (Gin *et al.,* 2014). The AAS technique made use of the wavelengths of light specifically absorbed by an element. The sample was fed into the nebulizer where it was bombard by light waves, the monochroator detects the number of photons emitted and transforms this data into metals concentrations present in the sample (Muriuki, 2015).

3.15 Experimental Design with RSM

The optimization of the removal efficiency of metal by sugarcane bagasse was determined using RSM and Central Composite Design (CCD) as a useful mathematical and statistical technique in evaluating the correlation between independent (x) and response (y) variables through experimental. In this study, contact/contact time, adsorbent dosage, temperature and pH of solution was taken as four independent variables; (x_i) and the percentage removal of heavy metals was the main response (y). The mathematical relationship between the main response 'y' and the set of independent values "x" is established according to the following second-order model Equation (3.10) (Tran *et al.*, 2017)

$$y = f(x) = \beta_o + \sum_{i=1}^{k} \beta_i x_i + \sum_{i=1}^{k} . \sum_{j=1}^{k} \beta_{ij} x_i x_j + \sum_{i=1}^{k} \beta_{ii} x^2{}_i \qquad (3.10)$$

Where y is the predicted response; x_i and x_j are the independent variables (i,j= 1,2,3,4…k).

The independent variables matrix used in the experiment is shown in Table 3.4.

Table 3.4: Independent variables matrix and their encoded levels

S/N	Name	Units	Code	-1level	+1level	-alpha	+alpha
1	Contact time	Minutes	A	40	100	10	130
2	pH		B	4	8	2	10
3	Temperature	^oC	C	30	70	10	90
4	Adsorbent dosage	Grams	D	0.5	1	0.25	1.25

The center variables (encoded 0) were utilized to determine the experimental error and the reproducibility of the data. The margin points including the low (encoded -1), high

(encoded +1) and rotaTable (encoded ±α) levels are manipulated. In addition, CCD matrix for four independent variables (k = 4) enumerates the 2k factorial experiments, 2k axial experiments and six replication experiments as following formula as reported by Tran *et al.,* 2017.

$$N = 2^k + 2k + c = 2^4 + 2(4) + 6 = 30$$

Where N is the number of experiments required for four independent variables (k = 4). The Analysis of variance was calculated using Design-Expert version 13.0.1.0 (DX13).

3.16 Batch Adsorption Experiments

Adsorption experiment was carried by adding raw SCB, modified SCB and SCB activated carbon in a 100 ml conical flask containing 50 mL of industrial effluent solution. The mixture was shaken for at 200 rpm using a water bath shaker. Input factors were investigated including contact time, temperature, adsorbent dosage and pH of the solution (Tran *et al.,* 2017). In other to maintain pH of the solutions, NaOH and HCL were used. After the agitated time, the content of each solution was then filtered. The residual concentrations were confirmed by AAS analysis (Man, 2018).

3.16.3 Determination of removal efficiency

The removal efficiency was calculated with Equation 3.8:

$$Removal\ efficiency\ (\%) = \frac{C_o - C_e}{C_o} \times 100 \qquad (3.8)$$

Where C_o and C_e are the initial and final metal concentration of ions (mg/L), respectively.

3.16.4 Determination of adsorbent capacity

The amount of adsorbed Cr and Zn ions by the adsorbents were determined by using Equation 3.9

$$Adsorbent\ capacity\ (q_e)\ \left(\frac{mg}{g}\right) = \left(\frac{C_o - C_e}{W}\right) V \quad (3.9)$$

Where Ce (mg/L) is the final Cr and Zn ion concentrations, *V* (mL) is the volume of the metal solution, *W* (g) is the weight of the adsorbent, and *d* (g/L) is the dosage of the sugarcane bagasse (Priyadarshini *et al.,* 2018).

3.17 Estimation of the Adsorption Kinetics, Isotherm and Thermodynamics

3.17.1 Adsorption isotherm study

In adsorption process, the study of equilibrium adsorption is the basis for the modeling of an adsorption system. The adsorption capacities of the adsorbent were determined by fitting the experimental results into Langmuir and Temkin isotherm (Adegoke, 2017).

According to Olorundare (2017) the Langmuir isotherm model is given as Equation 3.10

$$\frac{1}{q_e} = \left(\frac{1}{bQ_m}\right)\frac{1}{C_e} + \left(\frac{1}{Q_m}\right) \quad (3.10)$$

Where C_e is the equilibrium concentration$\left(\frac{mg}{L}\right)$, q_e the amount adsorbed at equilibrum$\left(\frac{mg}{g}\right)$. $Q_o$and b is the Langmuir constants related to the model (Bolade & Sangodoyin, 2018). The model assumed that the maximum adsorption occurs when a saturated monolayer of solute molecules is present on the adsorbent surface, the energy of adsorption constant and that there is no migration of adsorbate molecules in the surface plane (Kong *et al.,* 2014)

The equilibrium parameter, R_l Equation 3.12 represents the essential characteristics of Langmuir isotherm (Giusto *et al.,* 2017)

$$R_l = \frac{1}{1 + K_l C_o} \tag{3.11}$$

The linear form of the Temkin isotherm model is represented by the Equation 3.12

$$q_e = \frac{RT}{b} lnA + \frac{RT}{b} lnC_e \tag{3.12}$$

To obtain the liner plot of Temkin isotherm, the Equation 3.13 can modified as

$$q_e = B\ lnA + B\ lnC_e \tag{3.13}$$

Where, A and B are constants of Temkin isotherm model; $B = \frac{RT}{b}$ and corresponds to the gas constant (8.314 J/mol/K) and T is temperature. Temkin isotherm model was presented by plotting a linear curve of $q_e$versus C_e and A($\frac{L}{g}$) and B was calculated from the plot (Mishra *et al.,* 2016).

3.17.2 Adsorption kinetics study

The kinetic study is important for the adsorption process because not only does it describes the uptake rate of adsorbate, but it controls also the residual time of the process. The pseudo-first order model, pseudo-second order model was used for the kinetic study (Gholizadeh, 2013).

The pseudo-first order Equation 3.14

$$\ln (q_e - q_t) = \ln q_e - \frac{K_1 t}{2.303} \tag{3.14}$$

Where q_e is the amount of selected compounds adsorbed at equilibrium$\left(\frac{mg}{g}\right)$, $q_t$is the amount of selected compounds adsorbed at time t $\left(\frac{mg}{g}\right)$, K_1 $\left(\frac{1}{min}\right)$ is the pseudo-first order rate constant. The linear plot between ln $(q_e - q_t)$ and t was used to evaluate the coefficients like K_1 and q_e from the slope and intercept respectively.

The linear pseudo-second order Equation 3.15

$$\frac{t}{q_t} = \frac{1}{K_2 {q_e}^2} + \frac{1}{q_e}\ t \tag{3.15}$$

Where K_2 is the rate constant of pseudo second order adsorption $\left(\frac{\frac{g}{mg}}{min}\right)$, the slope and intercept was used to determine the second order rate constant K_2

3.17.3 Adsorption thermodynamics study

The activation energy and isosteric heat of adsorption were calculated from the Arrhenius Equation and Clausius-Clapeyron Equation, respectively. The activating parameters, Gibbs energy change (ΔG^o), enthalpy change (ΔH^o), and entropy (ΔS^o), were calculated using Eyring Equation. Van't Hoff plots were employed for the calculation of $\Delta H°$ and $\Delta S°$ based on the following Equations: (Kim and Kim, 2018).

$$K_c = \frac{q_e}{C_e} \tag{3.16}$$

$$\Delta G = -RT\ lnK_c \tag{3.17}$$

$$\ln K_c = \left(\frac{\Delta S}{R}\right) - \left(\frac{\Delta H}{RT}\right) \tag{3.18}$$

Where K_c is the equilibrium constant, C_e is the adsorbate concentration at the equilibrium $\left(\frac{mg}{mol}\right)$. The $\Delta H\ and\ \Delta S$ value was calculated from slope and intercept of the linear plot of $\ln K_c$ versus $\frac{1}{T}$, respectively.

CHAPTER FOUR

4.0 RESULTS ND DISCUSSION

This chapter presents the results and discussion of the characterization of the raw SCB, modified SCB and SCB based activated carbon and their application for adsorption studies. Also, presented are the experiment results and discussion of effect of selected process parameters on the adsorption of heavy metals.

4.1 Proximate and Ultimate Analysis

The proximate analysis of the raw SCB was carried out and the experimental result obtained are presented in Table 4.1

Table 4.1: Results of Proximate Analysis of the Raw SCB (Balasundram *et al.,* 2018)

S/N	Property	SCB values in this study (% wt)	SCB Brazil* (% wt)
1	Moisture Content	6.79	6.30
2	Volatile Matter	74.07	83.03
3	Ash Content	3.79	4.00
4	Fixed Carbon	15.35	12.97

The proximate analysis result of raw sugarcane bagasse determined the distribution of its contents. It was noted that the volatile matter present in the bagasse contributed maximum to its contents. The moisture content present in the sample can also be considered as water vapor when it is heated to high temperatures. Hence, about 80.86% of the contents tend to leave the sample when heated, of which 74.07% was volatile matter and 6.79% was moisture content. The values from Table 4.1 indicated that the ash content of the sample was 8.4% and the fixed carbon content of the sample was 15.35%. This gives an overview

about the properties and components of bagasse. According to Akl *et al*. (2014) when the moisture and ash content of raw sugarcane bagasse (precursor of bagasse) is very low the efficiency of it producing activated carbon is high.

The ultimate analysis of the raw SCB was carried ou result obtained are presented in Table 4.2

Table 4.2: Ultimate Analysis of the Raw SCB

S/N	Property	Unit	SCB values in this study
1	Carbon Content	% wt	43.46
2	Hydrogen Content	% wt	5.39
3	Oxygen Content	% wt	39.87
4	Nitrogen	% wt	0.46

The ultimate analysis of the raw SCB was carried out and experimental result obtained are presented in the Table 4.2. The elemental analysis showed that the carbonaceous SCB contains heteratom mixture of carbon, hydrogen, oxygen and nitrogen. This analysis revealed high contents of carbon (43.46%) and oxygen (39.87%) in the SCB, supporting the lignocellulose structure for this sample (Bachrun *et al.,* 2016).

4.2 The TGA Analysis

The thermal property of the dried raw sugarcane bagasse was investigated, the result is shown in Figure 4.1. The weight loss consists of three distinct steps in the curves. The first stage at the temperature range of (25-111ºC) corresponds to rapid loss of about 4% of the sample weight due to non-dissociative physically absorbed water molecules as well

as water held on the surface by hydrogen bonding (Teixerira, 2004). The second weight loss is 69.3% at the cellulose/hemicellulose and lignin. In the temperature range (425-870C) there was a third weight loss 25.7%, which is corresponding to carbonaceous residues (Giusto *et al.,* 2017). Therefore, stage II was mainly the decomposition of hemicellulose, and stage III correspond to lignin.

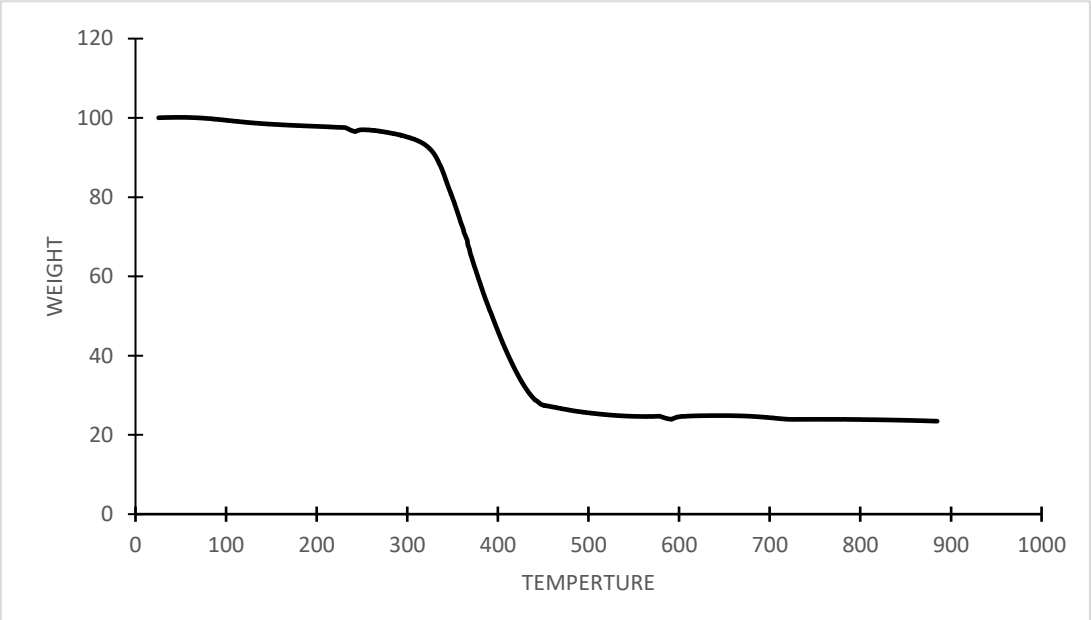

Figure 4.1: TGA curve of Raw Sugarcane bagasse

4.3 BET Analysis

The textural properties of solids were conventionally determined from the adsorption of nitrogen at 77 K, the result is shown in table 4.3. The surface area, pore volume and pore diameter of the raw sugarcane bagasse was 177.961 m^2/g, 0.09277 cm^3/g and 2.105 nm respectively. The surface area of the raw sugarcane bagasse was low. The MSCB treated at different concentration of H_3PO_4 showed an increased from 210 m^2/g to 423 m^2/g due to enhancement of the pore development. The activated carbon showed a large surface area of 954 m^2/g, this increase in surface area could be attributed to the change in textural

surface and formation of new pores in the surface. This increase in the result is in agreement with Adib *et al.,* 2018, the more micropores form in activated carbon, the bigger the surface area, hence the performance of activated carbon.

Table 4.3 shows the BET analysis summary result of the RSCB, MSCB and SCBAC.

Table 4.3: BET Result of Sugarcane Bagasse

S/N	SCB	Surface Area (m2/g)	Pore Volume (cm3/g)	Pore size (nm)
1	RSCB	178	0.0928	2.105
2	10% H_3PO_4	210.1	0.1214	2.107
3	20% H_3PO_4	311.8	0.1512	2.110
4	30% H_3PO_4	375	0.2000	2.116
5	40% H_3PO_4	406	0.2123	2.123
6	50% H_3PO_4	423	0.6000	2.132
7	SBAC	954.4	0.6279	2.853

4.4 FTIR Spectroscopy analysis

The FTIR spectroscopy was used to determine the functional groups of the raw sugarcane bagasse. The FT-IR spectra of SCB was performed to determine the vibration frequency changes in their functional groups within the range of 4000-400cm^{-1} Figure 4.3. The spectra measurements are in agreement with Chao *et al.,* (2014). The wavenumbers and chemical groups of RSCB, MSCB and SCBAC are shown in Table 4.4 to 4.6 and Figure in 1-3 in the appendix.

Table 4.4: Wavenumbers and Chemical Groups of FT-IR Bands for RSCB

S/N	SCB Wavelength (cm-1)	Bond/Functional group
1	1035.87	C-O stretching/ alcohol, carboxylic acids
2	1252-1402	O-H Bending (m)
3	1458.79	C-H stretching (m)
4	1685.54-1735.1	C=O stretching (s)
5	2345	O=C=O, N-H
6	3346.93	O-H Bending (s,b)
7	3627.72-3736	O-H stretching (m, sh)

(b=broad, m=medium, sh= sharp, s=strong).

Table 4.5: Wavenumbers and chemical groups of FT-IR for MSCB

S/N	SCB Wavelength (cm-1)	Bond/Functional group
1	941.69	O-H head/ Carboxylic acid (m)
2	1437.90	C-C stretch/ Aromatics
3	1458.74	C-H bend/Alkanes
4	1508.27-1545.05	N-O symmetric stretch
6	1560.13	C–C stretch (in–ring) m
7	1637.02-1654.31	C=O stretch (s), N–H bend/1st amine
9	1685.27-1701.17	C=O stretch (s)
10	2140.95- 2365.63	H-C=O: C-H stretch (m)
11	2746.99-3367.20	O-H
12	3568.18-3650.50	O-H stretch, free hydroxyl (s, sh)

Table 4.6: Wavenumbers and chemical groups of FTIR bands for SCBAC

S/N	SCBAC Wavelength (cm-1)	Bond/Functional group
1	669.18	O-H head/ Carboxylic acid (m)
2	1035.38	C-C stretch/ Aromatics
3	1458.47	C-H bend/ Alkanes
4	1508.03	N-O symmetric stretch
5	1541.84	N–O asymmetric stretch (s)
7	1560.13	C–C stretch (in–ring) m
7	1577.43	C=O stretch (s), N–H bend/1st amine
8	1637.01	C=O stretch (s), N–H bend/1st amine
9	1647.84	C=O stretch (s)
10	1654.29	C=O stretch (s)
11	1685.24	C=O stretch (s)
12	1701.21	C=O stretch (s)
13	1735.07	H-C=O: C-H stretch (m)
14	2345.59	H–C=O: C–H stretch (m)/Alkanes
15	2923.47	O-H
16	3568.19	O-H stretch (br, s), N-H stretch (m)/1,2, amines
17	3588.43	O-H stretch, free hydroxyl (s, sh)/Alcohol
18	3620.18	O-H stretch, free hydroxyl/phenols
19	3650.50	O-H stretch, (s, sh)/Alcohol

Table 4.4 – 4.6 shows the FTIR of sugarcane bagasse raw, modified, and activated carbon with the corresponding chemical group in Table 4.4 to 4.6. Peaks measured were in the

range of 4000 – 400 cm^{-1}. The IR spectra provide fingerprints of different functional groups present in the sugarcane adsorbent surface. The mechanism for the adsorption for heavy metals by sugarcane bagasse is linked to the role played by the essential stretching functional groups like hydroxyl (-OH), carboxylic (-COOH), carbonyl (C=O) and other aromatic and phenolic groups. Analysis showed the presence of alkanes, primary and secondary amines, alkynes, and alcohol and phenol functional groups. The acidic functional groups on the carbon surface, such as hydroxyl and carboxyl were able to attract molecules. This is in agreement with the work reported by Alhassan *et al.,* (2017).

SEM Analysis of the Sugarcane Bagasse

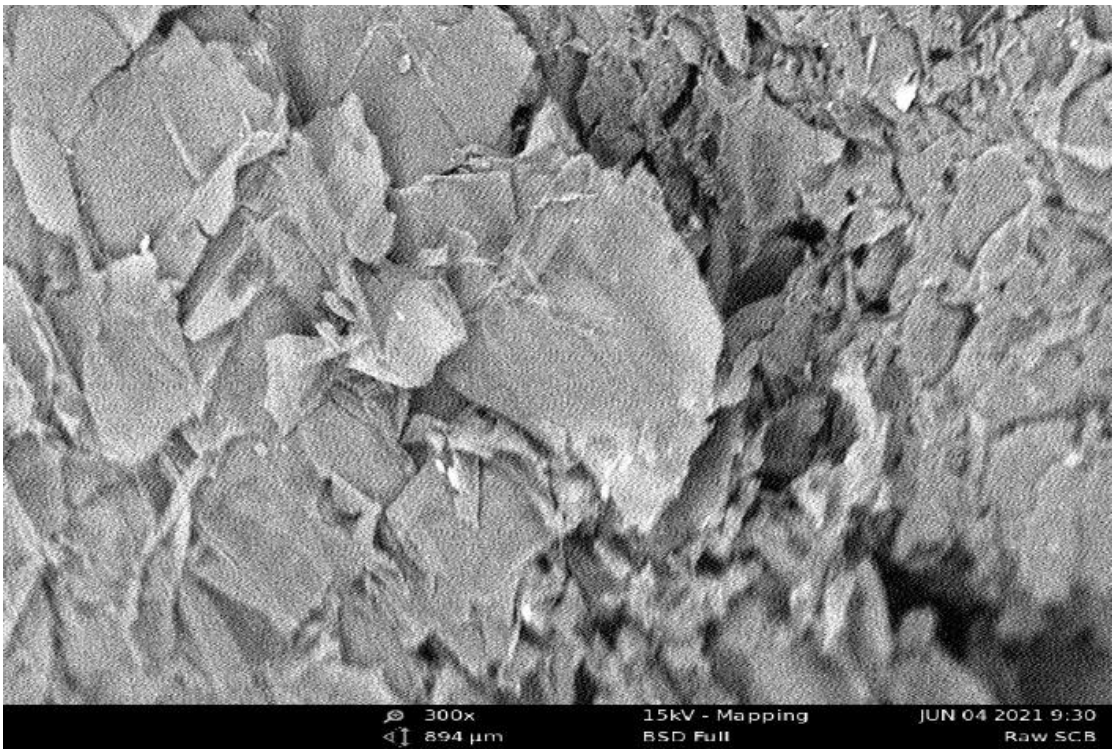

Plate I: RSCB 300x (894 µm)

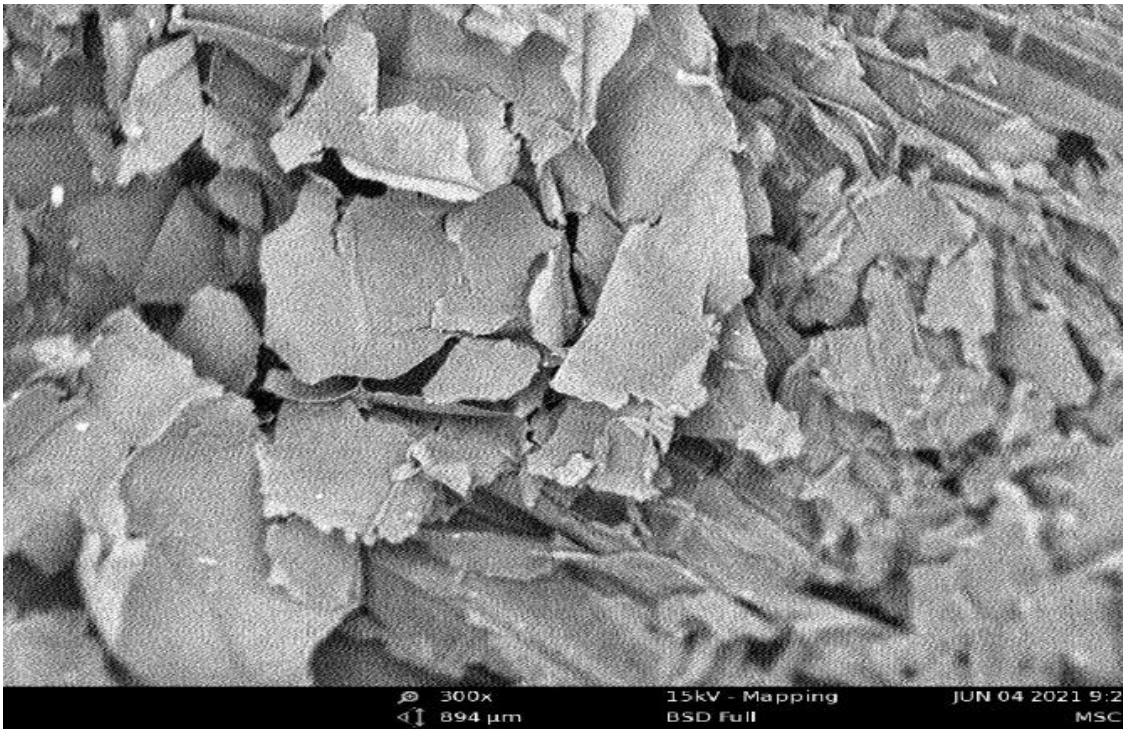

Plate II: MSCB 300x (894 µm)

Plate III: SCBAC

Plate I, II and III show the SEM images of the RSCB, MSCB and SBAC at different magnifications, Plate II showed an improvement in the plate I after treatment with phosphoric acid. The surface morphology of SCBAC in Plate III shows decomposition of lignin Putra (2014). Plate III shows a change in the surface morphology of the materials, which is observed after activation and carbonization. The smaller pore texture is important for adsorption process.

4.5 Heavy metal analysis

After the collection of the wastewater, the effluent was analyzed and shown in the Table 4.7. From the Table, it was observed that the AAS analysis of the effluent sample revealed the presence of Zn, Pb, Cd, and Cr at different concentrations even beyond the permissible limits set by the regulatory authorities.

Table 4.7: Initial Concentration of Metal Ions In Wastewater

S/N	Metal	Effluent sample (mg/L)	Safe limit (mg/L)	
			WHO (1993)* & EU (1998)*	NIS-554-2015*
1	Zinc	38.1858	33	3
2	Lead	3.6748	0.01	0.01
3	Cadmium	0.831810	0.003-0.005	0.003
4	Chromium	233.3611	50	0.05

NIS-554-2015: Nigeria Industrial Standard (Nigeria Standard for Drinking Water Quality approved by SON)

WHO: World Health Organization Drinking Standards

EU: European Union Drinking Standards

4.6 Optimization Studies

The optimization studies were carried out using response surface methodology (RSM) Central Composite Design (CCD). The process parameters investigated include the contact time, adsorbent dosage, temperature and pH of solution. Table 4.9 Presents the process parameters and their range used for the adsorption study.

Table 4.9: Process Parameters for Adsorption Study

S/N	Name	Units	Code	-1level	+1level	-alpha	+alpha
1	Contact time	Minutes	A	40	100	10	130
2	pH		B	4	8	2	10
3	Temperature	ºC	C	30	70	10	90
4	Adsorbent dosage	Grams	D	0.5	1	0.25	1.25

The result of Cr and Zn ions removal efficiency are shown with the experimental design on Table 4.10 to 4.12. The contact time was varied between 10 and 130 minutes, pH of 1 to 13, temperature of 10 to 90ºC and adsorbent dosage of 0.25 to 1.25 g. The result of the adsorption was presented in terms of percentage removal efficiency.

Table 4.10: Combined Experimental Design for the Simultaneous Adsorption of Heavy Metals (Cr and Zn) From Electroplating Wastewater-RSCB

Run No	Factor 1 A:Contact time min	Factor 2 B:pH	Factor 3 C:Temperature ^{0}C	Factor 4 D:RSCB Dosage g	Cr Removal %	Zn Removal %
1	130	6	50	0.75	62.90	46.48
2	100	4	70	1	69.05	49.67
3	70	6	50	1.25	63.01	46.05
4	70	2	50	0.75	60.43	44.77
5	40	4	70	1	65.01	48.11
6	40	8	70	0.5	45.35	38.65
7	40	8	70	1	62.22	44.77
8	40	8	30	1	60.99	40.80
9	40	4	30	0.5	46.23	37.30
10	100	4	30	1	62.66	44.48
11	70	6	50	0.75	61.92	45.90
12	70	10	50	0.75	60.38	40.76
13	70	6	10	0.75	59.49	38.99
14	100	4	30	0.5	52.34	39.30
15	70	6	50	0.75	64.87	42.56
16	70	6	50	0.75	65.20	46.35
17	70	6	50	0.75	63.89	48.35
18	70	6	50	0.75	60.45	45.34
19	70	6	50	0.25	30.42	32.45
20	100	4	70	0.5	55.65	43.50
21	70	6	90	0.75	63.93	46.42
22	70	6	50	0.75	62.90	45.29
23	100	8	30	0.5	51.09	39.15
24	100	8	30	1	61.46	44.28
25	40	4	70	0.5	48.66	41.31
26	100	8	70	1	61.33	48.05
27	40	4	30	1	56.65	43.31
28	40	8	30	0.5	47.94	35.51
29	10	6	50	0.75	54.41	41.37
30	100	8	70	0.5	46.44	42.29

Table 4.11: Combined Experimental Design Results for the Simultaneous Adsorption of Heavy Metals (Cr and Zn) From Electroplating Wastewater-MSCB

Run	Factor 1 A:Contact time min	Factor 2 B:pH	Factor 3 C:Temperature ºC	Factor 4 D:MSCB Dosage g	Cr Removal %	Zn Removal %
1	130	6	50	0.75	59.96	60.79
2	70	6	10	0.75	61.22	59.60
3	70	6	90	0.75	58.32	58.35
4	100	8	30	0.50	53.35	51.36
5	40	4	70	1.00	68.97	62.53
6	70	6	50	1.25	59.64	58.83
7	40	4	70	0.50	61.56	52.32
8	100	8	70	0.50	51.91	53.34
9	70	6	50	0.75	59.45	64.17
10	70	6	50	0.75	57.65	64.45
11	40	4	30	0.50	65.30	57.65
12	40	8	30	0.50	54.68	58.44
13	100	8	30	1.00	56.60	58.45
14	40	8	70	0.50	53.28	55.55
15	70	2	50	0.75	70.88	61.32
16	40	8	70	1.00	57.60	60.63
17	100	8	70	1.00	56.41	58.90
18	40	8	30	1.00	57.57	62.03
19	70	6	50	0.75	59.24	64.41
20	100	4	70	0.50	57.21	51.91
21	70	6	50	0.25	47.15	40.23
22	100	4	30	0.50	60.45	54.00
23	70	10	50	0.75	51.75	59.89
24	70	6	50	0.75	59.09	62.99
25	10	6	50	0.75	64.93	66.00
26	100	4	30	1.00	66.72	63.11
27	70	6	50	0.75	59.56	64.05
28	70	6	50	0.75	60.40	65.67
29	100	4	70	1.00	64.80	61.23
30	40	4	30	1.00	70.01	64.88

Table 4.10-4.12 showed the Combined experimental design results for the simultaneous adsorption of Cr and Zn from electroplating wastewater using RSCB, MSCB and SCBAC as the adsorbent respectively with varying contact time, pH, temperature and adsorbent dosage. It can be observed that in Table 4.10 that a significant increase in reaction time, adsorbent dosage and temperature increased the adsorption rate while an increase in pH played a little role meanwhile more adsorption occurred at acidic pH. The optimum conditions for removal of Cr and Zn ions were at reaction time of 70 minutes, temperature of 50^{o}C, pH of 6 and RSCB dosage of 0.75 g. The maximum removal of Cr and Zn ions were 69.05% and 49.48% which occurred at reaction time of 100 minutes, pH of 4, temperature of 70^{o}C and RSCB dosage of 1 g, this finding is in agreement with Yu *et al.,* (2016). From Table 4.11 the result of adsorption of Cr and Zn ions using MSCB, the maximum adsorption efficiency was 70.01% and 64.88% at reaction time of 40 minutes, pH of 4, temperature of 30^{o}C and MSCB dosage of 1 g while the optimum conditions were at reaction time of 70 minutes, temperature of 50^{o}C, pH of 6 and MSCB dosage of 0.75 g. In the adsorption of Cr and Zn ions, basic pH led lead to a decrease in removal efficiency, lower contact time and reaction time had better adsorption rate while and increase in MSCB dosage increased adsorption rate, this is in agreement with Man (2018). The resulted for the adsorption of Cr and Zn ions using SCBAC showed a maximum removal efficiency of 91.63% and 84.88% respectively at reaction time of 100 minutes, pH of 4, temperature of 70^{o}C and SCBAC dosage of 1 g. In the adsorption of Cr and Zn ions acidic pH and increase in adsorbent play a major role. The optimum conditions for the adsorption were at reaction time of 70 minutes, temperature of 50^{o}C, pH of 6 and SCBAC dosage of 0.75 g. The result is in agreement with Putra *et al.,* 2014 and Ullah, *et al.,* 2013.

Table 4.12: Combined experimental design results for the simultaneous adsorption of Heavy metals (Cr and Zn) from electroplating wastewater -SCBAC

Run	Factor 1 A:Contact time min	Factor 2 B:pH	Factor 3 C:Temperature ºC	Factor 4 D:SCBAC Dosage g	Response 1 Cr %	Response 2 Zn %
1	40	8	30	1	82.81	77.65
2	70	6	50	0.75	77.50	75.26
3	100	4	70	0.5	68.80	65.54
4	100	8	70	1	90.08	79.69
5	130	6	50	0.75	88.83	77.32
6	70	2	50	0.75	65.97	69.60
7	70	6	50	0.75	75.69	78.05
8	70	6	50	0.75	78.09	76.92
9	70	6	50	0.75	75.94	77.61
10	40	8	70	1	83.21	80.14
11	10	6	50	0.75	76.46	72.37
12	70	6	50	1.25	91.59	76.03
13	70	10	50	0.75	72.74	64.86
14	70	6	50	0.75	76.11	78.45
15	70	6	10	0.75	71.13	73.41
16	100	8	70	0.5	67.64	59.31
17	100	8	30	0.5	64.27	61.06
18	70	6	50	0.75	75.87	77.36
19	40	4	30	1	81.40	74.13
20	40	8	70	0.5	66.74	58.90
21	40	8	30	0.5	65.18	60.09
22	100	8	30	1	86.31	78.55
23	40	4	70	0.5	65.26	64.66
24	70	6	50	0.25	54.35	45.14
25	40	4	30	0.5	62.63	61.38
26	70	6	90	0.75	76.36	78.92
27	40	4	70	1	81.77	79.46
28	100	4	30	0.5	65.30	66.21
29	100	4	70	1	91.63	84.88
30	100	4	30	1	87.69	79.91

Table 4.13: Analysis of Variance (ANOVA) For the Adsorption of Cr (Using RSCB) From Electroplating Wastewater

Source	Sum of Squares	df	Mean Square	F-value	p-value	
Model	1950.08	14	139.29	45.66	< 0.0001	significant
A-Contact time	80.46	1	80.46	26.38	0.0001	
B-pH	15.89	1	15.89	5.21	0.0375	
C-Temperature	22.48	1	22.48	7.37	0.0160	
D-Adsorbent Dosage	1216.25	1	1216.25	398.71	< 0.0001	
AB	23.35	1	23.35	7.66	0.0144	
AC	1.27	1	1.27	0.4169	0.5282	
AD	3.72	1	3.72	1.22	0.2872	
BC	44.32	1	44.32	14.53	0.0017	
BD	1.38	1	1.38	0.4508	0.5121	
CD	18.81	1	18.81	6.17	0.0253	
A^2	47.28	1	47.28	15.50	0.0013	
B^2	21.04	1	21.04	6.90	0.0191	
C^2	8.28	1	8.28	2.72	0.1202	
D^2	506.75	1	506.75	166.13	< 0.0001	
Residual	45.76	15	3.05			
Lack of Fit	29.20	10	2.92	0.8819	0.5969	not significant

From the ANOVA analysis on Table 4.13 the Model F-value of 45.66 implies the model is significant. P-values less than 0.0500 indicate model terms are significant. In this case A, B, C, D, AB, BC, CD, A^2, B^2, D^2 are significant model terms. Values greater than 0.1000 indicate the model terms are not significant. The Lack of Fit F-value of 0.88

implies the Lack of Fit is not significant relative to the pure error. Non-significant lack of fit is good. Similarly, the model gave a correlation factor (R^2) which equals to 97.71% indicating a close fit between the experimental data and the predicted data as such indicating the model fits.

The model produced the following coded Equation (4.1)

$$\text{Cr (RSCB)Removal efficiency} = 63.205 + 1.83101 * A + -0.813785 * B + 0.967917 * C + 7.11878 * D + -1.20812 * AB + -0.281927 * AC + -0.481875 * AD + -1.66437 * BC + 0.293177 * BD + 1.08438 * CD + -1.31293 * A^2 + -0.875799 * B^2 + -0.549549 * C^2 + -4.2983 * D^2 \quad (4.1)$$

The Equation in terms of coded factors can be used to make predictions about the response for given levels of each factor. By default, the high levels of the factors are coded as +1 and the low levels are coded as -1. The coded Equation is useful for identifying the relative impact of the factors by comparing the factor coefficients. Negative coefficient values indicated that the individual or interaction effects factors negatively affect adsorption while positive coefficient values represents that factors increase removal percentage with higher coefficient terms indicating a larger effect on the adsorption process.

Table 4.14: Analysis of Variance (ANOVA) For the Adsorption of Zn (RSCB) From Electroplating Wastewater

Source	Sum of Squares	df	Mean Square	F-value	p-value	
Model	458.15	14	32.73	24.51	< 0.0001	significant
A-Contact time	40.54	1	40.54	30.36	< 0.0001	
B-pH	19.28	1	19.28	14.44	0.0017	
C-Temperature	92.42	1	92.42	69.21	< 0.0001	
D-Adsorbent Dosage	226.10	1	226.10	169.32	< 0.0001	
AB	3.17	1	3.17	2.38	0.1441	
AC	0.0077	1	0.0077	0.0058	0.9406	
AD	0.2474	1	0.2474	0.1853	0.6730	
BC	1.10	1	1.10	0.8219	0.3790	
BD	0.2140	1	0.2140	0.1603	0.6946	
CD	0.6588	1	0.6588	0.4933	0.4932	
A^2	3.66	1	3.66	2.74	0.1186	
B^2	11.78	1	11.78	8.82	0.0095	
C^2	12.33	1	12.33	9.24	0.0083	
D^2	64.54	1	64.54	48.33	< 0.0001	
Residual	20.03	15	1.34			
Lack of Fit	2.42	10	0.2417	0.0686	0.9997	not significant
Pure Error	17.61	5	3.52			
Cor Total	478.18	29				

$R^2 = 0.9581$

The result of ANOVA of Zn ion (RSCB) on Table 4.14 shows that the Model F-value of 24.51 implies the model is significant. P-values less than 0.0500 indicate model terms are significant. In this case A, B, C, D, B^2, C^2, D^2 are significant model terms. Values greater than 0.1000 indicate the model terms are not significant. The Lack of Fit F-value of 0.07 implies the Lack of Fit is not significant relative to the pure error. Non-significant lack of fit is good. Similarly, the model gave a correlation factor (R^2) which equals to 95.81% indicating a close fit between the experimental data and the predicted data as such indicating the model fits.

$$Zn\ (RSCB) removal\ efficiency$$
$$= 45.6319 + 1.29968 * A + -0.896353 * B + 1.96237 * C + 3.06933 * D + 0.445294 * AB + 0.0219086 * AC + -0.124341 * AD + -0.2619 * BC + -0.11565 * BD + 0.202913 * CD + -0.365278 * A^2 + -0.655226 * B^2 + -0.670547 * C^2 + -1.53398 * D^2 \quad (4.2)$$

The Equation 4.2 in terms of coded factors can be used to make predictions about the response for given levels of each factor. The coded Equation is useful for identifying the relative impact of the factors by comparing the factor coefficients. Negative coefficient values indicated that the individual or interaction effects factors negatively affect adsorption while positive coefficient values represents that factors increase removal percentage with higher coefficient terms indicating a larger effect on the adsorption process.

Table 4.15: ANOVA for the Adsorption of Cr (MSCB) From Electroplating Wastewater

Source	Sum of Squares	df	Mean Square	F-value	p-value	
Model	879.40	14	62.81	117.40	< 0.0001	significant
A-Contact time	41.21	1	41.21	77.02	< 0.0001	
B-pH	521.45	1	521.45	974.57	< 0.0001	
C-Temperature	14.64	1	14.64	27.37	0.0001	
D-Adsorbent Dosage	181.01	1	181.01	338.31	< 0.0001	
AB	8.70	1	8.70	16.27	0.0011	
AC	0.0257	1	0.0257	0.0480	0.8296	
AD	0.3250	1	0.3250	0.6074	0.4479	
BC	3.02	1	3.02	5.64	0.0314	
BD	7.58	1	7.58	14.17	0.0019	
CD	2.81	1	2.81	5.25	0.0368	
A^2	21.91	1	21.91	40.95	< 0.0001	
B^2	10.25	1	10.25	19.16	0.0005	
C^2	1.39	1	1.39	2.60	0.1276	
D^2	51.34	1	51.34	95.95	< 0.0001	
Residual	8.03	15	0.5351			
Lack of Fit	3.98	10	0.3985	0.4931	0.8403	not significant
Pure Error	4.04	5	0.8082			

Table 4.15 results show that the Model F-value of 117.40 implies the model is significant. There is only a 0.01% chance that an F-value this large could occur due to noise. P-values less than 0.0500 indicate model terms are significant. In this case A, B, C, D, AB, BC, BD, CD, A^2, B^2, D^2 are significant model terms. Values greater than 0.1000 indicate the model terms are not significant. The Lack of Fit F-value of 0.49 implies the Lack of Fit

is not significant relative to the pure error. Non-significant lack of fit is good. Similarly, the model gave a correlation factor (R2) which equals to 99.10% indicating a close fit between the experimental data and the predicted data as such indicating the model fits.

The model produced the following coded Equation (4.3)

$$Cr\,(MSCB) = 59.2325 + -1.31041 * A + -4.66122 * B + -0.78111 * C + 2.7463 * D + 0.737523 * AB + -0.040051 * AC + 0.142523 * AD + 0.434113 * BC + -0.68846 * BD + 0.419113 * CD + 0.893804 * A^2 + 0.611356 * B^2 + 0.225243 * C^2 + -1.3681 * D^2 \quad (4.3)$$

The Equation (4.3) in terms of coded factors can be used to make predictions about the response for given levels of each factor. The coded Equation is useful for identifying the relative impact of the factors by comparing the factor coefficients. The model Equation describes how the adsorption of Chromium unto MSCB was affected by individual variables of linear and quadratic or interaction effects. Negative coefficient values indicated that the individual or interaction effects factors negatively affect adsorption while positive coefficient values represents that factors increase removal percentage with higher coefficient terms indicating a larger effect on the adsorption process.

Table 4.16: ANOVA for the Adsorption of Zn (MSCB) From Electroplating Wastewater

Source	Sum of Squares	df	Mean Square	F-value	p-value	
Model	870.93	14	62.21	59.17	< 0.0001	significant
A-Contact time	43.05	1	43.05	40.95	< 0.0001	
B-pH	5.78	1	5.78	5.50	0.0332	
C-Temperature	10.67	1	10.67	10.15	0.0061	
D-Adsorbent Dosage	371.24	1	371.24	353.11	< 0.0001	
AB	3.49	1	3.49	3.32	0.0885	
AC	6.82	1	6.82	6.48	0.0224	
AD	1.54	1	1.54	1.47	0.2445	
BC	5.99	1	5.99	5.69	0.0307	
BD	13.21	1	13.21	12.57	0.0029	
CD	0.6185	1	0.6185	0.5883	0.4550	
A^2	1.88	1	1.88	1.79	0.2011	
B^2	25.26	1	25.26	24.03	0.0002	
C^2	51.24	1	51.24	48.74	< 0.0001	
D^2	381.21	1	381.21	362.60	< 0.0001	
Residual	15.77	15	1.05			
Lack of Fit	12.06	10	1.21	1.63	0.3078	not significant
Pure Error	3.71	5	0.7410			
Cor Total	886.70	29				

Table 4.16 shows that the P-values less than 0.0500 indicate model terms are significant. In this case A, B, C, D, AC, BC, BD, B^2, C^2, D^2 are significant model terms. Values greater than 0.1000 indicate the model terms are not significant. The Lack of Fit F-value

of 1.63 implies the Lack of Fit is not significant relative to the pure error. Non-significant lack of fit is good. The model gave a correlation factor (R^2) which equals to 98.22% indicating a close fit between the experimental data and the predicted data as such indicating the model fits. The model gave a correlation factor (R^2) which equals to 98.22% indicating a close fit between the experimental data and the predicted data as such indicating the model fits.

The model produced the following coded Equation (4.4)

$$Zn\,(MSCB) = 64.2892 + -1.33927 * A + -0.490903 * B + -0.666875 * C + 3.93299 * D + -0.466979 * AB + 0.652708 * AC + 0.310521 * AD + 0.611615 * BC + -0.908698 * BD + 0.196615 * CD + -0.261797 * A^2 + -0.959714 * B^2 + -1.3668 * C^2 + -3.72805 * D^2 \quad (4.4)$$

The Equation (4.4) in terms of coded factors can be used to make predictions about the response for given levels of each factor. By default, the high levels of the factors are coded as +1 and the low levels are coded as -1. The coded Equation is useful for identifying the relative impact of the factors by comparing the factor coefficients. The model Equation describes how the adsorption of Zinc ion unto MSCB was affected by individual variables of linear and quadratic or interaction effects. Negative coefficient values indicated that the individual or interaction effects factors negatively affect adsorption while positive coefficient values represents that factors increase removal percentage with higher coefficient terms indicating a larger effect on the adsorption process.

Table 4.17: ANOVA for the Adsorption of Cr (SCBAC) From Electroplating Wastewater

Source	Sum of Squares	df	Mean Square	F-value	p-value	
Model	2697.30	14	192.66	87.51	< 0.0001	significant
A-Contact time	137.58	1	137.58	62.49	< 0.0001	
B-pH	9.75	1	9.75	4.43	0.0526	
C-Temperature	37.50	1	37.50	17.03	0.0009	
D-Adsorbent Dosage	2273.00	1	2273.00	1032.38	< 0.0001	
AB	9.00	1	9.00	4.09	0.0613	
AC	5.78	1	5.78	2.63	0.1259	
AD	25.84	1	25.84	11.73	0.0038	
BC	0.1132	1	0.1132	0.0514	0.8237	
BD	0.2327	1	0.2327	0.1057	0.7496	
CD	0.4143	1	0.4143	0.1882	0.6706	
A^2	78.71	1	78.71	35.75	< 0.0001	
B^2	72.79	1	72.79	33.06	< 0.0001	
C^2	7.75	1	7.75	3.52	0.0802	
D^2	14.43	1	14.43	6.56	0.0217	
Residual	33.03	15	2.20			
Lack of Fit	27.99	10	2.80	2.78	0.1354	not significant
Pure Error	5.04	5	1.01			
Cor Total	2730.32	29				

The ANOVA Table 4.17 shows that The Model F-value of 87.51 implies the model is significant. P-values less than 0.0500 indicate model terms are significant. In this case A,

C, D, AD, A^2, B^2, D^2 are significant model terms. Values greater than 0.1000 indicate the model terms are not significant. The Lack of Fit F-value of 2.78 implies the Lack of Fit is not significant relative to the pure error. Non-significant lack of fit is good. The model gave a correlation factor (R2) which equals to 98.79% indicating a close fit between the experimental data and the predicted data as such indicating the model fits.

The model produced the following coded Equation (4.5)

$$Cr\ (SCBAC) = 76.5326 + 4.78849 * A + 0.637501 * B + 1.24996 * C + 9.73181 * D + -1.50041 * AB + 1.20231 * AC + 2.54149 * AD + -0.0840975 * BC + -0.120606 * BD + -0.160922 * CD + 6.77608 * A^2 + -1.62906 * B^2 + -0.531556 * C^2 + -0.725397 * D^2 \quad (4.5)$$

This Equation (4.5) in terms of coded factors can be applied to find the predictions about the response for given levels of each factor. Each parameter that has the high positive value of the coefficient, it evidenced a highly positive effect on the response. While, the negative number of parameters demonstrated the inverse relationship between the response and the parameter, denoting that the negative amount leading to the gaining of maximum responses.

Table 4.18: ANOVA for the Adsorption of Zn (SCBAC) From Electroplating Wastewater

Source	Sum of Squares	df	Mean Square	F-value	p-value	
Model	2347.34	14	167.67	114.42	< 0.0001	significant
A-Contact time	34.18	1	34.18	23.33	0.0002	
B-pH	38.16	1	38.16	26.04	0.0001	
C-Temperature	25.27	1	25.27	17.25	0.0008	
D-Adsorbent Dosage	1650.72	1	1650.72	1126.51	< 0.0001	
AB	14.23	1	14.23	9.71	0.0071	
AC	2.42	1	2.42	1.65	0.2181	
AD	1.30	1	1.30	0.8904	0.3603	
BC	9.33	1	9.33	6.37	0.0234	
BD	16.17	1	16.17	11.03	0.0046	
CD	12.71	1	12.71	8.67	0.0100	
A^2	5.27	1	5.27	3.60	0.0773	
B^2	150.47	1	150.47	102.68	< 0.0001	
C^2	0.3219	1	0.3219	0.2197	0.6460	
D^2	439.51	1	439.51	299.94	< 0.0001	
Residual	21.98	15	1.47			
Lack of Fit	15.69	10	1.57	1.25	0.4266	not significant
Pure Error	6.29	5	1.26			
Cor Total	2369.32	29				

$$R^2 = 0.9907$$

From the analysis of Table 4.18, the Model F-value of 114.42 implies the model is significant. P-values less than 0.0500 indicate model terms are significant. In this case B,

D, AB, BC, BD, CD, B^2, D^2 are significant model terms. Values greater than 0.1000 indicate the model terms are not significant. The Lack of Fit F-value of 1.25 implies the Lack of Fit is not significant relative to the pure error. Non-significant lack of fit is good. The model gave a correlation factor (R^2) which equals to 99.07% indicating a close fit between the experimental data and the predicted data as such indicating the model fits. This work is in agreement with Trans *et al.,* (2016).

The model produced the following coded Equation (4.6)

$$Zn\,(SCBAC) = 77.2753 + 2.38675 * A + -1.26094 * B + 1.02621 * C + 8.29338 * D + -1.88613 * AB + -0.778056 * AC + 0.571133 * AD + -0.763735 * BC + 1.00527 * BD + 0.891235 * CD + -1.75364 * A^2 + -2.34216 * B^2 + -0.108328 * C^2 + -4.00299 * D^2 \quad (4.6)$$

The Equation (4.6) in terms of coded factors can be used to make predictions about the response for given levels of each factor. By default, the high levels of the factors are coded as +1 and the low levels are coded as -1. The coded Equation is useful for identifying the relative impact of the factors by comparing the factor coefficients. The model Equation describes how the adsorption of Zn unto SCBAC was affected by individual variables of linear and quadratic or interaction effects. Negative coefficient values indicated that the individual or interaction effects factors negatively affect adsorption while positive coefficient values represents that factors increase removal percentage with higher coefficient terms indicating a larger effect on the adsorption process.

4.7 Combined Effect of Process Parameters on the Adsorption Process

The combined/interaction effect of the process parameters on the adsorption process were analyzed using 3-D response surface plots. The plots are as presented in Figure 4.2 – 4. 19

4.7.1 3-D response surface plot on the adsorption of Cr (RSCB)

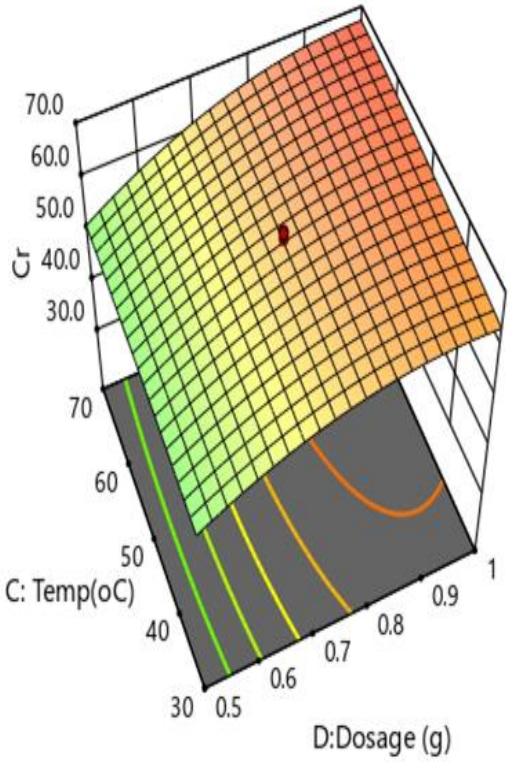

Figure 4.2: 3-D Response plot of adsorbent dosage and temperature on the removal efficiency of Cr (RSCB)

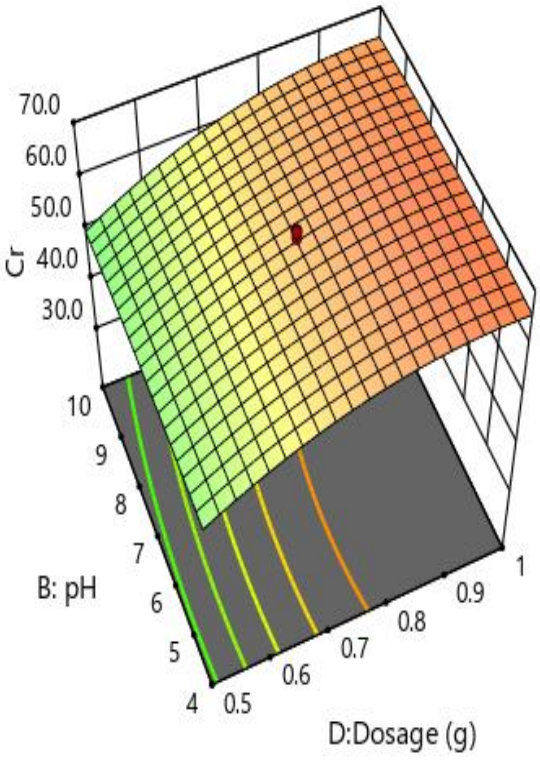

Figure 4.3: 3-D Response plot of adsorbent dosage and pH on the removal efficiency of Cr (RSCB**)**

Figure 4.2 shows the response surface plot of the interaction effect of adsorbent dosage and temperature on the removal efficiency of Cr at a contact time of 70 minutes and pH of 6. In terms of interaction, effect of adsorbent dosage and temperature an optimum removal efficiency of 63.21% at an adsorbent of 0.75 g and temperature of 50^{o}C. The interaction can be explained thus, at lower temperature and lower RSCB dosage, there was minimal adsorption rate. Increase in dosage with temperature brought about a better removal efficiency of Cr ion.

Figure 4.3 shows the response surface plot of the interaction effect of adsorbent dosage and pH on the removal efficiency of Cr at a contact time of 70 minutes and temperature of 50^{o}C. In terms of interaction, effect of adsorbent dosage and pH an optimum removal efficiency of 63.21% at an adsorbent of 0.75 g and pH of 6. It can be observed from the plot that acidic pH at increased dosage favoured more adsorption of Cr ion.

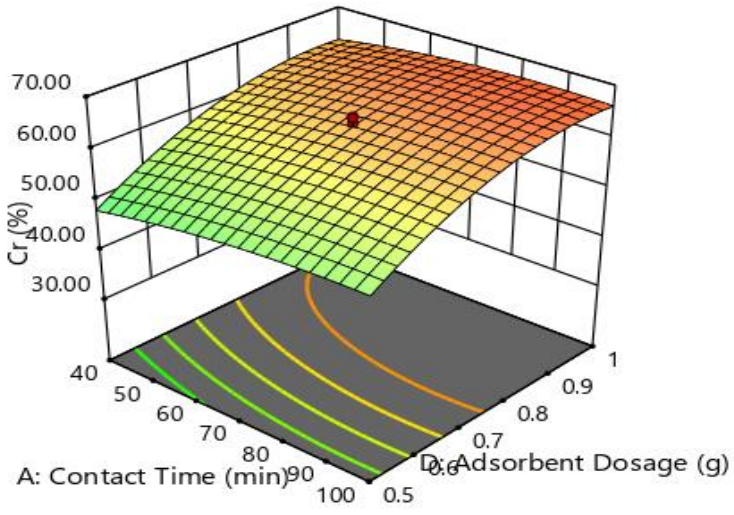

Figure 4.4: 3-D Response plot of adsorbent dosage and contact time on the removal efficiency of Cr (RSCB)

Figure 4.4 shows the response surface plot of the interaction effect of adsorbent dosage and contact time on the removal efficiency of Cr at a pH of 6 and temperature of 50^{o}C. In terms of interaction effect of adsorbent dosage and contact time an optimum removal efficiency of 63.21% at an adsorbent of 0.75 g and contact time of 70 minutes. The plot revealed that increase in contact time and increase RSCB dosage produce a better adsorption of Cr ion.

4.7.2 3-D Response Surface Plot on the adsorption of Zn (RSCB)

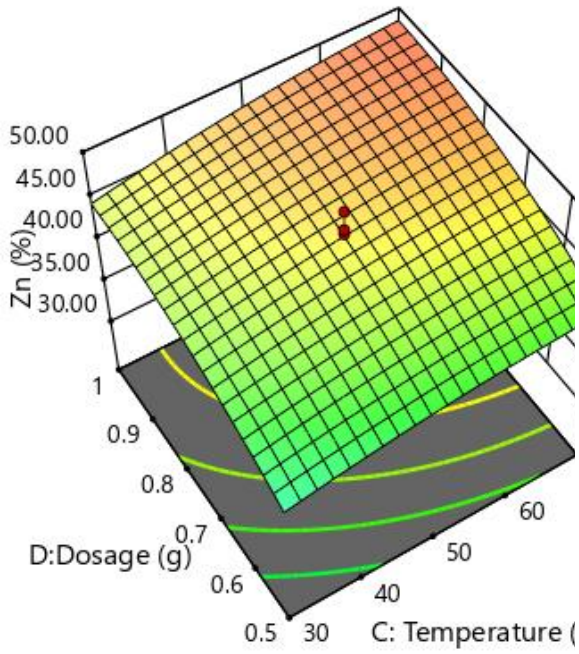

Figure 4.5: 3-D Response plot of RSCB dosage and temperature on the removal efficiency of Zn

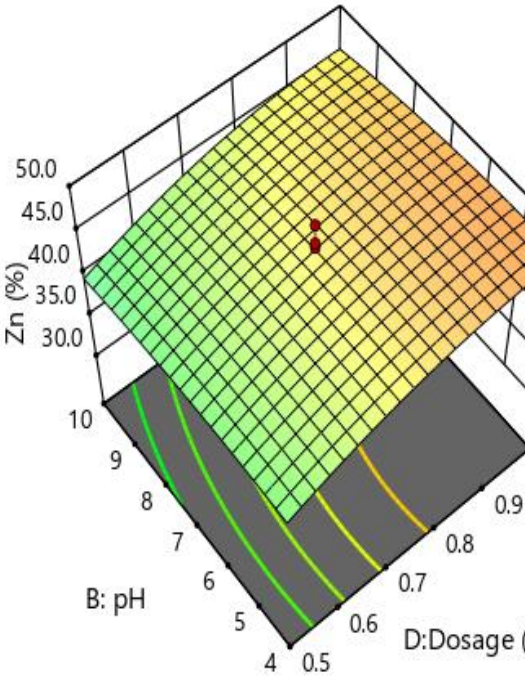

Figure 4.6: 3-D Response plot of adsorbent (RSCB) dosage and pH on the removal efficiency of Zn

Figure 4.5 shows the response surface plot of the interaction effect of adsorbent (RSCB) dosage and temperature on the removal efficiency of Zn at a contact time of 70 minutes and pH of 6. In terms of interaction, effect of adsorbent dosage and temperature an optimum removal efficiency of 45.63 % at an adsorbent of 0.75 g and temperature of 50^{o}C. The adsorption of Zinc ion best took place at higher dosage and high temperature.

Figure 4.6 shows the response surface plot of the interaction effect of adsorbent (RSCB) dosage and pH on the removal efficiency of Zn at a contact time of 70 minutes and temperature of 50^{o}C. In terms of interaction, effect of adsorbent dosage and pH an optimum removal efficiency of 45.63% at an adsorbent of 0.75 g and pH of 6. It can be observed from the plot that acidic pH at increased dosage favoured more adsorption of Zn ion while basic pH led to a decrease even with high dosage.

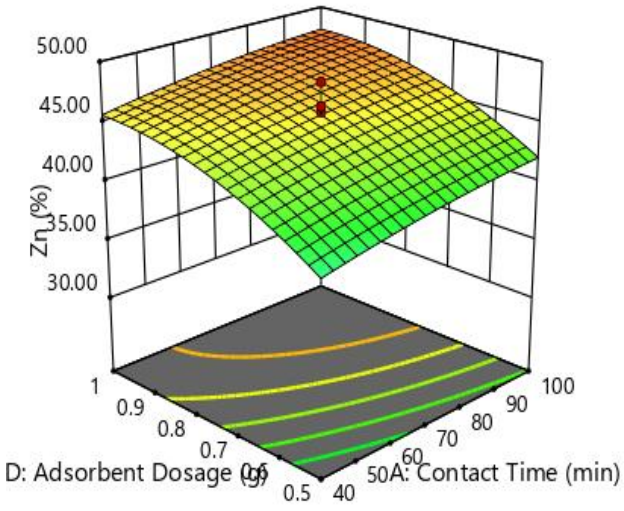

Figure 4.7: 3-D Response plot of adsorbent dosage (RSCB) and contact time on the removal efficiency of Zn

Figure 4.7 shows the response surface plot of the interaction effect of adsorbent (MSCB) dosage and contact time on the removal efficiency of Zn at a pH of 6 and temperature of 50^{o}C. In terms of interaction effect of adsorbent dosage and contact time an optimum removal efficiency of 45.63% at an adsorbent of 0.75 g and contact time of 70 minutes. It can be observed from the graph that at high dosage and increased contact time Zinc ion was better absorbed.

4.7.3 3-D response surface plot on the adsorption of Cr (MSCB)

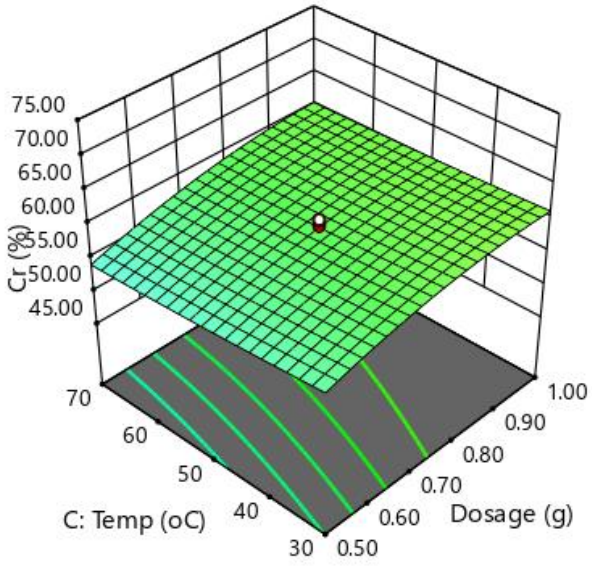

Figure 4.8:3- D Response plot of adsorbent dosage (MSCB) and temperature on the removal efficiency of Cr

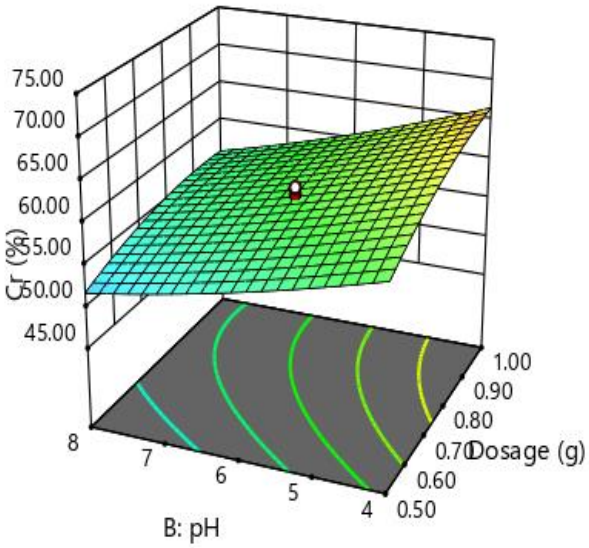

Figure 4.9: 3-D Response plot of adsorbent (MSCB) dosage and pH on the removal efficiency of Cr

Figure 4.8 shows the response surface plot of the interaction effect of adsorbent dosage and temperature on the removal efficiency of Cr at a contact time of 70 minutes and pH

of 6. In terms of interaction, effect of adsorbent dosage and temperature an optimum removal efficiency of 59.23% at an adsorbent of 0.75 g and temperature of 50^{o}C. The plot showed that increased dosage at minimal temperature favoured the adsorption of Chromium ion.

Figure 4.9 shows the response surface plot of the interaction effect of adsorbent dosage and pH on the removal efficiency of Cr at a contact time of 70 minutes and temperature of 50^{o}C. In terms of interaction, effect of adsorbent dosage and pH an optimum removal efficiency of 59.23% at an adsorbent of 0.75 g and pH of 6. It can be observed from the plot that acidic pH at increased dosage favoured more adsorption of Cr ion while basic .pH led to a decrease even with high dosage.

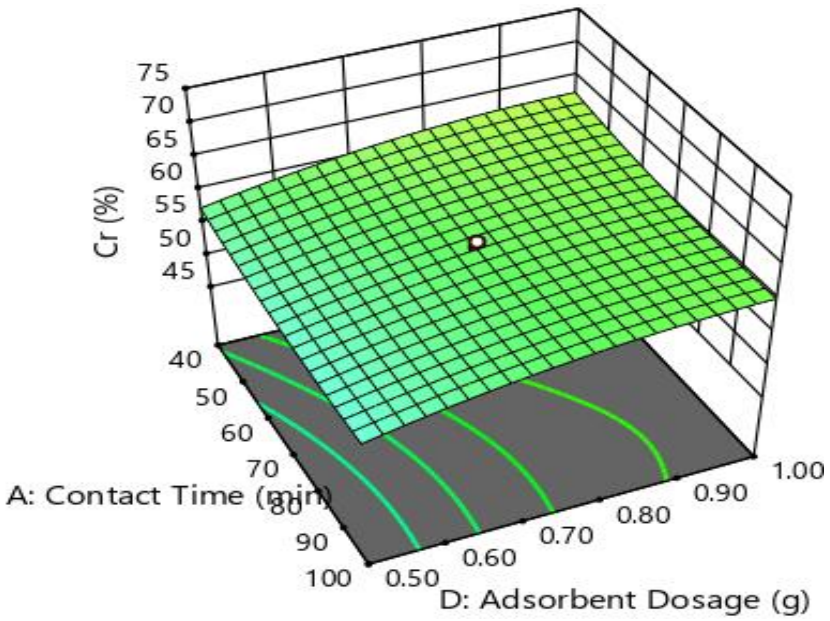

Figure 4.10: 3-D Response plot of adsorbent dosage (MSCB) and contact time on the removal efficiency of Cr

Figure 4.10 shows the response surface plot of the interaction effect of adsorbent dosage and contact time on the removal efficiency of Cr at a pH of 6 and temperature of 50^{o}C. In terms of interaction effect of adsorbent dosage and contact time an optimum removal efficiency of 59.23% at an adsorbent of 0.75 g and contact time of 70 minutes.

4.7.4 3-D response surface plot on the adsorption of Zn (MSCB)

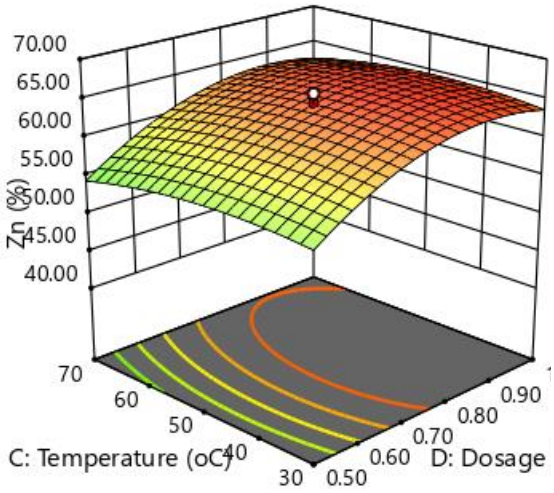

Figure 4.11: 3-D Response plot of adsorbent dosage (MSCB) and temperature on the removal efficiency of Zn

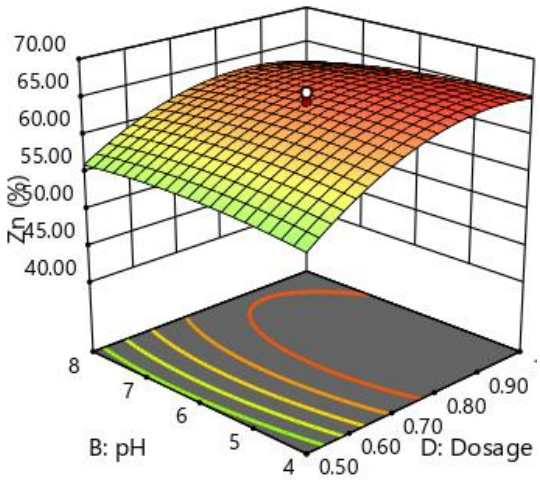

Figure 4.12: 3-D Response plot of adsorbent dosage (MSCB) and pH on the removal efficiency of Zn

Figure 4.11 shows the response surface plot of the interaction effect of adsorbent dosage and temperature on the removal efficiency of Zn at a contact time of 70 minutes and pH of 6. In terms of interaction, effect of adsorbent dosage and temperature an optimum removal efficiency of 64.29 % at an adsorbent of 0.75 g and temperature of 70^{o}C. More adsorption took place at temperature below 60 ^{o}C with increase in adsorbent dosage.

Figure 4.12 shows the response surface plot of the interaction effect of adsorbent dosage and pH on the removal efficiency of Zn at a contact time of 70 minutes and temperature of 50^{o}C. In terms of interaction, effect of adsorbent dosage and pH an optimum removal efficiency of 64.29% at an adsorbent of 0.75 g and pH of 6. More adsorption of Zn ion took place at the acidic pH with increased adsorbent dosage.

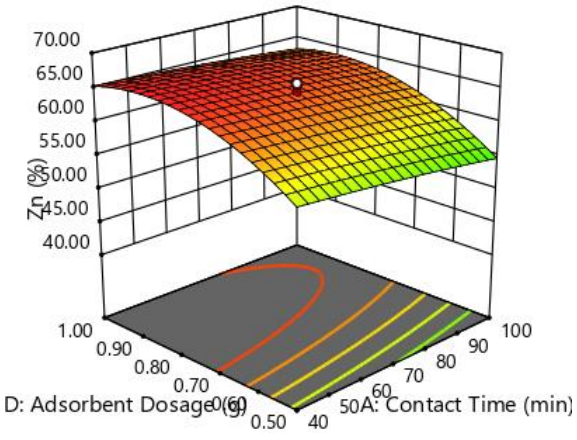

Figure 4.13: 3-D Response plot of adsorbent dosage (MSCB) and contact time on the removal efficiency of Zn

Figure 4.13 shows the response surface plot of the interaction effect of adsorbent dosage and contact time on the removal efficiency of Zn at a pH of 6 and temperature of 50^{o}C. In terms of interaction effect of adsorbent dosage and contact time an optimum removal efficiency of 64.29% at an adsorbent of 0.75 g and contact time of 70 minutes. It can be observed from the plot that increasing dosage with contact time led to increase in removal of MSCB.

4.7.5 3-D Response Surface Plot on the adsorption of Cr (SCBAC)

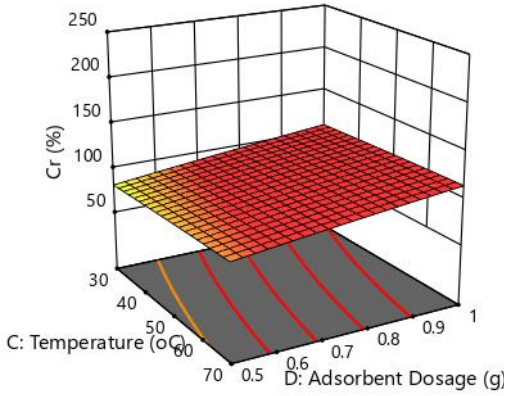

Figure 4.14: 3-D Response plot of adsorbent (SCBAC) dosage and temperature on the removal efficiency of Cr

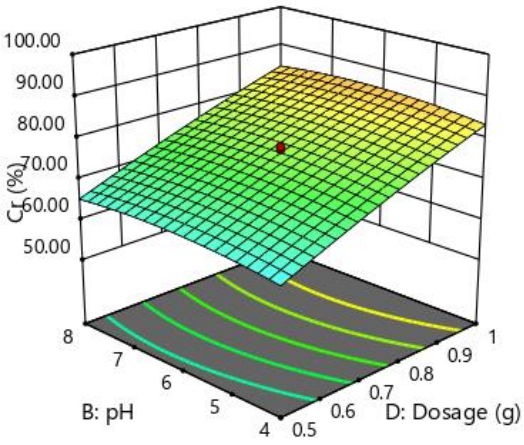

Figure 4.15: 3-D Response plot of adsorbent (SCBAC) dosage and pH on the removal efficiency of Cr

Figure 4.14 shows the response surface plot of the interaction effect of adsorbent (SCBAC) dosage and temperature on the removal efficiency of Cr at a contact time of 70 minutes and pH of 6. In terms of interaction, effect of adsorbent dosage and temperature an optimum removal efficiency of 76.53% at an adsorbent of 0.75 g and temperature of 50^{o}C. The result showed that increased temperature increased the adsorption of Chromium ions.

Figure 4.15 shows the response surface plot of the interaction effect of SCBAC dosage and pH on the removal efficiency of Cr at a contact time of 70 minutes and temperature of 50^{o}C. In terms of interaction, effect of adsorbent dosage and pH an optimum removal

efficiency of 77.53% at an adsorbent of 0.75 g and pH of 6. Increase in dosage and pH led to increase in the adsorption of chromium.

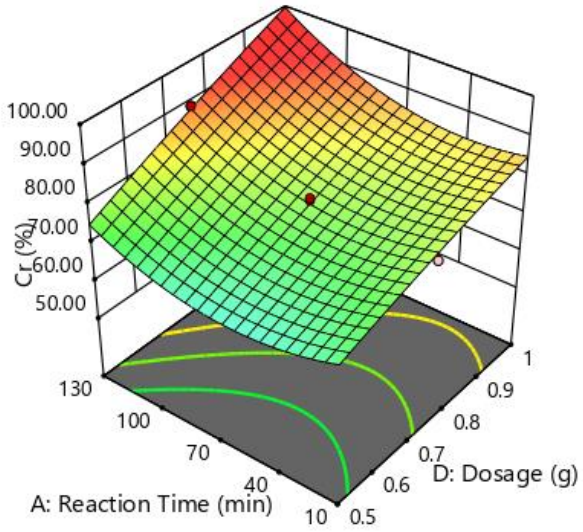

Figure 4.16: 3-D Response plot of adsorbent Cr (SCBAC) dosage and contact time on the removal efficiency of Cr ion

Figure 4.16 shows the response surface plot of the interaction effect of adsorbent dosage and contact time on the removal efficiency of Cr at a pH of 6 and temperature of 50^{o}C. In terms of interaction effect of adsorbent dosage and contact time an optimum removal efficiency of 76.53 at an adsorbent of 0.75 g and contact time of 70 minutes. Increase in contact time and dosage increased the adsorption of Cr ions.

4.7.6 3-D response surface plot on the adsorption of Zn (SCBAC)

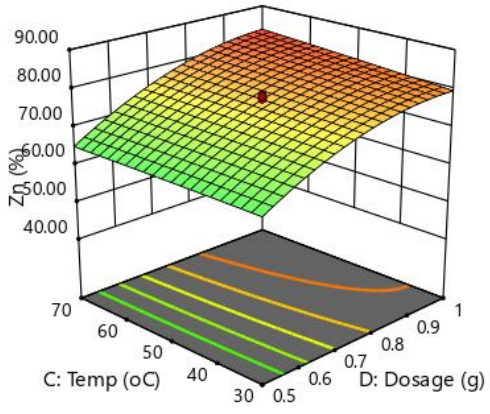

Figure 4.17: 3-D Response plot of adsorbent dosage (SCBAC) and temperature on the removal efficiency of Zn

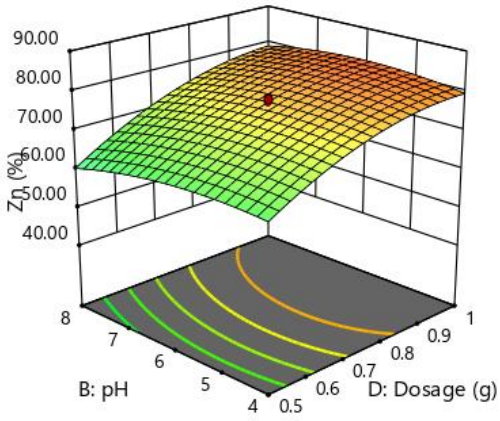

Figure 4.18: 3-D Response plot of adsorbent dosage (SCBAC) and pH on the removal efficiency of Zn

Figure 4.17 shows the response surface plot of the interaction effect of SCBAC dosage and temperature on the removal efficiency of Zn at a contact time of 70 minutes and pH of 6. In terms of interaction effect of adsorbent dosage and temperature an optimum removal efficiency of 77.28 % at an adsorbent of 0.75 g and temperature of 50^{o}C. The plot showed that higher dosage of SCBAC with temperature increased adsorption rate of Zinc ion.

Figure 4.18 shows the response surface plot of the interaction effect of SCBAC dosage and pH on the removal efficiency of Zn at a contact time of 70 minutes and temperature of 50^{o}C. In terms of interaction effect of adsorbent dosage and pH an optimum removal

efficiency of 77.28% at an adsorbent of 0.75 g and pH of 6. From the plot acidic pH with increase in dosage gave a better removal efficiency of Zinc ion.

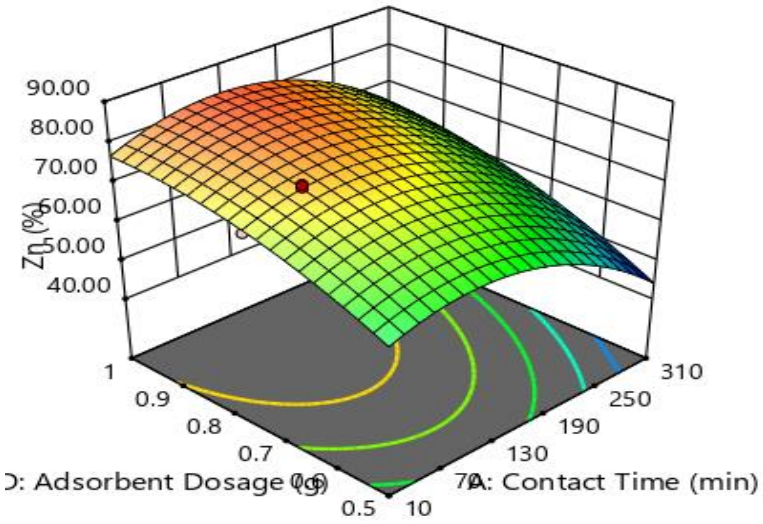

Figure 4.19: 3-D Response plot of adsorbent dosage and contact time on the removal efficiency of Zn (SCBAC)

Figure 4.19 shows the response surface plot of the interaction effect of SCBAC dosage and contact time on the removal efficiency of Zn at a pH of 7 and temperature of 50^{o}C. In terms of interaction effect of adsorbent dosage and contact time an optimum removal efficiency of 77.6% at an adsorbent of 0.76 g and contact time of 71 minutes. Increased time and dosage gave a better adsorption of Zn ions.

4.8 Effect of Process Parameters on the Adsorption Process

The effect of the process parameters: contact time, pH, temperature and adsorbent dosage on the percentage removal of Cr and Zn was studied.

4.8.1 Effect of contact time

The effect of the contact time on the percentage removal of Cr and Zn was studied in Figure 4.20

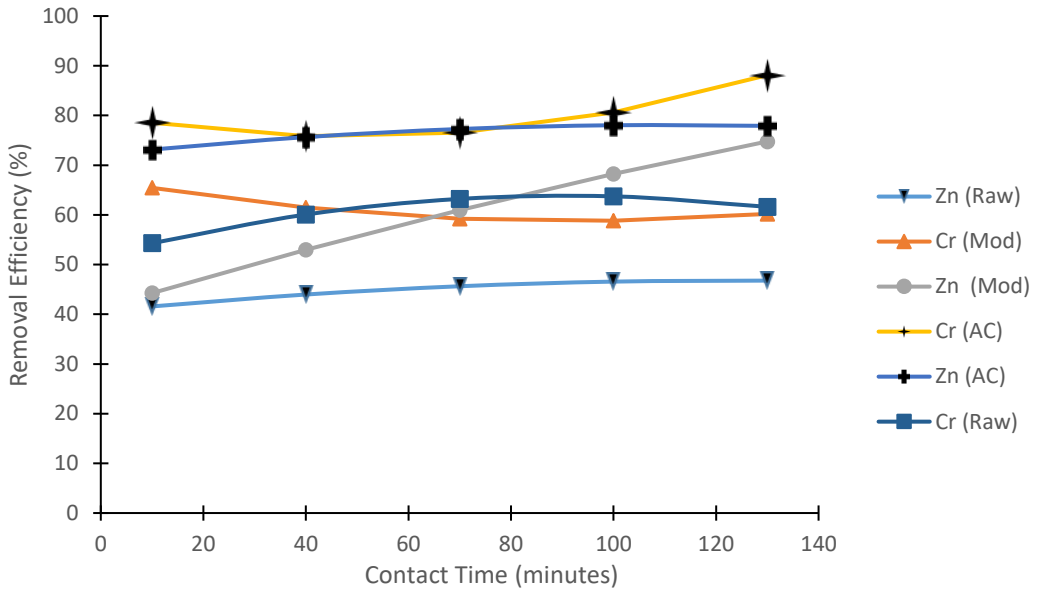

Figure 4.20: Effect of Contact time on Adsorption of Cr and Zn (Experimental conditions: temperature = 50ºC, and adsorbent dosage = .75g

From Figure 4.20 the effect of contact time was studied at optimum conditions of temperature, adsorbent dosage (RSCB, MSCB, and SCBAC) and pH of 50ºC, 0.75 and 6 respectively by varying contact time from 10 to 130 minutes. It was observed that incremental contact time favoured incremental removal efficiency for Cr for RSCB with a maximum removal of 63.7% and at 100 minutes and a subsequence decrease of 61.6% at 130 minutes while Zn continued to increase with time, the also occurred in MSCB removal of Zn and SCBAC removal of of Cr while Zn removal efficiency increased from 73% at 10 minutes to 78% at 100 minutes and then reduced to 77.9 at 130 minutes. RSCB

for Cr removal. However, at contact time exceeding 80 minutes the removal The fast adsorption may be due to the fact that at initial state higher driving force make transfer of metal ions faster to the surface of adsorbent particles and the presence of the unloaded metal ions on the surface area of the activated carbon. With the further increase in contact time it has taken a long time to attain equilibrium for the adsorption process diffusing slowly into the pores of activated carbon due to the decrease in the presence of the unloaded surface area, the active sites and less driving force. Hence, rate of adsorption process was observed slower. This finding is in agreement with Moubarik and Grimi (2014) findings that increase in contact time increased removal efficiency.

4.8.2 Effect of pH

The effect of the pH on the percentage removal of Cr and Zn was studied in Figure 4.21

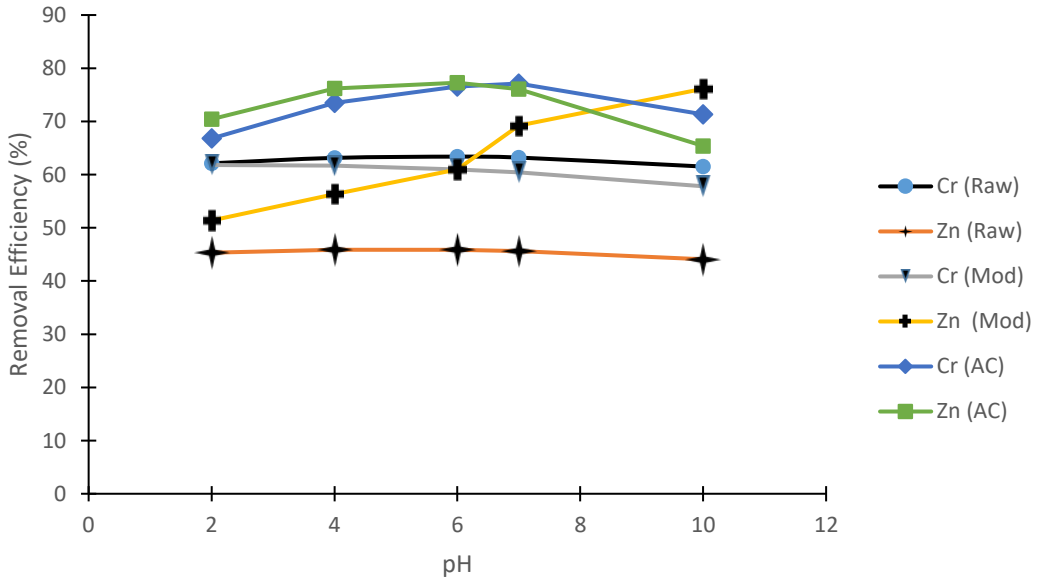

Figure 4.21: Effect of pH on Adsorption of Cr and Zn (Experimental conditions: temperature = 50^{o}C, Contact time = 70 minutes and adsorbent dosage = .75g

From the Figure 4.21 it can be observed increase in pH affected the removal efficiency of Cr upon the sugarcane raw, modified and AC. The solution's pH is significant to adsorption because of the ion-exchange nature of adsorption ions. The effect of pH was studied at constant temperature of 50^{o}C, contact time of 70 minutes and dosage of 0.75 g while varying the pH in the range of 2- 10. The result depicted in Figure 4.30 showed that in the pH range of 2-7 there was increase in removal efficiency Cr and Zn, meanwhile there was continuous increase in removal of Zn using SCB even after the pH was increased above 7 while pH of 8 where further increment led to a decrease in removal of Cr from 76% to 71% and Zn from 76% to 65% using SCBAC. This finding is in agreement with reported work of Man (2018) that the percentage of removal of Cr and Zn increased at acidic and decline at base pH due to the fact that more concentration of protons competes with the metal ions causing decrease in the adsorption process which can also be related to the electrostatic interactions between the adsorbent and the adsorbate in the acidic medium than in the basic medium (Salihi *et al.,* 2016).

4.8.3 Effect of temperature

The effect of the temperature on the percentage removal of Cr and Zn is shown in Figure 4.22

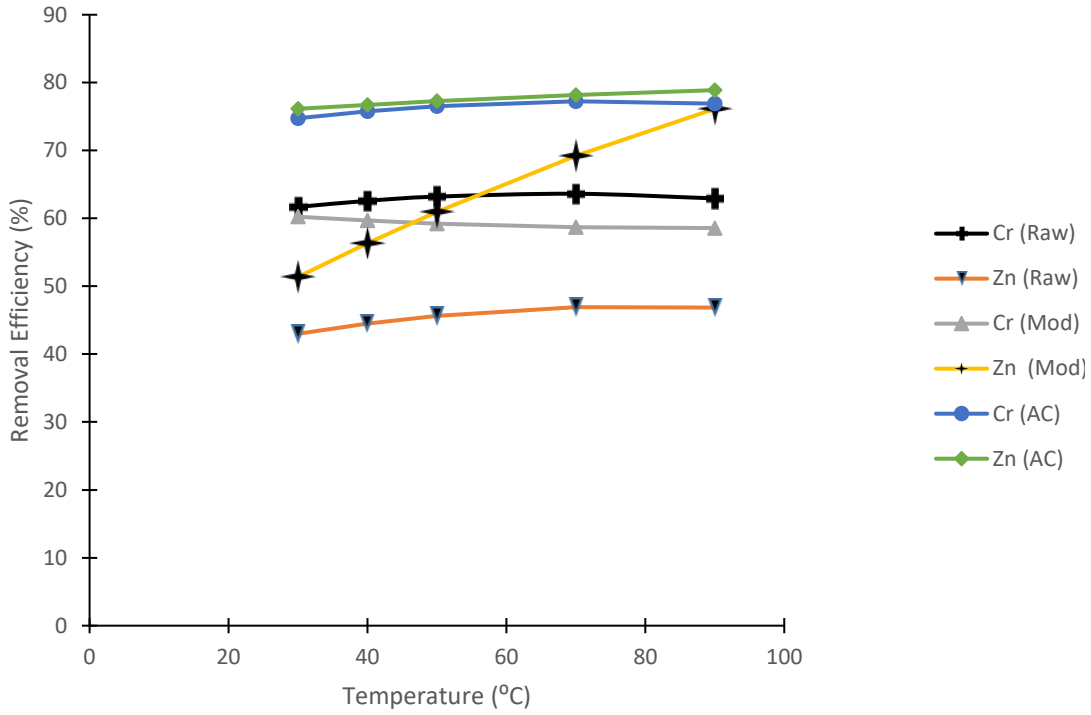

Figure 4.22: Effect of temperature on Adsorption of Cr and Zn (Contact time = 70 minutes and adsorbent dosage = .75 g)

Temperature is another parameter that affects the adsorption of metal ions. The effect is presented in Figure 4.22 at optimum condition of 70 minutes, 0.75 g and pH 6. The effect of temperature on the adsorption process was studied by varying the temperatures from 30℃ to 70℃. The result showed a little but gradual change in removal efficiency in the removal of Cr and Zn when using the raw and AC adsorbent as the temperature is being increased. Meanwhile, continuous increase in temperature in the removal of Zn when using the MSCB. This reveals that an increase in the adsorption temperature resulted in an increase in the removal efficiency, this increment is because increased in temperature facilitates the ionization of the functional groups (adsorption sites) which can increase their movement towards the adsorption of the selected impurities (Yu *et al.*, 2016).

4.8.4 Effect of adsorbent dosage

The effect of the adsorbent dosage on the percentage removal of Cr and Zn was studied for RSCB, MSCB and SCBAC as shown in Figure 4.23. The temperature, contact time and pH were kept constant at optimum conditions of 50°C, 70 minutes, and 6 respectively while varying the RSCB, MSCB and SCBAC dosage from 0.25 – 1.25 g. RSCB had a maximum removal of 66% and 47.2 % for Cr and Zn respectively at 1g, MSCB had a maximum removal of 60.6% and 62.5 % for Cr and Zn respectively at 1 g dosage and SCBAC dosage maximum removal efficiency for Cr at 1.25 g was 90% and Zn at 1 g was 81.6% Further increment of RSCB, lead to a decrease in removal efficiency. Further increase of SCBAC dose led to decrease in adoption. The increase in adsorption when the dosage was increased is due to the increase of surface area in the surface area in the activated carbon which produce more sorption site to be able to adsorb the Cr and Zn according to Adib *et al.,* (2018). Further increment in the dosage resulting to decrease in the removal efficiency can be attributed to the overlapping of the active sites in the adsorbent because of overcrowding thereby hindering further adsorption. This observation is in agreement with the work of Abel *et al.,* (2014).

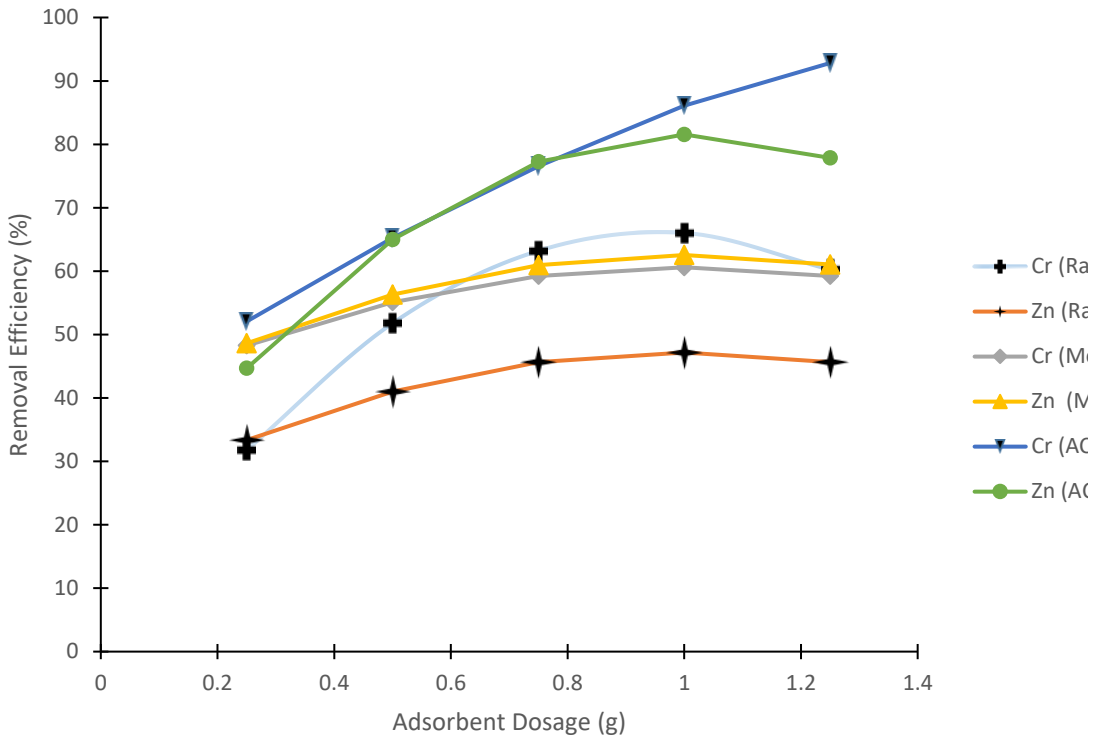

Figure 4.23: Effect of adsorbent dosage on Adsorption of Cr and Zn (Contact time = 70 minutes, temperature =50°C)

4.9 Adsorption Isotherm Studies

An adsorption isotherm can be used to characterize the interaction of adsorbate with adsorbents. The isotherm provides a relationship between the concentration of adsorbate in solution and the amount of adsorbate adsorbed on the solid phase when both phases are in equilibrium (Zhou, *et al.*, (2012). In this study according to the effect of temperature on adsorption, the equilibrium condition was kept at the optimum temperature of the adsorbate (Olorundare, *et al.*, 2014), and the adsoption isotherms were analyzed by Langmuir and Temkin models and thus shown in Table 4.19.

Table 4.19: Adsorption isotherm Values

Heavy Metal	Isotherm	Parameter	Value
Cr (Raw)	Langmuir	Q_o	31.055
		b	0.006
		R_L	0.851
		R^2	0.971
	Temkin	A	0.039
		B	8.027
		R^2	0.963
Zn (Raw)	Langmuir	Q_o	6.863
		b	0.0216
		R_L	0.870
		R^2	0.958
	Temkin	A	0.173
		B	1.653
		R^2	0.945
Cr (Modified)	Langmuir	Q_o	39.062
		b	0.0182
		R_L	0.583
		R^2	0.950
	Temkin	A	0.130
		B	9.808
		R^2	0.974
Zn (Modified)	Langmuir	Q_o	8.285
		b	0.0246
		R_L	0.832
		R^2	0.981
	Temkin	A	0.217

Table 4.19: continues

		B	1.855
		R^2	0.903
Cr (AC)	Langmuir	Q_o	104.166
		b	0.005
		R_L	0.639
		R^2	0.986
	Temkin	A	0.044
		B	26.465
		R^2	0.842
Zn (AC)	Langmuir	Q_o	18.315
		b	0.012
		R_L	0.819
		R^2	0.972
	Temkin	A	0.169
		B	2.996
		R^2	0.928

The model parameters obtained by applying Langmuir and Temkin models to the experimental data are given in Table 4.19. The regression coefficients R^2 values obtained from Langmuir isotherm is closer to one than that of the Temkin model in most cases, suggesting that the Langmuir isotherm fits better with the adsorption of Cr and Zn on raw, modified and AC sugarcane bagasse. The observation came about because the Langmuir isotherm gave higher values of 0.9712, 0.9588, 0.9509, 0.81, 0.9865 and 0. 9729 for Cr (raw), Zn (raw), Cr (modified), Zn (modified) and Cr (AC), Zn (AC) respectively unlike the lower values of R^2 of Temkin isotherm of 0.9632, 0.9454, 0.97478, 0.9036, 0.8427

and 0.9287 for Cr (raw), Zn (raw), Cr (modified), Zn (modified) and Cr (AC), Zn (AC) respectively. The R_L values obtained in all cases lie between 0 and 1 confirming that the adsorption is a favourable process. Hence, according to Akl *et al.*, (2014) it can be concluded that the monolayer Langmuir adsorption isotherm is more suiTable to explain the adsorption of Cr and Zn onto on raw, modified and AC sugarcane. Similar to Zhou, *et al.,* (2012) and Ullah, *et al.,* 2013 the adsorption process was depicted by the Langmuir isotherm model more correctly.

4.10 Adsorption Kinetics Studies

The essence of kinetic model investigation is to find out the stage that plays a vital role to the reaction rate of adsorption. The pseudo first-order and pseudo-second order models were used to test the best model in describing the kinetics of the adsorption process as shown in Table 4.20. The basis for kinetics study is the kinetic isotherms which is obtained experimentally by tracking the adsorbed amount against time.

Table 4.20: Kinetic Parameters for the Adsorption of Cr and Zn

Heavy Metal	Pseudo-first order parameters			Pseudo-second order parameters		
	Qe (mg/g)	k_1 (L min^{-1})	R^2	Qe (mg/g)	K_2 (L min^{-1})	R^2
Cr (Raw)	9.021	0.097	0.811	11.286	0.186	0.976
Zn (Raw)	1.486	0.089	0.716	1.822	1.854	0.966
Cr (Modified)	23.922	0.043	0.944	15.673	0.115	0.978
Zn (Modified)	1.104	0.064	0.963	2.188	0.170	0.970
Cr (AC)	184.048	0..299	0.943	19.762	0.256	0.980
Zn (AC)	5.010	0.148	0.946	2.402	3.126	0.980

The parameter represented in Table 4.20 compared the results obtained for pseudo-first order and pseudo-second order. The pseudo-second order kinetic model represents a better fit of experimental data for the removal of Cr and Zn with high regression coefficient of 0.98, 0.97, 0.98, 0.97, 0.98 and 0.98 respectively. Similarly, the pseudo order model gave a higher rate constant (k_2) and equilibrium adsorption capacity (Qe) for the adsorption process studied. The pseudo second order kinetics model agrees with a higher value for the rate constant (k_2) (which is a measure of the affinity of the adsorbent for the metal ion and has a direct relationship with the removal efficiency) for Cr and Zn. Such finding is also in good agreement with previous studies (Aloma, *et al.*, 2012).

4.11 Thermodynamic Studies

The Gibb's free energy (ΔG^o), enthalpy change (ΔH^o) and entropy change (ΔS^o) obtained for the thermodynamic studies are shown in Table 4.21.

Table 4.21: Thermodynamic parameters for the Uptake of Cr and Zn on RSCB, MSCB and SCBAC

Heavy Metal	Temperature (K)	LnKc=Ln(Q/C)	ΔH^o (kJ mol^{-1})	ΔS^o (kJ mol^{-1} K^{-1})	ΔG^o (kJ mol^{-1})
Cr (Raw)	303	2.466	-5.440	2.771	-6.212
	313	2.447			-6.367
	323	2.380			-6.391
	333	2.301			-6.372
	343	2.221			-6.364
Zn (Raw)	303	2.393	-3.721	7.875	-6.028
	313	2.392			-6.227

Table 4.21: continues

	323	2.369			-6.363
	333	2.302			-6.375
	343	2.219			-6.329
Cr (Mod)	303	1.704	-1.5876	3.7975	-4.293
	313	1.531			-3.986
	323	1.347			-3.618
	333	1.194			-3.306
	343	0.953			-2.719
Zn (Mod)	303	2.187	-5.168	0.865	-5.511
	313	2.036			-5.300
	323	2.032			-5.459
	333	1.991			-5.514
	343	1.912			-5.654
Cr (AC)	303	0.879	-4204	5.503	-2.215
	313	1.057			-2.752
	323	1.006			-2.703
	333	0.873			-2.417
	343	0.716			-2.043
Zn (AC)	303	1.730	-2.641	6.101	-4.360
	313	1.830			-4.504
	323	1.699			-4.564
	333	1.691			-4.683
	343	1.644			-4.690

The calculated values of the thermodynamic parameters are given in Table 4.21. As shown in the Table that ΔG^{o} values are the negative at all temperature indicate the feasibility of the process and the spontaneous nature of the adsorption of Cr and Zn onto (raw, modified, and AC) sugarcane bagasse with high affinity for Cr and Zn. The negative

value of ΔH^{o} reveals that the adsorption process for of Cr and Zn onto (raw, modified, and AC) sugarcane bagasse was exothermic and physical in nature (Adegoke *et al.*, 2017). Furthermore, positive values of ΔS^{o} indicates an irregular increase of randomness, reflects the affinity towards the adsorbent and increased disorderliness at the solid-solution interface and the driving force during the adsorption process (Zhou, *et al.*, (2012).

CHAPTER FIVE

5.0 CONCLUSION AND RECOMMENDATIONS

5.1 Conclusion

The proximate and ultimate analysis confirmed that SCB is carbonaceous, which has low moisture (6.79%) and ash (3.79%) content; presence of high carbon (43.6%) and oxygen contents (39.87). The FT-IR analysis showed the presence of hydroxyl, amine, carbonyl and phenolic groups, which are responsible for the adsorption of the Cr and Zn ions from the effluent. The BET method were used to deduce the effective surface area, the SCBAC BET was found to have surface area, pore volume and pore diameter of 954.4 m^2/g, 0.628 cm^3/g and 2.853 nm respectively which provided the active sites for the adsorption of the ions.

Response surface methodology and central composite rotatable design were appropriate for determining the optimal conditions for Cr and Zn ions adsorption onto RSCB, MSCB and SCBAC. The optimal conditions of adsorption established by RSM were as follows: temperature of 50ºC, contact time of 70 minutes, 0.75 g of adsorbent dosage and pH of 6 for RSCB, MSCB and SCBAC.

The Langmuir model better describes the adsorption of Cr and Zn ions using SCBAC process because the R_L (0.6 and 0.8 respectively) are between 0 & 1 and R^2 closer to 1 (0.99 and 0.97 respectively), indicating that the adsorption process is favourable and it is a mono layer adsorption. The pseudo-second-order kinetics of the adsorption of Cr and Zn ions using SCBAC was found to have better fit to the kinetics behavior of the adsorption process due to the R^2 are closer to 1 (0.98 and 0.98 respectively). The thermodynamic parameters for the adsorption process were evaluated, ΔS^o as positive which shows disorderliness, $\Delta H^o$was negative thus, exothermic reaction of the adsorption

process and $\Delta G^{o}$was negative which suggests the process is spontaneous. The results of this study however showed the potential of sugarcane residue to be used (SCB as a source to produce added value) for the removal of Cr and Zn ions.

5.2 Recommendations

This work involves the use of raw, modified and activated carbon sugarcane bagasse for the removal of heavy metals from electroplating water.

The following suggestions for future work are recommended:

1. Further characterization of the spent adsorbent and its reuse may be of further scope of research.
2. Development of a feasible economical method for the regeneration of the adsorbent.
3. Establishing a proper laboratory scale unit and extending the present work to include the effect of other operating conditions such as impregnation ratio, impregnation time, particle size and agitation speed on removal of heavy metals.should be optimized.

5.3 Contribution to knowledge

This research work compared the adsorption efficiency of the sugarcane bagasse in its raw, modified and activated carbon which was 69.05%, 70.88% and 91.63% respectively for Cr ion removal and 49.67%, 66.00% and 84.88% respectively for Zn ion.

The optimum condition for removal of Cr and Zn was at 50^{o}C, 70 minutes, 1 g and pH of 6 using H_3PO_4 as an activating agent.

REFERENCES

Abdelhafez, A. A., & Li, J. (2016). Removal of Pb (II) from aqueous solution by using biochars derived from sugar cane bagasse and orange peel. *J Taiwan Inst Chem Eng*, 61, 367–375

Adegoke, H. I., Adekola, F. A., & Abdulraheem, M. N. (2017). Kinetic and Thermodynamic Studies on Adsorption of Sulphate from Aqueous Solution by Magnetite, Activated carbon and Magnetite-Activated Carbon Composites. Nigerian Journal of Chemical Research, 22 (1), 39-69

Adib, M. R. M, Attahirah, M. H. M. N., & Amirza, A. R. M. (2018). Phosphoric acid activation of sugarcane bagasse for removal of o-toluidine and benzidine. *IOP Conf. Series: Earth and Environmental Science*. 140 012029 doi: 10.1088/1755-1315/140/1/012029

Adib, M. R. M., Suraya, W .M. W., Rafidah, H., Amirza, A. R. M., Attahirah, M. H. M. N, Hani, M. S. N. Q., & Adnan, M. S. (2015). Effect of Phosphoric Acid Concentration on the Characteristics of Sugarcane Bagasse Activated Carbon. *Soft Soil Engineering International Conference*, 136 012061, doi:10.1088/1757-899X/136/1/012061

Akl, A. A. M., Dawy, M. B. & Serage, A. A. (2014). Efficient Removal of Phenol from Water Samples Using Sugarcane Based Activated Carbon. *Journal of Analytical and Bioanalytical Techniques*, 5(2), 1-12

Alhassan, M., Andrew, I., Auta, M., Umar, M., Garba, M. U., Isah, A. G., & Alhassan, B. (2017). Comparative Studies of CO_2 Capture Using Acid and Base Modified Activated Carbon from Sugarcane Bagasse. *Biofuels*, DOI:10.1080/17597269.2017.1306680

Ali, I., Asim, M., & Khan, T. A. (2012). Low-Cost Adsorbent for the Removal of Organic Pollutants from Wastewater. *Journal of Environmental Management*, 113C, 170-183.

Aloma, I., Martın-Lara, M. A. Rodrı´guez, I.L, Bla´zquez, G., & Calero, M. (2012). Removal of nickel (II) ions from aqueous solutions by biosorption on sugarcane bagasse. *Journal of the Taiwan Institute of Chemical Engineers*, 43, 275–281

ALOthman, Z. A., Naushad, M. & Ali, R. (2013). Kinetic, Equilibrium Isotherm and Thermodynamic Studies of Cr (VI) Adsorption onto Low-Cost Adsorbent Developed from Peanut Shell Activated with Phosphoric Acid. *Environ Sci Polluct Res*, 20, 3351-3365.

Amari, A., Gannouni, H., Khan, M. I., Almesfer, M. K., Elkhaleefa, A. M., & Gannouni, A. (2018). Effect of structure and chemical activation on the adsorption properties of green clay minerals for the removal of cationic dye. Applied Sciences, 8(11), 2302. https://doi.org/10.3390/app8112302

Amin N. K (2008). Removal of reactive dye from aqueous solutions by adsorption onto activated carbons prepared from sugarcane bagasse pith. *Desalination*, 223, 152–161

Aragaw T. A., (2016)Proximate Analysis of Cane Bagasse and Synthesizing Activated Carbon: Emphasis on Material Balance. *Journal of Environmental Treatment Techniques,* 4(4), 102-110.

Awala, H. A., & El Jamal, M. M. (2011). Equilibrium and kinetics study of adsorption of some dyes onto feldspar. *Journal of the University of Chemical Technology & Metallurgy*, 46(1).

Aziz, H. A., Adlan, M. N., & Ariffin, K. S., (2008). Heavy metals (Cd, Pb, Zn, Ni, Cu and Cr(III)) removal from water in Malaysia: posttreatment by high quality limestone. *Bioresour. Technol*. 99, 1578–1583

Babel, S. and Kurniawan, T. A. (2004). Cr (VI) Removal from Synthetic Wastewater Using Coconut Shell Charcoal and Commercial Activated Carbomn Modified with Oxidizing Agents and/or Chitosan. *Chemosphere,* 54, 951-967.

Bachrun, S. Noni, A. R., Annisa, S.H & Arif, H. (2016). Preparation and Characterization of Activated Carbon from Sugarcane Bagasse by Physical Activation with CO_2 gas. *IOP Conference Series: Materials Science and Engineering*, 105, 1-9

Bahadur, K. D., & Paramatma, M. (2014). Adsorptive Removal of Cr (VI) from Aqueous Solution by Sugarcane Biomass. *Research Journal of Chemical Sciences,* 4 (5), 32-40.

Balasundram, V., Ibrahim, N., Kasmani, R. M., Isha, R., Hamid, M. K. A., Hasbullah, H. & Ali, R. R. (2018) Catalytic Upgrading of Sugarcane Bagasse Pyrolysis Vapours over Rare Earth Metal (Ce) Loaded HZSM-5: Effect of Catalyst to Biomass Ratio on the Organic Compound in Pyrolysis Oil. *Applied Energy*, 220, 787-799.

Barakat, M. A. (2011). New trends in removing heavy metals from industrial wastewater. *Arabian Journal of Chemistry*, 4, 361–377

Basmadjian, D. (1997). The little adsorption book. *United States of America: CRC Press*, 120.

Bediako J. K., Wei W., Kim S., & Yun Y. (2015). Removal of Heavy metals from Aqueous Phases Using Chemically Modified Waste LyocellFibre. *Journal of Hazardous Materials*, 299, 550-561.

Bradl, H. (2002). Heavy metals in the environment: origin, interaction and remediation. *Academic, London,* 6

Castro, J. B., Bonelli, P. R., Cerrella, E. G., & Cukierman. (2000). Phoshoric Acid Activation of Agricultural Residues and Bagasse from Sugarcane: Influence of

the Experimental Conditions on Adsorption Characteristics of Activated Carbons. *Incl. Eng. Chem. Res.*, 39, 4166-4172.

Castro-González, M. I. & Méndez-Armenta, M. (2008). Heavy metals: Implications associated to fish consumption, *Environmental Toxicology & Pharmacology*, 26, 263-271.

Chao, H., Chang, C., & Nieva, A. (2014). Bisorption of Heavy Metals on Citrus maxima peel, passion fruit shell, and sugarcane bagasse in a fixed-bed column. *Journal of Industrial and Engineering Chemistry*, 20, 3408-3414.

Chimenez, T. A., Gehlen, M. H, Marabezi, K. & Curvelo, A. A. S. (2013). Characterization Sugarcane Bagasse by Auto-fluorescence Microscope. *Cellulose*, 21(1), 653-664.

Cronje, K. J., Chetty, K. Carsky, M., Sahu, J. N., & Meikap, B. C. (2012). Optimization of Chromium (VI) Sorption Potential Using Developed Activated Carbon from Sugarcane Bagasse with Chemical Activation by Zinc Chloride. *Desalination*, 275, 276-285.

Dawood, S., & Sen, T. (2014). Review on dye removal from its aqueous solution into alternative cost effective and non-conventional adsorbents. Journal of Chemical and Process Engineering, 1(104), 1-11.

Deokar, S. K., Mandavgane, S. A., & Kulkarni, B. D. (2016). Adsorptive removal of 2, 4-dichlorophenoxyacetic acid from aqueous solution using bagasse fly ash as adsorbent in batch and packed-bed techniques. Clean Technologies and Environmental Policy, 18(6), 1971-1983.

Dos Santos V. C. G., De Souza J. V. T. M., Tarley C. R. T., & Dragunski D. C. (2012). Copper Ions Adsorption from Aqueous Medium Using the Biosorbent Sugarcane Bagasse in *Natura* and Chemically Modified. *Water Air Soil Pollution*, 216, 351-359.

Duffus, J. H (2002). Heavy metals—a meaningless term? *Pure Appl Chem* 74:793–807

Duran, C., Ozdes, D., & Seturk, H. M. (2011). Kinetic and Isotherm Analysis of Basis Dyes Adsorption onto Almond Shell (*Prunusdulcis*) as a Low-Cost Adsorbent. *Journal of Chemical Engineering Data*, 56(5), 2136-2147.

Edgar, T. F., Himmelblau, D. M, & Lasdon, L. S. (2001). Optimization of Chemical Processes. *McGraw-Hill Chemical Engineering Series*. Second Edition, 1-667

Fergusson J. E (1990). The heavy elements: chemistry, environmental impact and health effects. Pergamon, Oxford

Fomina, M. and Gadd, G.M. (2014). Bisorption: Current Perspectives on Concept, Definition and Application. *Bioresources Technology*, 160, 3-14.

Garg U. K., Kaur M. P., Sud D., & Garg V. K. (2009). Removal of Hexavalent Chromium from Aqueous Solution by Adsorption on Treated Sugarcane Bagasse Using Response Surface Methodological Approach. *Desalination*, 249, 475-479.

Gholizadehet, A., Kermani, M., Gbolami, M., & Farzadkia, M., (2013). Kinetic and isotherm studies of adsorption and bio-sorption processes in the removal of phenolic compounds from aqueous solutions: comparative study. *Journal of Environmental Health Sciences & Engineering*, 11, 29. Retrieved from http://www.ijehse.com/content/11/1/29

Gin, W. A., Jimoh, A., Abdulkareem, A. S. & Giwa, A. (2014). Kinetics and Isotherm Studies of Heavy Metal Removals from Electroplating Wastewater Using Cassava Peel Activated Carbon. *International Journal of Engineering Research & Technology (IJERT)*, 3(1), 25-34

Giusto, L. A. R., Pissetti, F. L., Castro, T. S., & Magalhaes, F. (2017). Preparation of Activated Carbon from Sugarcane Bagasse Soot and Methylene Blue Adsorption. *Water Air Soil Pollut*, 228-249

Gupta, V. K. & Ali, I. (2004) Removal of lead and chromium from wastewater using bagasse fly ash—a sugar industry waste. *J Colloid Interface Sci*, 271, 321–328

Hamelink, J. L, Landrum, P. F., Harold B. L, & William, B. H., (1994). Bioavailability: physical, chemical, and biological interactions. *CRC, Boca Raton,1,* 83–98

Harvey, L. J, & McArdle, H. J., (2008) Biomarkers of copper status: a brief update. *British Journal of Nutrition*, 99, S10-S13.

He Z. L., Yang X. E., & Stoffella P. J. (2005) Trace elements in agroecosystems and impacts on the environment. *J Trace Elem Med Biol* 19:125–14

Helen K. M., I.R., Magesh, G. P., & Lima R. M. (2009). Modelling, analysis and optimization of adsorption parameters for H_3PO_4 activated rubber wood sawdust using response surface methodology (RSM). *Colloids and Surfaces B: Biointerfaces* 70, 35–45

Joseph, C. G., Puma, G. L., Bono, A., Taufiq-Yap, Y. H. & Krishhnaiah D. (2011). Operating Parameters and Synergistic Effects of Combining Ultrasound and Ultraviolent Irradiation in the Degradation of 2, 4, 6-Trichlorophenol. *Desalination*, 276(1-3), 303-309.

Kabata-Pendia A., (2001). Trace Elements in Soils and Plants, *CRC, Boca Raton,* 3, 83–98.

Khadijah C. O., Fatimah C. O., Aina, N., Misnon, F., & Hanim, K. (2012). Utilization of sugarcane bagasse in the production of activated carbon for groundwater treatment. *International Journal of Engineering and Applied Sciences*, 1(2), 76-85

Khoo, R. Z., Chow W. S., & Ismail, H. (2018). Sugar Bagasse Fiber and Its Cellulose Nanocrystals for Polymer Reinforcement and Heavy-metals Adsorbent: A review. *Cellulose*, 25(8), 4303-4330

Khormzadeh, E., Nasernejad B., & Halladj, R. (2013). Mercury biosorption from Aqueous Solutions by Sugarcane Bagasse. *Journal of the Taiwan institute of chemical engineers*, 44, 266-269

Kim, Y. S. & Kim, J. H. (2018). Isotherm, kinetic and thermodynamic studies on the adsorption of paclitaxel onto Sylopute, *Journal of Chemical Thermodynamics*, doi: https://doi.org/10.1016/j.jct.2018.10.005

Klemm, D., Heublein, B., Fink, H. P., & Bohn A. (2005). Cellulose: Fascinating Biopolymer and Sustainable Raw Material. *Angewandte Chemie International Edition*, 44(22), 3358-3393.

Kolawole, M. Y., Aweda, J. O. & Abdulkareem, S. (2017). Archachatina marginata bio-shells as reinforcement material in metal matrix composites. *International Journal of Automotive and Mechanical Engineering,* 14(1), 4068 – 4079.

Kong, W., Ren, J., Wang, S., and Chen, Q. (2014). Removal of heavy metals from aqueous solutions using acrylic-modified sugarcane bagasse-based adsorbents: Equilibrium and Kinetic studies. *Bioresources*, 9(2), 3184 – 3196.

Krishman, K. A., Sreejalekshmi, K. G. & Baiju R. S. (2011). Nickel (II) Adsorption *Bioresources Technology* onto Biomass Based Activated Carbon Obtained from Sugarcane Bagasse Pith, 102, 10239-10247.

Kumar, A., Negi, Y. S., Choudhary, V., & Bhardwaj, N. K., (2013). Characterization of Cellulose Nanocrystals Produced by Acid-Hydrolysis from Sugarcane Bagasse as Agro-Waste. *Journal of Materials Physics and Chemistry*, 2(1), 1-8

Kurniawan, T. A., Chan, G. Y. S., Lo, W. H., & Babel, S., (2006). Physicochemical treatment techniques for wastewater laden with heavy metals. *Chem. Eng. J.* 118, 83–98.

Lavanya, D., Kulkarni, P. K., Dixit, M., Raavi, P. K. & Krishna, N. V. (2011). Sources of Cellulose and their Applications – A Review. *International Journal of Drug Formulation and Research*, 2 (6), 19-38

Leimkuehler, E. P. & Suppes, G. J. (2010). Production, Characterization and Applications of Activated Carbon. (Unpublished Master's Thesis). Faculty of Graduate School, University of Missouri.

Li, Z., Kong, Y. & Ge, Y. (2015). Synthesis of Porous Lignin Xanthate Resin for Pb2+ Removal from Aqueous Solution. *Chemical Engineering Journal*, 270, 229-234.

Loh, Y. R., Sujan, D. & Das, C.A. (2013). Sugarcane Bagasse-The Future of Composite Material: A Literature Review. *Resource Conserve Recycle*, 75, 14-22.

Man, S.R. (2018). Studies on Adsorption Isotherms and Adsorption Kinetics of the Removal of Pb(II) from Aqueous Solution onto Activated Carbon Prepared from Lapsi Seed Stone. *International. Journal of Advanced Social Science*, 1(2), 1-10.

Ming-Ho, Y. (2005). Environmental Toxicology: Biological and Health Effects of Pollutants, Chap.12, CRC Press LLC, ISBN 1-56670-670-2, 2nd Edition, BocaRaton, USA

Mishra, S. R., Chandra, R., Kaila A. J., & Darshi B. S., (2016). Kinetics and Isotherm studies for the adsorption of metal ions onto two soil types. *Environmental Technology & Innovation*, http://dx.doi.org/10.1016/j.eti.2016.12.006

Mohanty, S., Verma, S. K., & Nayak, S. K. (2006). Dynamic Mechanical and thermal properties of MAPE Treated Jute/HDPE Composites. *Composites Science and Technology*, 66 (3-4), 538-547.

Mohlala, L. M., Bodunrin, M. O., Awosusi, A. A., Daramola, M. O., Cele, N. P. & Olubambi, P. A. (2016). Beneficiation of Corncob and Sugarcane Bagasse or Energy Generation and Materials Development in Nigeria and South Africa: A Short Overview. *Alexandra Engineering Journal*, 1-12

Moore, P. H., Paterson, A. P., & Tew, T. (2014). Sugarcane: The Crop, the Plant, and Domestication. *Sugarcane: Physiology, Biochemistry, and Functional Biology*, 1, 1-17.

Morais, S., Garciaa e Costa, F., & Pereira, M. (2014). Human Metals and Human Health. *Environmental Health-Emerging Issues and Practice*, 227-246

Moubarik, A. & Grimi, N. (2015). Valorization of Olive Stone and Sugarcane Bagasse By-Products as Bisorbents for the Removal of Cadiumfrom Aqueous Solution. *Food Res In*t, 73, 169-175.

Mugure, W. N. (2014). Investigation of the Performance of Natural Fibres as a Micro Reinforcement in Concrete. (Unpublished Bachelor Dissertation). Department of Civil and Construction Engineering, University of Nairobi, Kenya.

Muriuki, C. W. (2015). *Evaluation of Banana Peels, Pumice and Charcoal Potential to Adsorb Chromium Ions from Tannery Wastewater.*

Nmadu, J. N., Ojo, M. A., and Ibrahim, F. D. (2013). Prospects of Sugar Production and Imports: Meeting the Sugar Demand of Nigeria by Year 2020. *Russian Journal of Agriculture and Socio-Economic Sciences*, 2(14), 15-25.

Olorundare, O. E., Msagati, T. A., Karuse, R. W. M., Okonkwo, B. B., & Mamba, B.B. (2014). Activated Carbon from Ligneocellulosic Waste Residues: Effect of

Activating Agent on Porosity Characteristics and Use as Adsorbents for Organic Species. Water Air Soil Pollut, 225

Pehlivan, E., peg, H. T., Ouedraogo, W. K. I., Schmidt, C., Zachmann, D. & Bahadir, M. (2013). Sugarcane Bagasse Treated with Hydrous Ferric Oxide as A Potential Adsorbent for the Removal of As (V) from Aqueous Solutions. *Food Chemistry*, 138, 133-138.

Pereira, P. H. F., Voorwarld, H. L. C., Cioffi, M. O. H., Mulinari, D. R., Lux, S. M. D. & Silva, M. L. C. P. (2011). Sugarcane Bagasse Pulping and Bleaching: Thermal and Chemical Characterization. *Bio Resources*, 6, 2471-2482.

Priyadarshini, B., Rath, P. P., Behera, S. S., Panda, S. R., Sahoo, T. R. & Parhi, P. K.; (2018). Kinetics, Thermodynamics and Isotherm studies on Adsorption of Eriochrome Black-T from aqueous solution using Rutile TiO2. IOP Conf. Series: Materials Science and Engineering 310 012051 doi:10.1088/1757-899X/310/1/012051

Putra, P. W., Kamari, A., Yusoff, S. N. M., Ishak, C. F., Mohamed, A., Hashim N. & Illyas, M. A. (2014). Biosorption of Cu (II), Pb (II) and Zn (II) Ions from Aqueous Solution Using Selected Waste Materials: Adsorption and Characterisation Studies. *Journal ofEncapsulation AdsorptionScience*, 4, 25-35.

Putro, J. N., Kurniawan, A., Suryadi I., & Ju, Y. (2017). Nanocellulose based biosorbents for wastewater treatment: Study of isotherm, kinetic, thermodynamic and reusability, *Environmental Nanotechnology. Monitoring and Management*. http://dx.doi.org/10.1016/j.enmm.2017.07.002.

Raghuvanshi S. P., Singh R, Kaushik C. P., & Raghav A. K. (2004) Kinetics study of methylene blue dye bioadsorption on baggase. *Appl Ecol Environ Res*, 2, 35–43

Renu, A. M., & Singh, K. (2017). Methodologies for Removal of Heavy-Metal ions from wastewater: An Overview. *Interdisciplinary Environmental Review*, 18(2), 124-142.

Richardson, J. F., & Harker J. H. and Backhurst, J. R. (2002). Particle Technology and Separation Processes. *Coulson and Richardson's Chemical Engineering*, 2(5), 974

Ruthven, D. M. 1984. Principles of adsorption & adsorption processes. *Canada: Wiley Interscience Publications.*

Sarker, C. T., Shah, G. A., Ahmed M. A. E., Salvatore A. G., & Giuliano B. (2017). Sugarcane bagasse: a potential low‑cost biosorbent for the removal of hazardous materials. *Clean Techn Environ Policy*, DOI 10.1007/s10098-017-1429-7

Salihi, I. U., Kutty, S. R. M., Isa, M. H., Umar, U. A., & Olisa, E. (2016). Sorption of Copper and Zinc from Aqueous Solutions by Microwave Incinerated Sugarcane Ash. *Applied Mechanics and Materials*, 835, 378-385.

Salmam, J. M. Njoku, V. O. & Hameed B. H. (2011). Adsorption of Pesticides from Aqueous Solution onto banana stalk Activated carbon. *Chemical EngineeringJournal,* 174(1), 41-48.

Sulaiman, M., Abdulsalam, Z., & Damisa, O. (2015). Profitability of Sugarcane Production and Its Contribution to Farm Income of Farmers in Kaduna State, Nigeria. *Asian Journal of Agricultural Extension, Economics & Sociology*, 7(2): 1-9

Tadda, M. A., Ahsan, A., Shitu, A., ElSergany, M., Arunkumar T., Jose, B, Razzaque, M. A, & Daud, N. N. N. (2016). A review on activated carbon: process, application and prospects. *Journal of Advanced Civil Engineering Practice and Research*, 2(1), 7-13.

Tchounwou, P. B., Yedjou, C. G., Patlolla, A. K., & Sutton D. J. (2012). Heavy Metal Toxicity and the Environment.

Teixera, C. R & Arruda, M. A. (2004). Bisorption of heavy metals using rice-milling by-products. Characterization and application for removal of metals from aqeous effluents. *Chemosphere*, 54, 987-995.

Tran, V. T., Quynh, B. T. P., Phung, T. K., Ha, G. N., Nguyen, T. T., & Bach, L. G. (2017). Preparation of Activated Carbon from Sugarcane Bagasse Using Zncl2for the Removal of Cu (II) Ion from Aqueous Solution: Application of Response Surface Methodology (RSM). *Journal of Science and Technology*, 54 (1A), 277-284.

Ullah, I., Nadeem, R., Iqbal, M., & Manzoor, Q. (2013). Biosorption of Chromium onto Native and Immobilized Sugarcane Bagasse Waste Biomass. *Ecological Engineering* 60, 99-107.

USEPA (United States Environmental Protection Agency). (1979). Human Health Effects of Molybdenum in Drinking Water. EPA, 65-77.

Weber Jr., W. J. (1985). Adsorption theory, concepts, and models, in: F.L. Slejko (Ed.), Adsorption Technology: A step-by-step approach to process evaluation and application. *United States of America: Marcel Dekker, Inc.* 3-18

WHO/FAO/IAEA (1996) Trace elements in human nutrition and health. World Health Organization, Geneva

Winarno, A., Amijaya, D. H., & Harijoko, A. (2018). Geochemical characterization of Kutai coals using proximate and ultimate analysis. *IOP Conf. Series: Earth and Environmental Science*, 212, 1-10

Yu, F., Sun, S., Han, S., Zheng, J., & Ma, J. (2016). Adsorption removal of ciprofloxacin by multi-walled carbon nanotubes with different oxygen contents from aqueous solutions. *Chemical engineering journal*, *285*, 588-595.

Yu, J., Wang, L., Chi, R., Zhang Y., Xu, Z., & Guo, J. (2013). Competitive Adsorption of Pb^{2+} and Cd^{2+} on Magnetic Modified Sugarcane Bagasse Prepared by Two Simple Steps. *Applied Surface Science,* 268, 163-170.

Zaini, L.H., Jonoobi, M., Tahir, P.M., & Karimi, S. (2013). Isolation and Characterization of Cellulose Whiskers from Kenaf (Hibiscus cannabinus L.) Bast Fibers. *Journal of Biomaterials and Nanobiotechnology, 2013, 4, 37-44*

Zhou, Y., Jin, Q., Hu, X., Zhang, Q., & Ma, T. (2012). Heavy Metal Ions and Organic Dyes Removal from Water by Cellulose Modified with Maleic Anhydride. *J.Mater. Sci.,* 47, 5019-5029.

APPENDIX A

Langmuir and Temkin Isotherms

I. Chromium (Raw)

W (g)	Co (mg/L)	Ce (mg/L)	V (mL)	Qe (mg/g)	Ce (mg/g)	lnCe	1/Ce=x	1/Qe=y
0.1	233.3611	199.4866	0.05	16.93723	199.4866	5.295747	0.005013	0.059042
0.2	233.3611	173.3489	0.05	15.00304	173.3489	5.155306	0.005769	0.066653
0.3	233.3611	150.05	0.05	13.88518	150.0500	5.010969	0.006664	0.072019
0.4	233.3611	129.5899	0.05	12.9714	129.5898	4.864375	0.007717	0.077093
0.5	233.3611	111.9685	0.05	12.13926	111.9685	4.718218	0.008931	0.082377

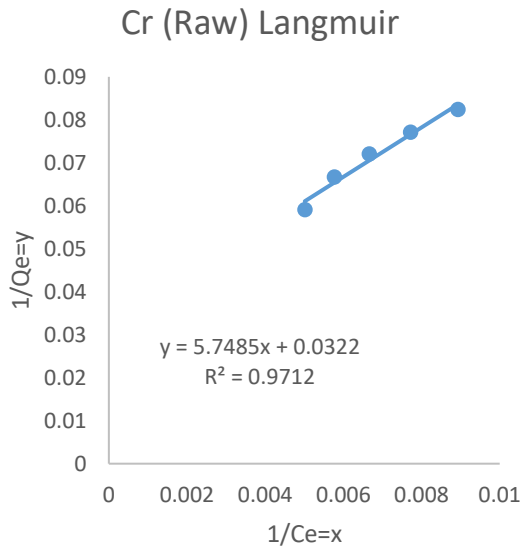

-Figure A1: Langmuir plot of Cr (Raw)

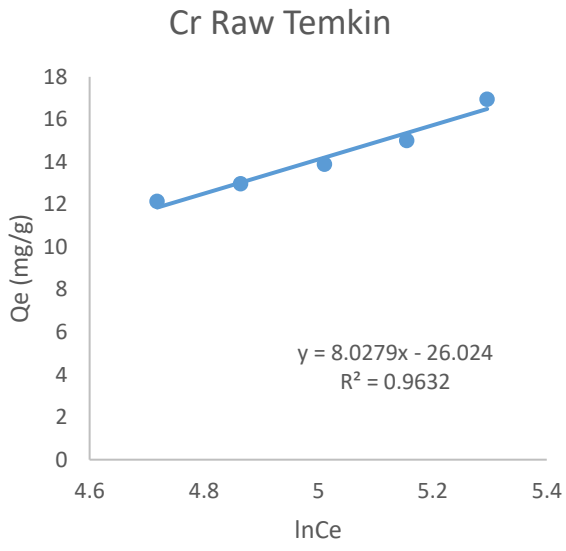

Figure A2: Temkin plot of Cr (Raw)

II. For Zn (Raw)

W (g)	Co (mg/L)	Ce (mg/L)	V (mL)	Qe (mg/g)	LnCe	1/Ce=x	1/Qe=y
0.1	38.186	28.19611	0.05	4.994944	3.339184	0.035466	0.200202
0.2	38.186	23.26892	0.05	3.729271	3.147118	0.042976	0.268149
0.3	38.186	18.21542	0.05	3.32843	2.902269	0.054899	0.300442
0.4	38.186	15.43562	0.05	2.843797	2.736678	0.064785	0.351643
0.5	38.186	13.02952	0.05	2.515648	2.567218	0.076749	0.397512

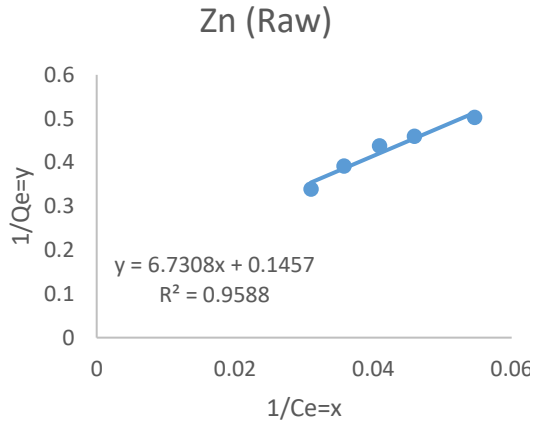

Figure A3: Langmuir plot of Zn (Raw)

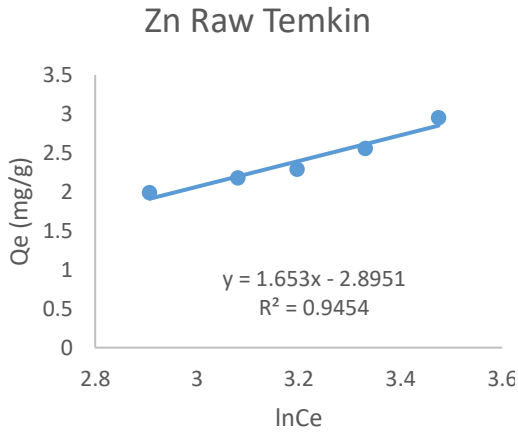

Figure A4:Temkin plot of Zn (Raw)

III. Chromium (Modified)

W (g)	Co (mg/L)	Ce (mg/L)	V (mL)	LnCe	Qe (mg/g)	1/Ce=x	1/Qe=y
0.1	233.3611	171.1108	0.05	5.1423	31.12516	0.005844	0.032128
0.2	233.3611	125.1616	0.05	4.8296	27.04987	0.00799	0.036969
0.3	233.3611	91.18285	0.05	4.5129	23.69637	0.010967	0.042201
0.4	233.3611	68.17451	0.05	4.2221	20.64832	0.014668	0.04843
0.5	233.3611	40.13657	0.05	3.9148	19.32245	0.019946	0.051753

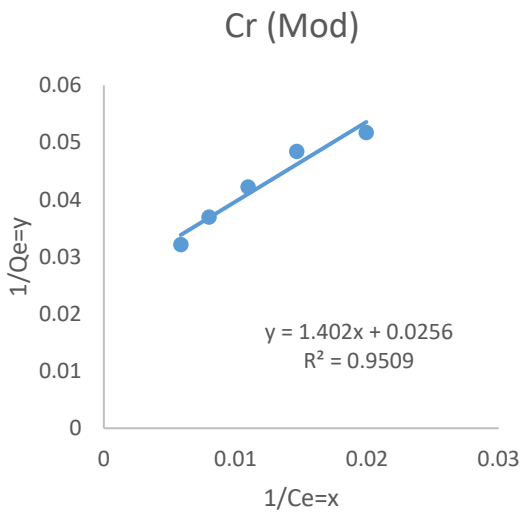

Figure A5: Langmuir plot of Cr (Modified)

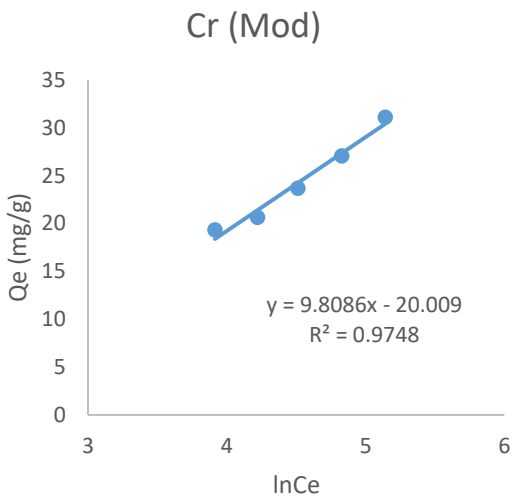

Figure A6:Temkin plot of Cr (Modified)

IV. Zn (Modified)

W (g)	Co (mg/L)	Ce (mg/L)	V (mL)	lnCe	Qe (mg/g)	1/Ce=x	1/Qe=y
0.1	38.186	31.18901	0.05	3.440066	3.498496	0.032063	0.285837
0.2	38.186	25.09432	0.05	3.222641	3.272921	0.03985	0.305537
0.3	38.186	21.38411	0.05	3.062648	2.800316	0.046764	0.357103
0.4	38.186	18.25837	0.05	2.904624	2.490954	0.054769	0.401453
0.5	38.186	15.41712	0.05	2.735478	2.276888	0.064863	0.439196

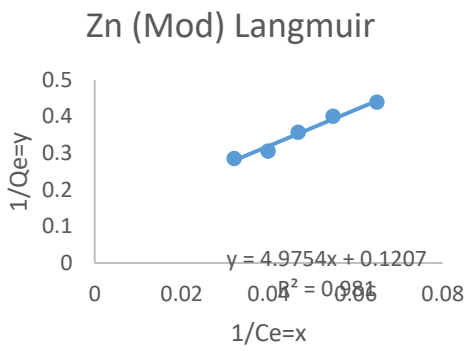

Figure A7: Langmuir plot of Zn (Modified)

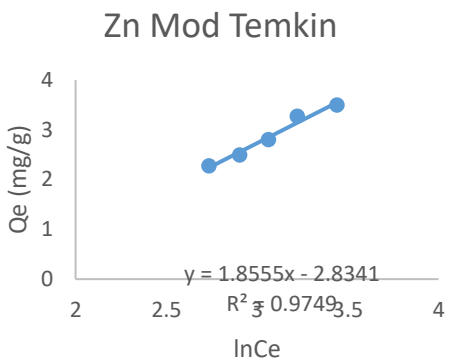

Figure A8: Temkin plot of Zn (Modified)

V. Chromium (AC)

W (g)	Co (mg/L)	Ce (mg/L)	V (mL)	Qe (mg/g)	LnCe	1/Ce=x	1/Qe=y
0.1	233.3611	127.528	0.05	52.91654	4.848336	0.007841	0.018898
0.2	233.3611	97.68899	0.05	33.91803	4.581789	0.010237	0.029483
0.3	233.3611	73.09847	0.05	26.71044	4.291807	0.01368	0.037439
0.4	233.3611	53.75648	0.05	22.45058	3.984464	0.018602	0.044542
0.5	233.3611	39.66296	0.05	19.36981	3.680418	0.025212	0.051627

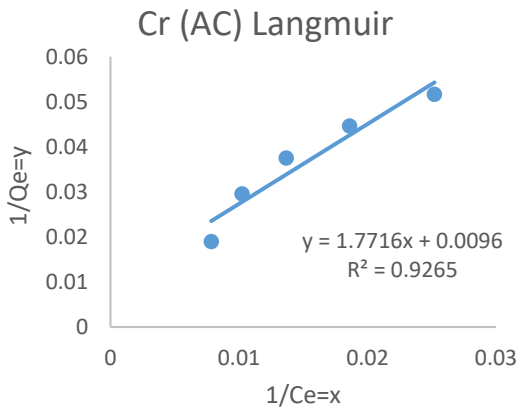

Figure A9: Langmuir plot of Cr (AC)

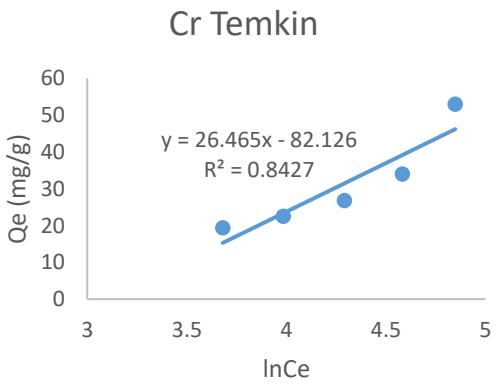

Figure B10: Temkin plot of Cr (AC)

VI. Zn (AC)

W (g)	Co (mg/L)	Ce (mg/L)	V (mL)	Qe (mg/g)	LnCe	1/Ce=x	1/Qe=y
0.1	38.186	28.19611	0.05	4.994944	3.339184	0.035466	0.200202
0.2	38.186	23.26892	0.05	3.729271	3.147118	0.042976	0.268149
0.3	38.186	18.21542	0.05	3.32843	2.902269	0.054899	0.300442
0.4	38.186	15.43562	0.05	2.843797	2.736678	0.064785	0.351643
0.5	38.186	13.02952	0.05	2.515648	2.567218	0.076749	0.397512

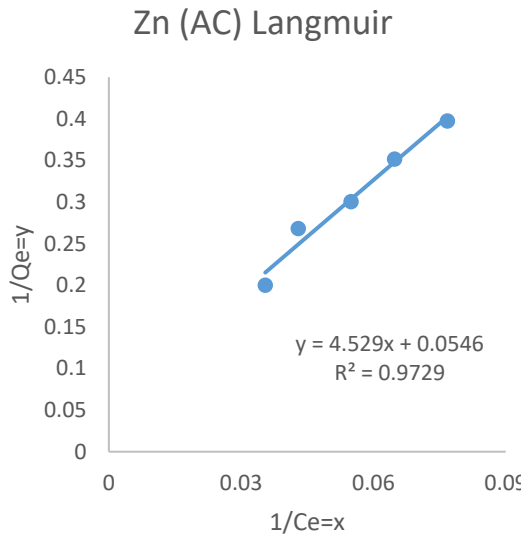

Figure B11: Langmuir plot of Cr (AC)

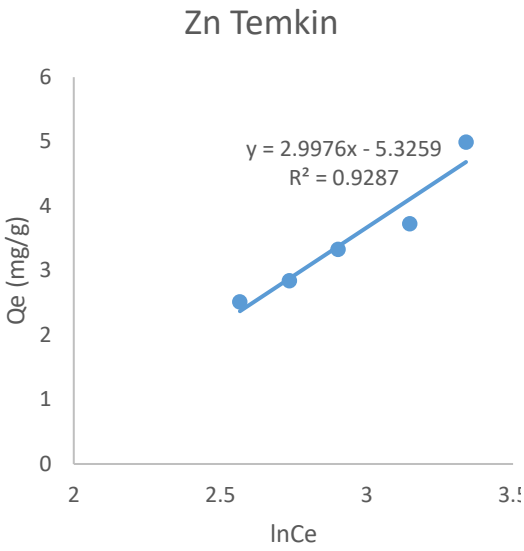

Figure B12: Temkin plot of Cr (AC)

APPENDIX B

Pseudo First and Second Order

I. Chromium (Raw)

t (min)	Co (mg/L)	Ct	Co-Ct	Qt (mg/g)	Qe-Qt	ln(Qe-Qt)	t/Qt
10	233.3611	34.34386	3.842142	1.921071	3.073873	2.117827	5.205429
20	233.3611	27.21442	10.97158	2.742894	0.986377	1.128724	7.291568
30	233.3611	23.89712	14.28888	2.381479	0.94695	0.698076	12.59721
40	233.3611	18.07634	20.10966	2.513708	0.330089	0.233436	15.91275
50	233.3611	15.15224	23.03376	2.303376	0.212271	0.438213	21.70727

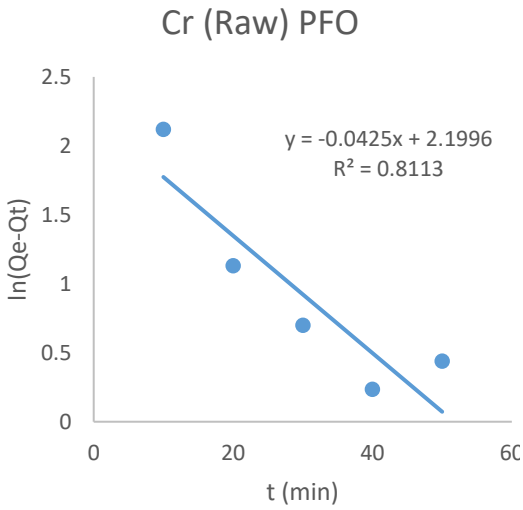

Figure B13: Pseudo First Order plot of Cr (Raw)

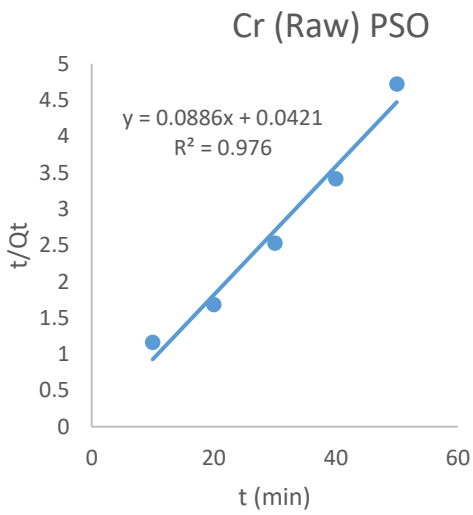

Figure B14: Pseudo Second Order plot of Cr (Raw)

II. For Zn (Raw)

t (min)	Co (mg/L)	Ct (mg/L)	Co-Ct	Qt (mg/g)	Qe-Qt	Ln (Qe-Qt)	t/Qt
10	38.186	35.56553	2.620467	1.310233	1.63917	0.4941	7.6322
20	38.186	29.56333	8.622673	2.155668	0.399216	-0.9182	9.2778
30	38.186	26.79223	11.39377	1.898962	0.388446	-0.9456	15.7981
40	38.186	23.25222	14.93378	1.866722	0.309971	-1.1712	21.42793
50	38.186	20.94332	17.24268	1.724268	0.264415	-1.3302	28.99782

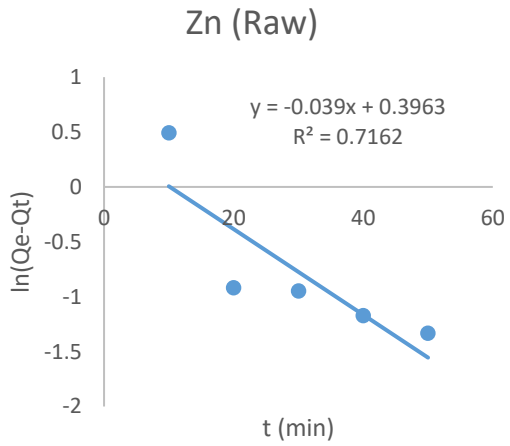

Figure B15: Pseudo First Order plot of Zn (Raw)

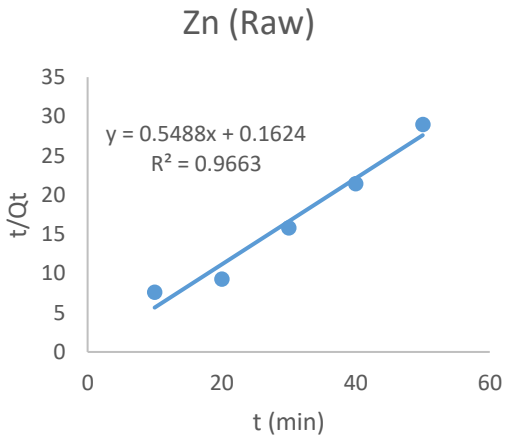

Figure B16: Pseudo Second Order plot of Zn (Raw)

III. Chromium (Modified)

t (min)	Ct	Co-Ct	Qt	Qe-Qt	ln(Qe-Qt)	t/Qt
20	200.9063	32.4548	16.2274	14.89776	2.701211	1.232483
40	173.3261	60.03504	15.00876	12.04111	2.488327	2.66511
60	135.2152	98.14585	16.35764	7.338732	1.993166	3.66801
80	119.5739	113.7872	14.2234	6.424921	1.860184	5.624533
100	70.40193	162.9592	16.29592	3.026537	1.107419	6.136507

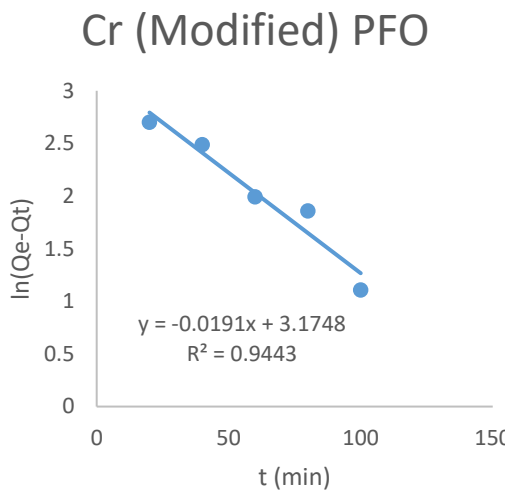

Figure B17: Pseudo First Order plot of Cr (Modified)

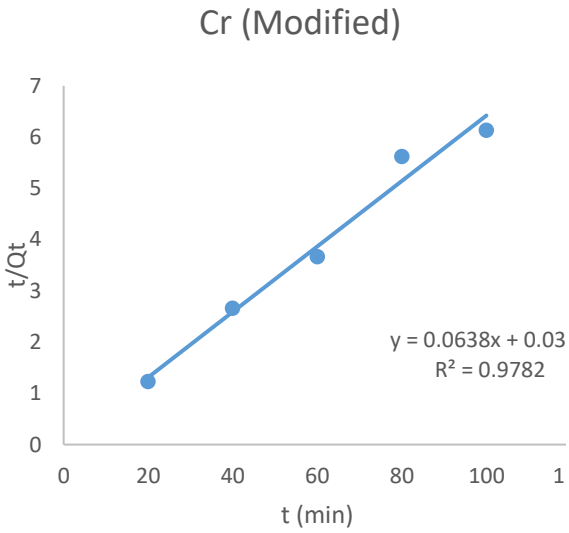

Figure B18: Pseudo Second Order plot of Cr (Modified)

IV. Zinc (Modified)

t (min)	Ct	Co-Ct	Qt	Qe-Qt	ln(Qe-Qt)	t/Qt
20	34.93812	3.24788	1.62394	1.874556	0.628372	12.31573
40	28.20245	9.983553	2.495888	0.777032	-0.25227	16.02636
60	24.0219	14.1641	2.360683	0.439632	-0.82182	25.41637
80	20.32691	17.85909	2.232386	0.258568	-1.3526	35.8361
100	17.39947	20.78653	2.078653	0.198235	-1.6183	48.10807

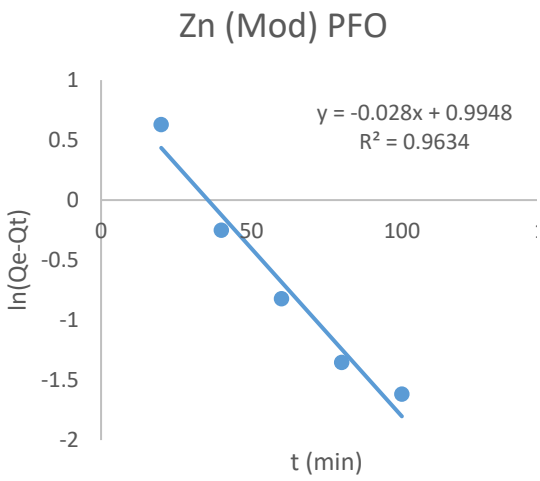

Figure B19: Pseudo First Order plot of Zn (Modified)

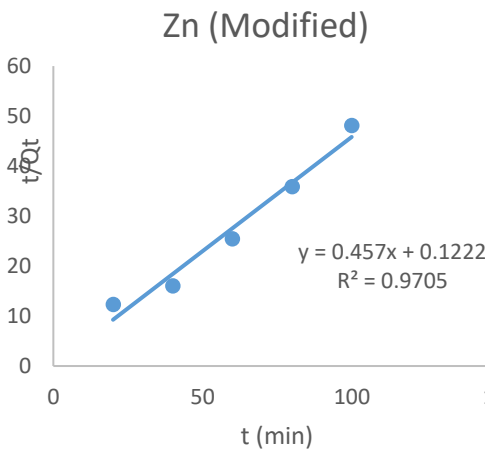

Figure B20: Pseudo First Order plot of Zn (Modified)

V. Chromium (AC)

t (min)	Ct	Co-Ct	Qt	Qe-Qt	ln(Qe-Qt)	t/Qt
10	190.8428	42.51829	21.25914	31.6574	3.454972	0.470386
20	158.797	74.5641	18.64103	15.277	2.726348	1.072902
30	122.9408	110.4203	18.40338	8.307062	2.117106	1.630136
40	61.17441	172.1867	21.52334	0.927241	-0.07554	1.858448
50	41.59764	191.7635	19.17635	0.193468	-1.64264	2.607379

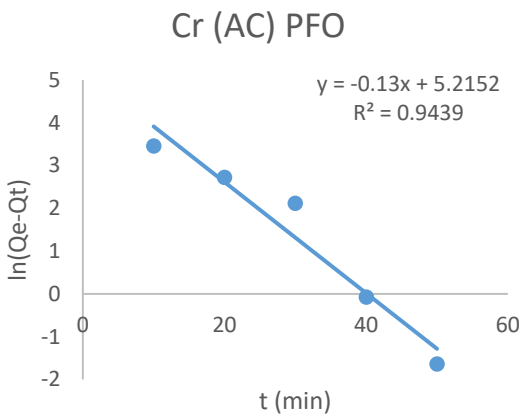

Figure B21: Pseudo First Order plot of Cr (AC)

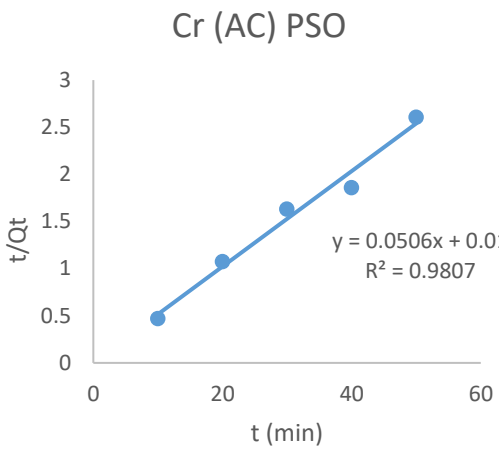

Figure B22: Pseudo Second Order plot of Cr (AC)

VI. Zinc (AC)

t (min)	Ct	Co-Ct	Qt	Qe-Qt	ln(Qe-Qt)	t/Qt
10	34.34386	3.842142	1.921071	3.073873	1.122938	5.205429
20	27.21442	10.97158	2.742894	0.986377	-0.01372	7.291568
30	23.89712	14.28888	2.381479	0.94695	-0.05451	12.59721
40	18.07634	20.10966	2.513708	0.330089	-1.10839	15.91275
50	15.15224	23.03376	2.303376	0.212271	-1.54989	21.70727

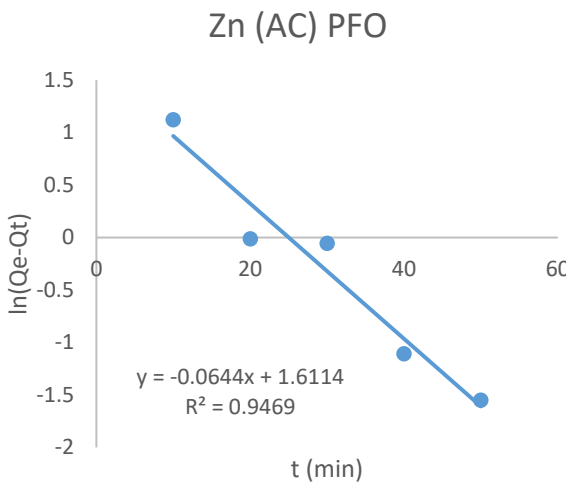

Figure B23: Pseudo First Order plot of Zn (AC)

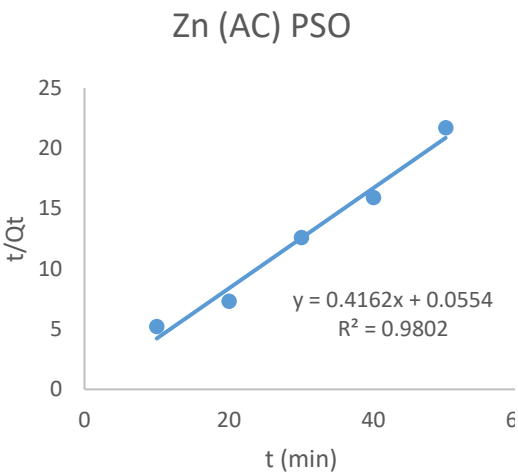

Figure B24: Pseudo Second Order plot of Zn (AC)

APPENDIX C

Thermodynamic Calculations

I. Chromium (Raw)

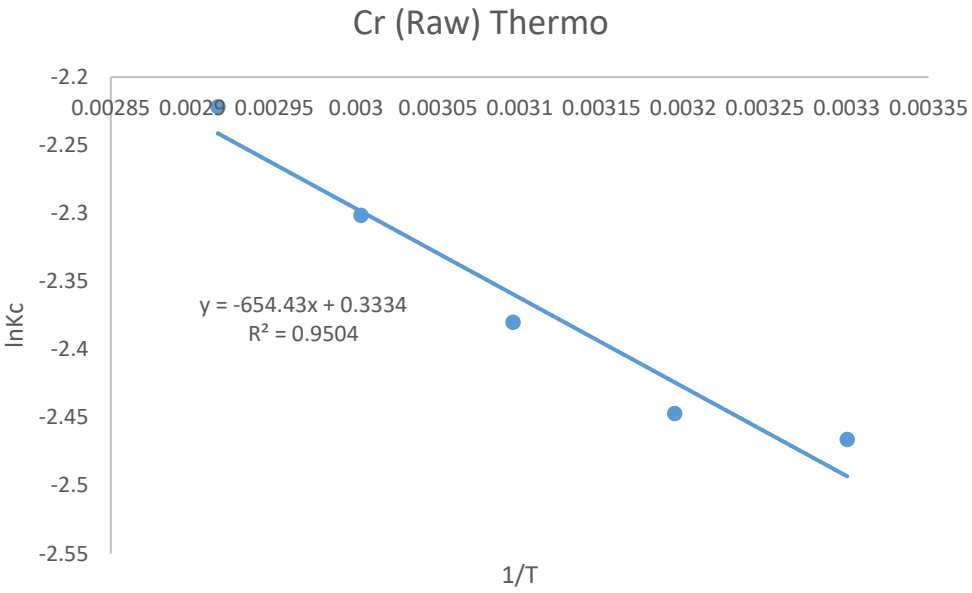

II. Zinc (Raw)

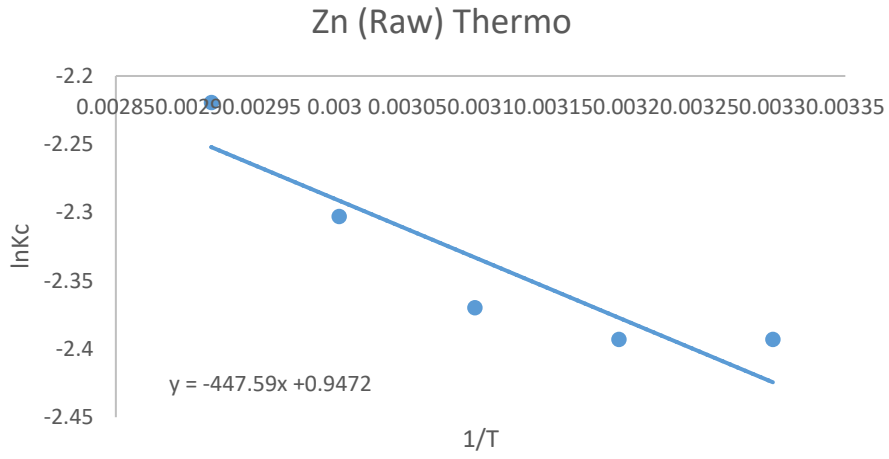

III. Chromium (Modified)

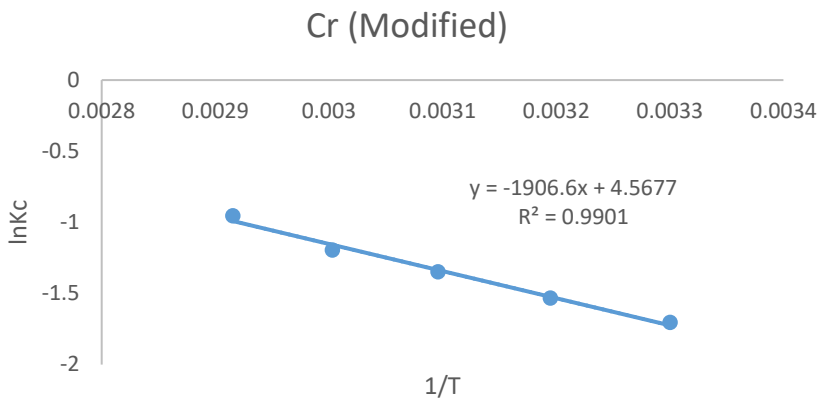

IV. Zinc (Modified)

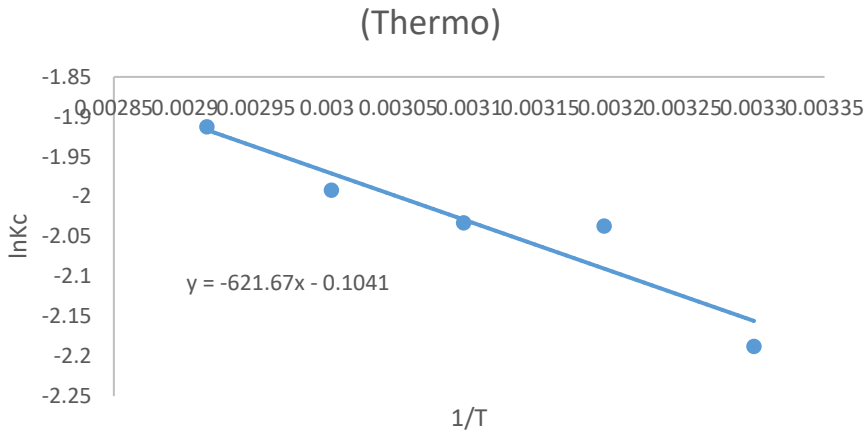

V. Chromium (AC)

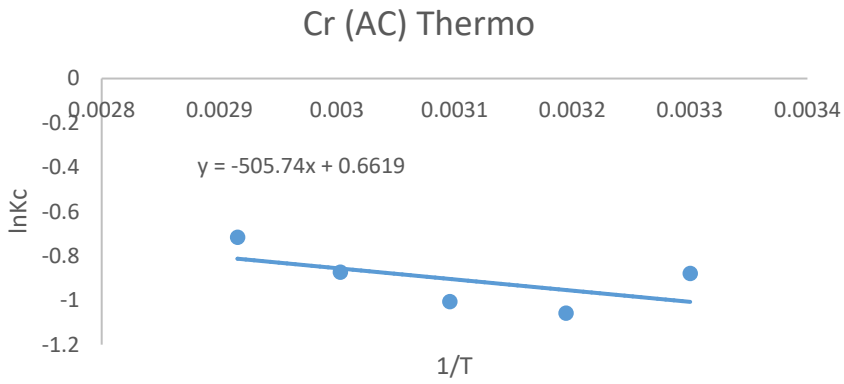

VI. Zinc (AC)

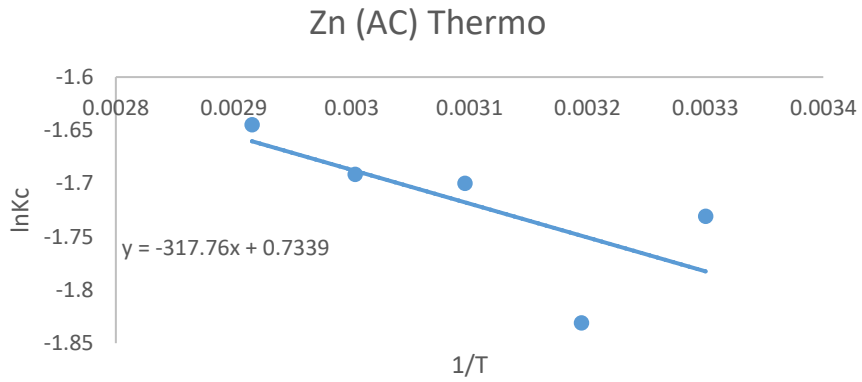

APPENDIX D

FT-IR Analysis

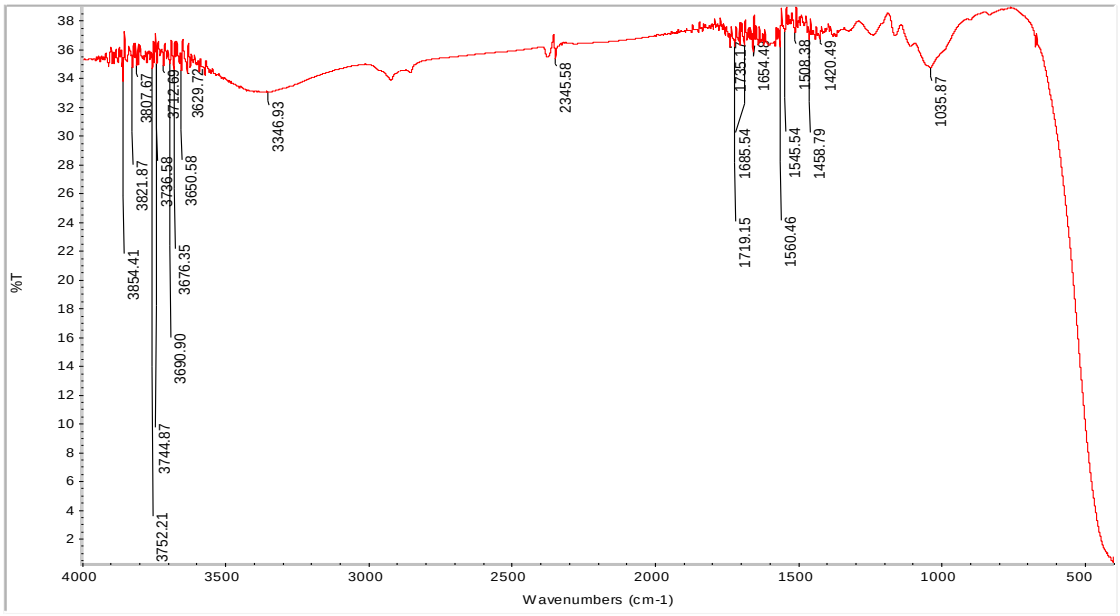

Figure 1: FT-IR Spectra of raw sugarcane bagasse

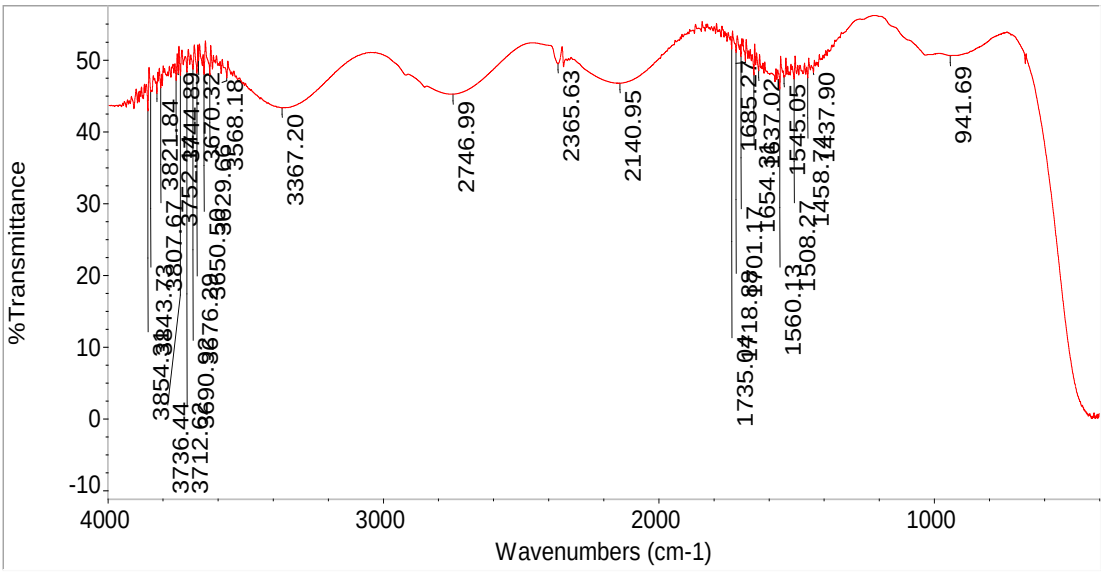

Figure 2: FTIR of modified sugarcane

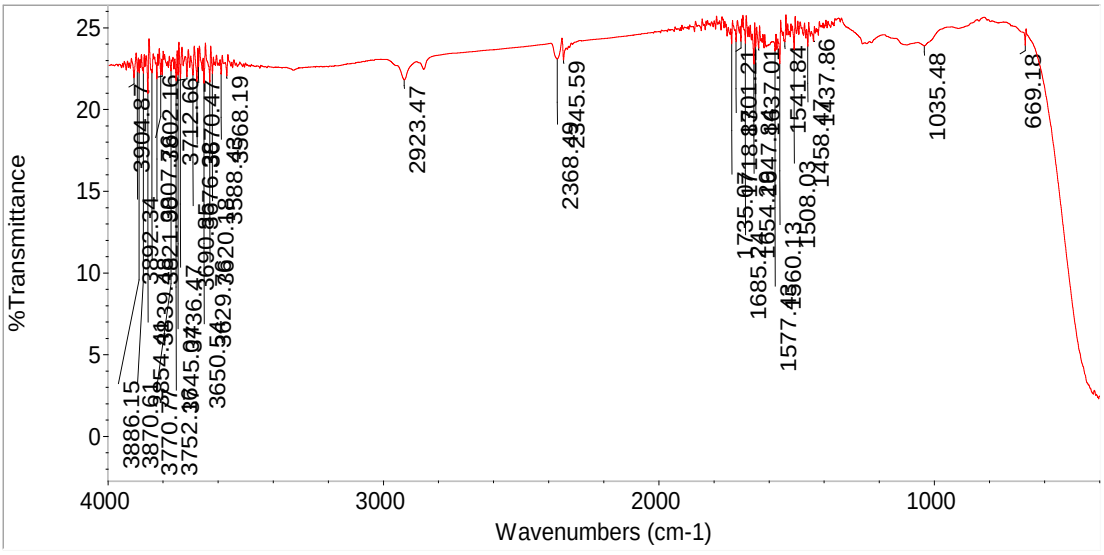

Figure 3: FT-IR Spectra of sugarcane bagasse activate